DJ-1, A NOVEL ANDROGEN RECEPTOR BINDING PROTEIN, ACTIVATES RECEPTOR SIGNALING IN PROSTATE CANCER AND CORRELATES WITH THE DEVELOPMENT OF ANDROGEN-INDEPENDENT DISEASE

By

Jennifer Erin Tillman

Dissertation

Submitted to the Faculty of the

Graduate School of Vanderbilt University

in partial fulfillment of the requirements

for the degree of

DOCTOR OF PHILOSOPHY

in

Cancer Biology

May, 2007

Nashville, Tennessee

Approved	**Date**
Susan Kasper, PhD	3/16/2007
Robert Matusik, PhD	3/16/2007
Neil Bhowmick, PhD	3/16/2007
Fiona Yull, PhD	3/16/2007

To my beloved fiancée Alex S. Flynt, had you not been by my side,

I might never have achieved this goal.

I eagerly await the joys our new life together will bring.

ACKNOWLEDGEMENTS

This work would not have been possible without the following financial support: from the NIDDK (R01DK60957 and R01DK059142 to Susan Kasper), the Frances Williams Preston Laboratories of the T.J. Martell Foundation (to Susan Kasper) and the NIH/NCI Training Grant CA09592 (to Lynn Matrisian) that provided stipend support to me for two years.

I would like to express my gratitude to the following individuals for their encouragement and support which helped me complete my PhD research and training. Foremost I would like to thank my mentor, Dr. Susan Kasper for her guidance and training. I would also like to thank Susan and the rest of my committee members Dr. Fiona Yull, Dr. Neil Bhowmick, and Dr. Robert Matusik for their time, expertise, and thoughtful suggestions regarding experiments, organization of manuscripts, and presentation of my data. Their helpful suggestions have truly made me a better scientist and encouraged me to carefully think about experimental design and data interpretation. Additionally, I would like to thank Dr. Simon Hayward for experimental suggestions and for the opportunity to present my work at the fall meeting of the Society for Basic Urologic Research in 2006. This was an exceptional opportunity for my research career and made me appreciate the interest in and importance of my research. I would also like to thank Dr. Peter Clark for conversations relating to the tissue array data and providing a clinical view of possible future directions of this project.

I want to thank everyone in the Kasper lab, both past and present, but especially: Dr. Tiina Pitkanen-Arsiola, my friend and colleague for training advice; Dr. Guangyu Gu

for his friendship, expertise, and guidance in more areas than I could possibly list here; Jialing Yuan, our invaluable lab manager who's smile and organization make the entire lab "work"; and Ritwik Ghosh, my friend and fellow student, who has been there through it all – lab work, incredible stress, personal matters, and of course "happy hour." Finally, thank you to the entire Prostate Cancer Center for being such an open, inviting, helpful, and collegial group of people.

Finally, I want to thank my family and friends for their continued support during the last several years. I especially want to thank my parents, Dickie and Cheryl Tillman, and my brother, Lee Tillman, for encouraging and supporting me throughout graduate school. They may not have always understood the problems I was having with experiments, but they were always there to encourage me to persevere.

PREFACE

The American Cancer Society was founded in 1913, and since that time, has promoted cancer awareness. Educational efforts began with medical professionals and later expanded to include the general public. Over the last century, their efforts, and others like theirs, have greatly improved public awareness of the disease, funding, and advocacy for cancer related programs. There have been many advances in basic knowledge of most cancers. Pioneering research in prostate cancer in 1941 by Huggins and Hodges demonstrated that castration caused cancer regression. Castration caused disease regression by removing androgens and therefore preventing the activation of the androgen receptor. This breakthrough provided a way to control tumor growth, but unfortunately they discovered that prostate cancer recurred independently of androgens. Although their work provided perhaps the biggest breakthrough in the prostate cancer field, earning them the Nobel Prize, the mechanisms by which prostate cancer and androgen-independent disease develops remains elusive some 66 years later. The androgen receptor remains a persistently pursued target in prostate cancer research today and anti-androgen therapy remains the most effective treatment. Laboratories throughout the world strive to understand how it is controlled in all stages of prostate development and cancer progression. Our laboratory has developed the hypothesis that there is a sub-set of anti-androgen-regulated genes that may allow the androgen receptor to escape anti-androgen therapy and promote disease progression. This is a compelling idea – **perhaps the treatment itself drives disease progression**. This research project specifically addresses this hypothesis by focusing on the oncogene DJ-1 in prostate cancer. We

determined that DJ-1 is a novel androgen receptor binding partner regulated by androgens and anti-androgens and that DJ-1 expression increases in primary prostate cancer following androgen deprivation (anti-androgen) therapy. Thus, increased DJ-1 expression may promote androgen receptor activity and serve as a marker for the development of hormone-refractory prostate cancer.

TABLE OF CONTENTS

V. ADDITIONAL STUDIES TO DETERMINE FUNCTION OF DJ-1

LIST OF TABLES

LIST OF FIGURES

LIST OF ABBREVIATIONS

ACTH ..... Adrenocorticotropic Hormone

AD ..... Androgen Dependent

ADT ..... Androgen Deprivation Therapy

AI ..... Androgen Independent

AIPC ..... Androgen Independent Prostate Cancer

AP ..... anterior prostate

ARE ..... Androgen Responsive Element

BPH ..... Benign Prostatic Hyperplasia

CAT ..... chloramphenicol acetyl transferase

CK ..... cytokeratin

CHX ..... cyclohexamide

DHEA ..... Dihydroepiandrosterone

DHT ..... Dihydrotestosterone

DLP ..... dorso-lateral prostate

Dox ..... doxycycline

DP ..... Dorsal prostate

EM ..... Electron microscopy

GnRH ..... Gonadotropin-releasing Hormone

HGPIN ..... High-Grade Prostatic Neoplasia

HPE ..... Human Prostate Epithelial (Cells)

IP ..... immunoprecipitation

LGPIN ..... Low-Grade Prostatic Intraepithelial Neoplasia

LH..... Leutenizing Hormone

LHRH ..... Leutenizing Hormone Releasing Hormone

LP ..... lateral prostate

LUTS ..... Lower Urinary Tract Symptoms

OHF ..... hydroxy-flutamide

PB ..... Probasin

PCa ..... Prostate Cancer

PIN ..... Prostatic Intraepithelial Neoplasia

PSA..... Prostate Specific Antigen

PZ ..... Peripheral zone

RTKs..... Receptor Tyrosine Kinases

SV40 ..... Simian Virus 40

TH..... Tyrosine Hydroxylase

TIGR..... Transiently Infected Gene Reporter

TMA ..... Tissue Microarray

TZ ..... Transitional zone

VP ..... ventral prostate

CHAPTER I

INTRODUCTION

Prostate Biology and Structure

The prostate is a male accessory reproductive gland found in all mammals that aids in liquefying the seminal fluid. Physiologic parallels are numerous between species, but there are few anatomic similarities. For example, in humans and dogs, the prostate is located at the bladder neck, while in mice and rats, the prostate is a combination of paired glandular organs (1). Mouse and rat prostate is discussed in Chapter V.

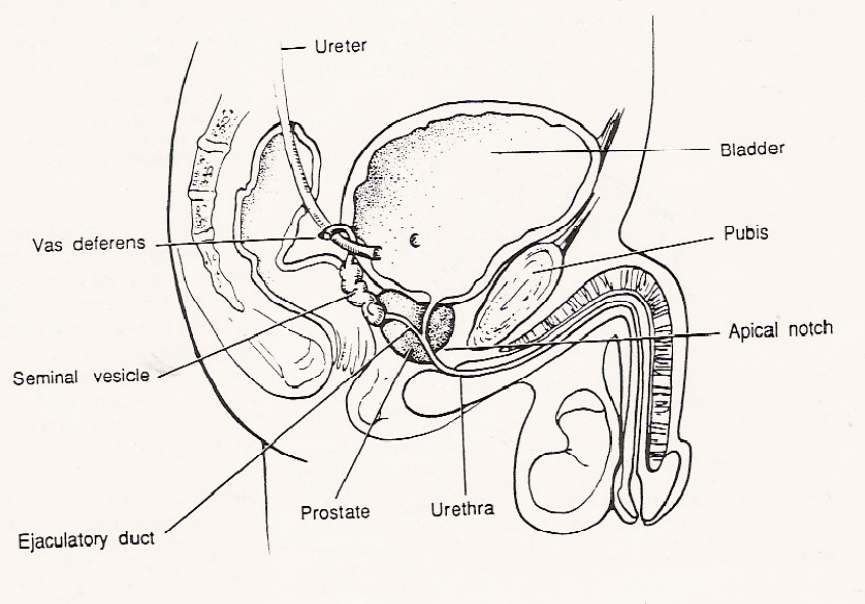

Figure 1. The adult prostate and surrounding structures. The base of the prostate is located at the bladder neck. The urethra bisects the prostate. Image taken from (1).

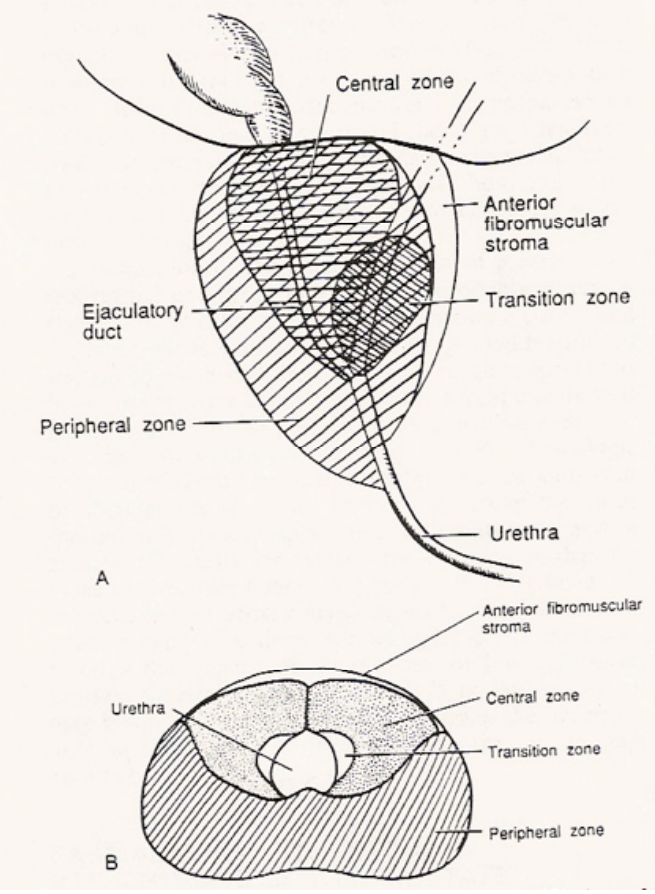

Figure 2: Prostatic Zones. Lateral **A)** and Coronal **B)** views of the prostatic zones. The four histologically distinct zones are shown: anterior fibromuscular stroma, the central zone, the transitional zone, and the peripheral zone. Figure taken from (1).

The human prostate changes little in size from birth until puberty. At puberty, the prostate undergoes rapid growth and reaches an average adult weight of approximately 40 grams. Structurally, the human prostate resembles a truncated cone that is bisected by the urethra (Figure 1). Distinct anatomic lobes were not defined for the human prostate until 1975. Tissel and Salander described four anatomically distinct lobes that were arranged in an "onion" pattern. The anatomical pattern they defined was confirmed by other investigators and is used today. The prostate is composed of the central, transition,

peripheral zones, and a region of anterior fibromuscular stoma (Figure 2). As the name indicates, the anterior fibromuscular stroma is the most anterior prostatic structure. Posteriorly to the stromal region are the paired central zones. Interior to the central zones are the transition zones which are located on either side of the urethra. The transition zones represent the smallest zone in the normal prostate. Lastly, the peripheral zone is located on the posterior side of the prostate. The peripheral zone is the largest region of the normal adult prostate (Figure 2)

Histologically, prostatic glands are composed of several cell types (Figure 3). The predominant cells are tall columnar luminal epithelial cells which are androgen-dependent and produce prostatic secretions (2, 3). Luminal epithelial cells are characterized by expression of androgen receptor and cytokeratins 8 and 18. Basal cells are the second most abundant cell type. Basal cells form a continuous layer between the luminal cells and the basement membrane/basal lamina (2). Cytokeratins 4 and 14 as well as p63 are basal cell markers. The third prostatic epithelial cell type is neuroendocrine cells which are androgen-independent and are dispersed throughout the basal layer (4). Neuroendocrine cells are a minor population of cells in the normal prostate and express chromogranin A, serotonin, and neuropeptides. A thick layer of stroma surrounds the epithelial glands and is composed primarily of smooth muscle but also contains fibroblastic, neuronal, vascular, and lymphatic cell types (5). Stromal markers include smooth muscle alpha-actin and vimentin.

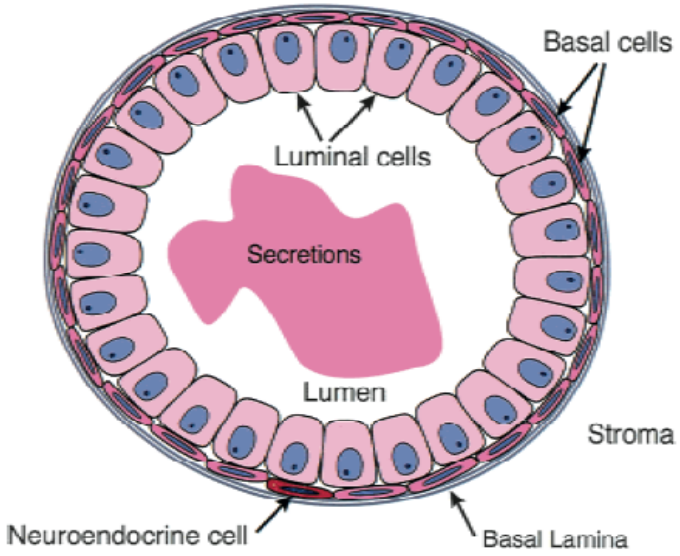

Figure 3: Schematic Diagram of the Cell Types in an Adult Human Prostatic Duct. Relative abundance of epithelial cell types is depicted. Figure from (2).

In most mammals, the prostate is not of great pathological significance. For humans, this is not the case. The human prostate is associated with a number of diseases which are discussed.

Prostatic Diseases

Unlike most mammals, the human prostate is associated with both benign and malignant conditions. The presence of LUTS, or Lower Urinary Tract Symptoms, such as frequent urination, urgent need to urinate, and nocturia are common to all prostatic diseases and are typically the reason men see their doctor. These symptoms alone could be evidence of either a benign or a malignant condition. Prostatitis and Benign Prostatic

Hyperplasia are two common non-malignant conditions that affect the prostate while adenocarcinoma is the most common malignant prostatic disease.

Prostatitis

Prostatitis is an inflammation of the prostate that encompasses four disorders: acute bacterial prostatitis, chronic bacterial prostatitis, chronic pelvic pain syndrome, and asymptomatic inflammatory prostatitis. Acute prostatitis is the least common of the four types. It is caused by a bacterial infection that often results in fever, lower back pain, and a burning sensation during urination in addition to general LUTS symptoms. Acute prostatitis is easily cured with antibiotics. Chronic bacterial prostatitis is also relatively uncommon and is essentially acute prostatitis accompanied by an underlying problem in the prostate allowing chronic infection. This type of prostatitis is treated with antibiotics, but may not be curable. The third, and most common, type of prostatitis is known as chronic pelvic pain syndrome. It can be either inflammatory or non-inflammatory and symptoms often appear and disappear unexpectedly. This type of prostatitis is the least well understood and the treatments vary between patients. Asymptomatic inflammatory prostatitis is the fourth variety and occurs when the patient has no symptoms, but inflammatory cells are present in the semen.

Prostatitis in itself is a relatively minor disorder of the prostate, but inflammatory markers have recently been correlated with cancer risk (6, 7). However, other studies determined that clinical prostatitis did not increase occurrence of prostate cancer (8).

These controversial results indicate that the effects of prostattis on prstate cancer risk or initiation require further investigation.

Benign Prostatic Hyperplasia (BPH)

BPH is another common disease of the prostate. BPH occurs in the transitional zone resulting in an age-dependent enlargement of the gland. Early development of BPH usually occurs after age 40 with prevalence rising to over 50% by age 60, and may reach 90% in men over 85 years (9, 10). Approximately 50% of men diagnosed have moderate to severe LUTS (9). Both stromal and epithelial hyperplasia have been documented in BPH, but it is typically accepted that the stromal:epithelial cell ratio is higher in BPH than normal prostate (9).

BPH is diagnosed by testing the rate of urine flow, digital rectal examination, as well as prostate-specific antigen (PSA) levels. Decreased urine flow rate may indicate that a patient has an enlarged prostate, which can be confirmed with a digital rectal examination. Blood tests are performed to determine the levels of PSA, a serine protease that functions to liquefy semen. If the prostate is enlarged but PSA levels are normal (lower than 4 ng/mL), then BPH rather than prostate cancer is likely the cause of the patient's LUTS.

Prostate Cancer

The most common prostate malignancy is adenocarcinoma. Unlike BPH, prostate adenocarcinoma occurs primarily in the peripheral zone. Prostate Cancer (PCa) is the most prevalent cancer in males, affecting 1 in 9 men between 60 and 70 years old. There are multiple risk factors for the development of PCa, but age is the most significant. Other risk factors include race, family history, and environmental aspects such as diet (11). Studies of age-specific incidence have revealed that risk increases significantly after age 55 and peaks at age 70-74. Autopsy studies have revealed the long latency of PCa because lesions have been found in the prostates of men in their 20s and 30s (11). Race has been added to the risk factor list due to the 60% higher incidence in African-Americans as compared to whites (11). Mortality rates are also higher in African-Americans, although the causes are unclear (11). Since the 1950s epidemiological studies determined that having a first-degree relative with PCa increased an individual's risk of developing the disease by 2-3 fold, (reviewed in (11)). Further, epidemiology has determined that the prevalence of PCa is much higher in the United States than in other parts of the world. In Asia for example, PCa rates are very low, but Asian men who immigrate to the United States have similar rates of PCa to American men, indicating that this difference is related to dietary and environmental differences rather than genetic ones (2). There is a genetic component to PCa risk, however. Two familial susceptibility loci have been mapped to the X chromosome and to a region of chromosome 1q (2, 12, 13). The impact of these factors on the development and progression of PCa is currently an area of intense investigation.

Although controversy exists as to whether prostatitis or BPH increase PCa risk or the development of pre-neoplastic lesions, prostatic-intraepithelial neoplasia (PIN) has been accepted as a precursor to cancer (14). PIN lesions can be described as either low-grade (LGPIN) or high-grade (HGPIN) depending on the level of architectural abnormalities. LGPIN resembles normal prostate, but tufting of the luminal epithelial cells exists. HGPIN is considered an immediate precursor to early invasive carcinoma. Figure 4 depicts the progression from normal prostate epithelium to metastatic cancer and well-defined architectural changes that occur during this progression. For example, there is typically a loss of basal cells in PIN, but the basal lamina/basement membrane is intact. Once epithelial cells invade the basal lamina, the lesion would be classified as invasive carcinoma. Metastasis is defined by migration and growth of prostatic epithelial cells to distant sites in the body (Figure 4).

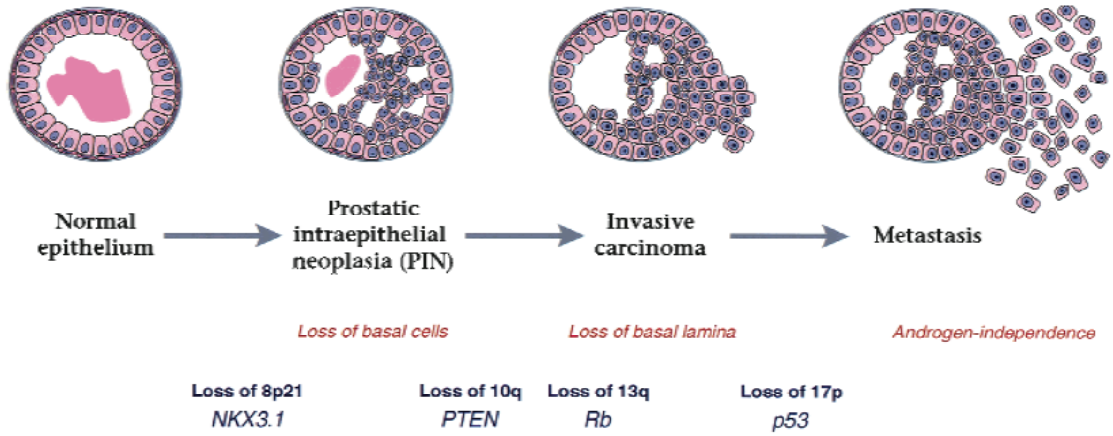

Figure 4: Pathway for Human PCa Progression. Stages of progression are correlated with specific changes such as loss of basal cells or invasion of the basal lamina. Candidate genes for the progression of PCa are shown. Figure taken from (2).

Although there are relatively clear guidelines for classification of PIN versus carcinoma, the heterogeneous and multi-focal nature of PCa provides a challenge to researchers. When PCa samples are examined histologically, there will typically be a combination of normal, pre-neoplastic, and neoplastic foci of varying severity throughout the tissue. In regards to multifocality, microdissection of adjacent neoplastic lesions are not genetically identical, indicating that multiple foci may emerge and evolve independently (15, 16). This phenomena has made PCa research difficult due to the difficulty of getting a homogeneous sample that is large enough to study at the molecular level. Fortunately, new techniques such as cell sorting can now be used to isolate specific cell populations and many standard techniques have become more sensitive, allowing smaller samples to be examined.

In order to provide a standard pathological grading system despite the heterogeneous nature of PCa, Gleason developed a grading system that is the predominant one used by pathologists today. The data leading to the development of the system was collected by studies of the Veterans Administration Cooperative Urological Research Group between 1960 and 1975. The system was developed in the 1970s by Dr. D.F. Gleason by blindly correlating tumor histology with patient survival data to determine malignancy (17-20). The histological patterns were arranged into five groups (1-5), referred to as Gleason grades or patterns. To generate a score, the two most prevalent histologic patterns are evaluated and rated as Gleason pattern 1-5, with higher numbers representing more aggressive/advanced carcinoma. These numbers are then added to give the Gleason score. For example, if the most prevalent lesion is a Gleason pattern 4 and the second most prevalent is a Gleason pattern 3, then this is a Gleason (4 + 3), or Gleason score 7 (21). Each progressive Gleason pattern is represented by cellular and architectural changes as depicted in Figure 5. Gleason score 2-4 is considered low-grade, 5-7 is intermediate, and 8-10 is a high-grade tumor.

Figure 5: The Gleason Grading System. Pathologic grading system used to grade the malignancy of adenocarcinoma. Gleason patterns range from 1, representing small, round, normal glands, to a 5, which corresponds to a complete loss of glandular architecture. This figure represents Gleason's original description of glandular architecture of each grade (19).

Multiple molecular events have been associated with the development of PCa, but only several will be described here. One common early event in PCa progression is the loss of a region of chromosome 8p. This chromosomal loss occurs in approximately 80% of tumors as well as in lung and colon cancers (22-24). One region of 8p that is frequently

lost early in PCa progression is 8p12-21. The candidate gene for this locus is the homeobox gene, Nkx3.1(25). Nkx3.1 is required for normal prostate differentiation in mice, and deletion of one allele is sufficient to cause development of PIN lesions (26) (Figure 4).

Another step in prostate cancer progression occurs with the loss of chromosome 10q and the tumor suppressor PTEN (Phosphatase and Tensin deleted on chromosome 10). Loss of 10q occurs in 50%-80% of prostate tumors and also occurs in breast cancer and glioblastoma (27). Loss of this region is thought to occur after 8q since it is observed more frequently in carcinoma than in PIN (Figure 4). PTEN has been implicated in PCa due to frequent mutation in PCa cell lines and total loss in other cell lines and xenografts (28-30). Loss of PTEN activates the Akt signaling cascade and leads to increased cell proliferation (31). Increased Akt activity has been observed in xenografts as well as primary tumors, supporting a role for PTEN in PCa progression (31).

A third common event in PCa progression that results in carcinoma is the loss of chromosome 13q which includes the Retinoblastoma (Rb) tumor suppressor gene. This deletion occurs in at least 50% of prostate tumors (32-34). Rb mutations and loss of expression have been observed in localized and advanced carcinomas (35-38) (Figure 4). Rb plays an important role in PCa by regulating apoptosis in response to androgens (39-41). Homozygous deletion of Rb is lethal, but tissue rescue of the Rb null prostates revealed dysplasia and invasive carcinoma, which is exacerbated by treatment with androgens (27).

Deletion of chromosome 17p is a relatively late-stage event in the progression of PCa (42). This region encodes the well characterized p53 tumor suppressor gene. p53 mutations occur infrequently in early invasive carcinoma (43) (44). Mutations of p53 were identified in advanced carcinomas and metastatic lesions from immunohistochemical examination of accumulated protein and by direct mutational analyses (Figure 4) (2, 45-47).

Consistent with the heterogenous nature of PCa, there are many genes that have been implicated in the development and progression of PCa. A few of the most studied are listed and discussed briefly above. One simil arity in the molecular profile of PCa exists, however, the importance of the androgen receptor in prostate development and all stages of prostate cancer progression.

Androgen Receptor Signaling

Male steroid hormones

The androgen receptor (AR) is part of the superfamily of nuclear receptors which traditionally function by binding small cytoplasmic steroid or non-steroid ligands that enter cells through diffusion. The type-one receptors (androgen, progesterone, estrogen, glucocorticoid, and mineralcorticoid) share functional domains consisting of an N-terminal variable domain, a DNA binding domain, a hinge region, and a hormone binding domain. Type-one receptors are associated with heat shock proteins when

inactive, but upon ligand binding, the heat shock proteins are released, the receptor dimerizes, and translocates to the nucleus to activate transcription of target genes.

Prostatic growth and function is regulated predominantly by testicular androgens via the androgen receptor, but to a lesser degree by adrenal androgens. The endocrine pathway that ultimately results in synthesis of androgens begins in the hypothalamus. Lutenizing Hormone Releasing Hormone (LHRH) is synthesized and released from the hypothalamus which stimulates the pituitary to release lutenizing hormone (LH) and adrenocorticotropic hormone (ACTH). LH stimulates the production of testosterone in the testis while ACTH stimulates the adrenal glands to synthesize the adrenal androgens dihydroepiandrosterone (DHEA), DHEA sulfate, and androstenedione. Both testicular and adrenal androgens stimulate the prostate, but testosterone is responsible for the majority of effects (Figure 6). Testosterone circulates through the bloodstream where it is bound to albumin or sex-hormone binding globulin, or it is free (un-bound). When free testosterone reaches the prostate it diffuses across the plasma membrane and is converted to the more potent androgen, dihydrotestosterone (DHT), by 5 alpha-reductase. DHT binds the androgen receptor, causing a release of heat shock proteins and recruitment of co-regulators. Ligand-binding triggers AR dimerization and phosphorylation followed by translocation to the nucleus where AR binds the promoter regions of androgen-regulated genes, such as PSA, via an androgen responsive element (ARE) to activate transcription (Figure 7).

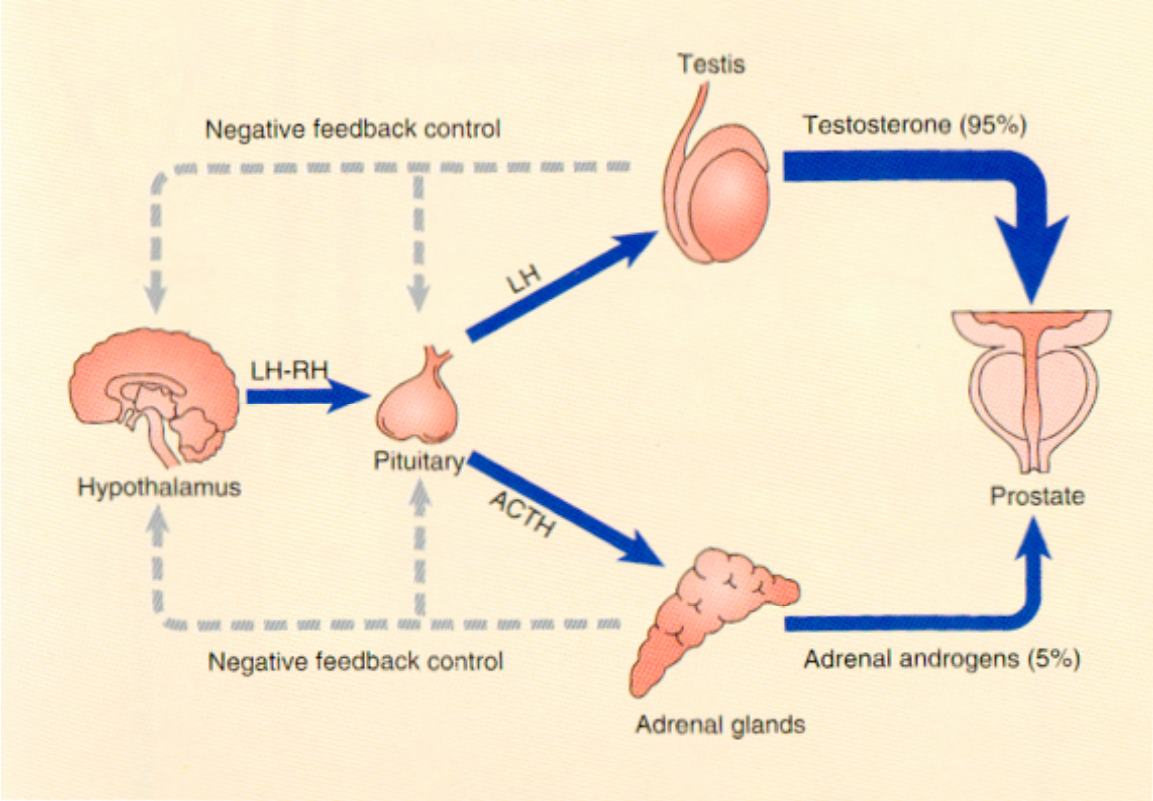

Figure 6: The Male Endocrine Pathway The hypothalamus releases LHRH stimulating the pituitary to generate LH and ACTH. LH stimulates the synthesis of testosterone in the testis, while ACTH stimulates production of adrenal androgens. Both testicular and adrenal androgens stimulate the prostate in the relative amount shown, 95% and 5% respectively. In addition to stimulating prostatic growth, androgens are also part of a negative feedback loop to the pituitary and hypothalamus to stop hormone production. Figure adapted from (1).

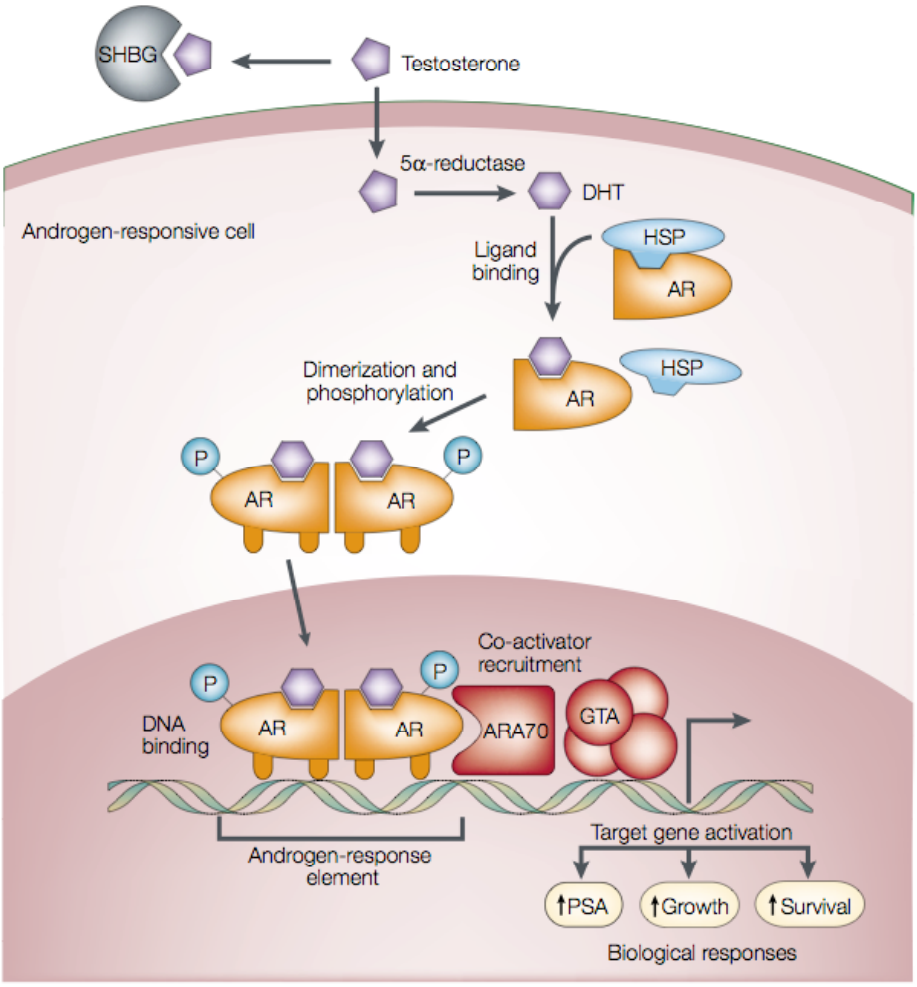

Figure 7: AR Action In the Prostate. Testosterone is released from sex-hormone binding globulin (SHBG) and diffuses into an androgen-responsive cell. Once in the cytoplasm, testosterone is converted to DHT, binds AR which causes the release of heat shock proteins (HSP). Ligand binding induces receptor dimerization and phosphorylation followed by translocation to the nucleus. Nuclear AR binds androgen-responsive elements in the promoter regions of androgen-regulated genes, recruits co-regulators such as ARA70, and the general transcription apparatus (GTA). Activation of target genes leads to biological responses such as production of PSA and promotion of growth and survival. Figure from (48).

Androgen Receptor in Normal Prostate and Prostate Cancer

Androgens and the AR are required for development and normal prostate function (2, 49-52). The prostates of AR knockout mice do not develop (52) nor do the prostates of testicular feminized (Tfm) mice or individuals with inactivating mutations of AR (49, 50, 53, 54). Once the prostate develops, androgens are the primary regulators of epithelial cell proliferation and apoptosis (48-50). Androgens promote cell survival and inhibit apoptosis (Figure 7) (48, 49). In the normal prostate, there is a balance between the number of cells proliferating and cells undergoing apoptosis resulting in maintenance of the size of the gland.

Unlike the genes discussed previously that have been implicated at specific times in PCa development and progression, AR is important at all stages (2, 49). AR is required for normal prostate function and is expressed in PIN and early carcinoma, however it is also expressed in advanced and metastatic carcinoma. Androgens regulate the proliferation rates of epithelial cells, the predominant cell type involved in adenocarcinoma, so increased androgen levels or AR activity could result in uncontrolled proliferation and cancer. This is one reason that PSA, an androgen-regulated gene, is used as a marker for PCa. Another mechanism by which PSA levels are increased in cancer is that abnormal ductal structures allow PSA to be secreted into the extra-cellular space, rather than prostatic lumens, resulting in increased PSA in the bloodstream (55, 56).

In addition to regulation of PSA, AR regulates a number of other genes through numerous interactions with co-activators and co-repressors. Once AR translocates to the

nucleus, nuclear AR co-regulators facilitate interactions with DNA and with the general transcription initiation complex.

Androgen Deprivation Therapy as a Treatment for PCa

Prostate cancer is initially dependent upon androgens for growth and survival and when androgens are removed, massive apoptosis and tumor regression occurs. This observation was made by Huggins and Hodges in 1941 when they reported that castration caused prostate cancer regression (57). Huggins performed surgical castration to treat prostate cancer, and it was highly effective for a period of time, but eventually the tumors recurred independently of androgens. Androgen deprivation therapy (ADT) is still the most commonly used therapy for androgen-dependent (AD) prostate cancer (58, 59). Today's physicians rely on chemical castration using mono- or combination therapy. Maximum androgen blockade has been initiated when anti-androgens were administered along with gonadotropin-releasing hormone (GnRH) to simultaneously block adrenal as well as testicular androgens or with LHRH analogs to block the synthesis of either testicular or adrenal androgens (60, 61). As with physical castration, the tumor initially responds to androgen deprivation but will eventually recur as an androgen-independent tumor. The mechanisms behind the progression from androgen-dependency to androgen-independency have been studied in depth, but appear to vary from patient to patient and thus remain difficult to study.

Mechanisms for the Development of AIPC

Feldman and Feldman have complied and discussed additional hypotheses for the development of androgen-independent disease (48). Their hypotheses focus on AR since it is likely at the center of the development of androgen-independent prostate cancer (AIPC). Their hypotheses include the hypersensitive AR pathway, the promiscuous AR, the outlaw AR, the AR bypass, and lurker cells (Figure 8). The hypersensitive and promiscuous AR hypotheses will be discussed in the most detail as they are closely related to this research, but all hypotheses have primary research supporting them which is discussed by Feldman (48).

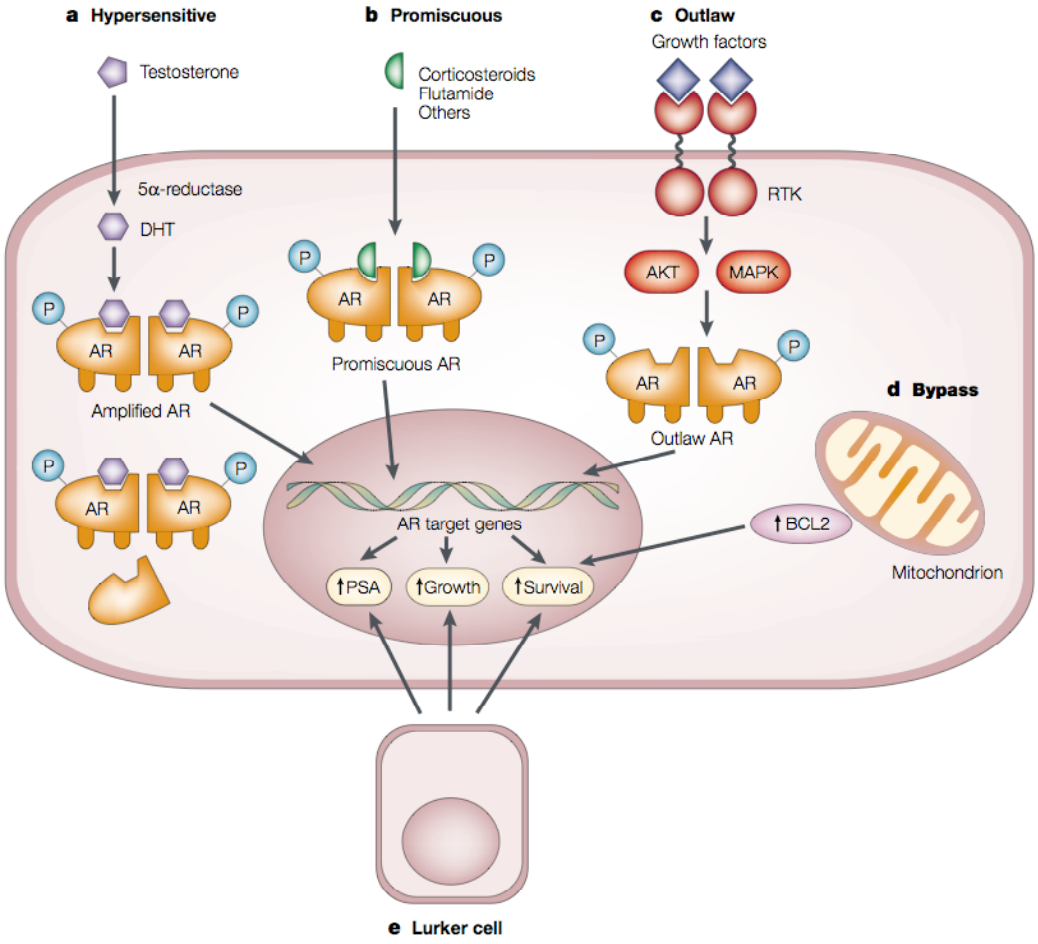

Figure 8: Hypotheses for the development of androgen-independent prostate cancer. Multiple mechanisms exist for a cancer cell to escape ADT and become androgen-independent. Several of these mechanisms involve AR. A) The hypersensitive pathway occurs when AR is amplified or is more sensitive to low androgen levels. B) In the promiscuous pathway, AR can be activated by steroids or anti-androgens typically due to mutations allowing these agents to act as agonists. C) Receptor Tyrosine Kinases (RTKs) can activate AR in the Outlaw pathway by phosphorylating AR in the absence of ligand D) The bypass pathway does not involve AR, but rather other pro-survival genes like bcl-2 stimulate the cell to survive in the absence of AR signaling E) The lurker cell hypothesis relies on the possibility that androgen-independent cells always exist in the prostate and are selected for by androgen-deprivation therapy (48).

Hypersensitive AR

The hypersensitive AR hypothesis is one possible mechanism for prostate cancer to circumvent ADT. If the tumor increases sensitivity to androgens it would be able to take advantage of the small amounts of androgens present after ADT. These tumors would not strictly be androgen-independent because they would still rely on androgens, just in much lower amounts than normal prostate. For a prostate tumor to become hypersensitive to androgens one of two things (or both) must occur. AR must either be amplified or become more sensitive to low levels of androgens (Figure 8a). If AR is amplified, there is an increase in the percentage of ligand-bound receptor even though androgen levels are low. Studies have indicated that approximately 30% of androgen-independent tumors after ADT have AR amplification, whereas none of them had AR gene amplification before androgen-ablation (62-64).

An alternate mechanism for prostate tumors to become hypersensitive to low-levels of androgens is through increased AR sensitivity. This mechanism was documented in an animal model for PCa where tumor cells exhibited increased expression of AR, increased stability, and enhanced nuclear localization of AR (65). These cells were more sensitive to DHT than expected: the growth-promoting concentration was 4-fold lower than the regular androgen-dependent LNCaP cells. Further, Balk (66) reported that AR mRNA levels rose up to 70-fold in metastatic AI compared to primary prostate cancer and that AR immunostaining was nuclear in androgen-independent (AI) prostate cancer cells, even in patients undergoing ADT/bicalutamide treatment. Examples of increased AR

expression and sensitivity demonstrate that these situations occur *in vivo* and that the hypersensitive AR pathway contributes to promotion of androgen-independence.

Promiscuous AR

A second hypothesis for tumor cells to escape ADT is through a promiscuous AR. This hypothesis is based upon the fact that most androgen-independent tumors express AR. It seems that many androgen-independent tumors do not arise from loss of androgen signaling, but rather from genetic changes that cause divergent activation of the AR signaling pathway (67). These changes are typically missense mutations of AR resulting in decreased ligand specificity allowing other non-androgen steroids or androgen-antagonists to activate AR (Figure 8b). The rate of AR somatic mutations in PCa has been debated in the literature, but seems that most mutations occur in metastatic samples (68). Further analysis revealed the mutation rate increased after androgen deprivation (58, 62, 69-71). It seems logical that gain-of-function mutations would be selected for in order to provide a growth advantage. There are many mutations that have been characterized and are reviewed thoroughly elsewhere (48, 49). Importantly, most somatic AR mutations discovered in AI prostate tissue localize to discrete regions of the receptor and suggest that altered androgen signaling provides a potential mechanism for the re-emergence of tumor growth during the course of ADT (67).

One of the most well known AR mutations is the T877A substitution mutation found in the LNCaP human PCa cell line (72). This mutation allows progestins, estrogens, and anti-androgens to act as agonists (48, 73, 74). Studies of primary prostate tumors

revealed that this mutation was present in 6 of 24 metastatic prostate cancer samples, indicating that it occurs relatively frequently in AIPC patients (75). AR mutations that allow anti-androgens to gain agonist function could explain the clinically observed phenomenon of "anti-androgen withdrawl syndrome" where patients worsen clinically with flutamide treatment, but improve when it is withdrawn (76-78). These patients experience rising PSA levels when treated with flutamide and seems to be due to selection of cells expressing a promiscuous AR. When flutamide treatment is withdrawn, PSA levels decrease as well as other parameters such as acid and alkaline phosphatases. In these studies, it seems that flutamide drives selection of cells expressing mutant ARs. The T877A mutation was documented in the bone marrow metastases of 5 out of 16 patients who had received flutamide treatment (69). As expected, these cells exhibited growth stimulation from flutamide treatment. Tumors in other patients who did not receive flutamide treatment had different mutations and did not grow in response to flutamide treatment. This suggests that flutamide treatment provided selective pressure for mutations resulting in a promiscuous AR.

A different mechanism whereby flutamide or other anti-androgens could result in promiscuous AR activity is through alterations to AR co-regulators. There are numerous co-activators and co-repressors of AR that have been described (49, 79). Studies have identified alterations in expression of AR co-regulators when there is no apparent mutation of AR (44). An increase in AR activity could be the result of increased expression of co-activators, or by decreased expression of co-repressors. Several AR co-regulators have been specifically linked to advanced and androgen-independent prostate

cancers. Two AR co-activators, steroid receptor co-activator 1 (SRC1) and transcriptional intermediary factor 2 (TIF2), are over-expressed in several prostate cancer cell lines and in some recurrent prostate cancers (80-82). These changes allowed activation of AR at physiologic (low) levels of adrenal androgens indicating that these co-activators could promote promiscuous AR activity *in vivo*. Nuclear accumulation of another AR co-activator, Tat interactive protein, 60kDa (Tip60), was increased in biopsies from patients with AIPC (83). Additionally, Tip60 expression was increased by androgen deprivation in the LNCaP and CWR22 xenograft models (82, 83) indicating that Tip60 may be part of a family of co-activators that are regulated by ADT to promote development of AIPC. The structurally similar AR co-activators, p300 and CBP (CREB binding protein), enhance ligand-independent activation of AR in the presence of interleukin 6 (IL-6) (82). IL-6 and other cytokines activate multiple signaling cascades, such as the JAK/STAT and MAPK pathways that have been identified in the outlaw receptor hypothesis (Figure 8c) (48, 82). The role of AR co-repressors in the development of AIPC is less well documented, but at least one example has been documented. The AR co-repressor, nuclear receptor co-repressor (NCoR), has been shown to differentially repress AR activity in the presence of different agonistic and antagonistic ligands. In LNCaP cells that express the T877A mutant AR, NCoR was unable to repress the agonistic activity of the anti-androgens flutamide and cyproterone acetate (84). This indicates that AR mutations can modify the effectiveness of AR co-repressors. The expression pattern of NCoR and other AR co-repressors has not been evaluated in androgen-independent disease, however, decreased expression of NCoR in breast cancer correlated with tamoxifen (an ER antagonist) resistance (85). Breast cancer patients that lacked functional

NCoR, tamoxifen became an ER agonist and led to the activation of ER responsive genes (85). These examples of nuclear receptor co-activators and co-repressors highlight the importance of these proteins in both normal tissues and in the development of hormone refractory cancers.

Finally, there are additional ligand-independent mechanisms involving receptor tyrosine kinases, anti-apoptotic genes like bcl-2, (48, 86, 87) or growth factors such as insulin-like growth-factor-1 (IGF-1), keratinocyte growth factor (KGF) and epidermal growth factor (EGF) (88, 89) that could alter AR activity in the absence of androgen, thereby facilitating progression towards androgen resistant disease (Figure 8C and D). A final hypothesis for the development of AIPC is known as the lurker cell. Some believe that androgen-independent cells always exist in small numbers in the prostate, potentially as prostate stem cells or cancer stem cells, and that ADT provides a growth advantage to these cells (Figure 8E) (48) (71).

DJ-1

Human DJ-1 is located in at 1p36.33-1p36.12 and is composed of 7 exons encoding a 20 kilo-Dalton protein (NCBI accession numbers: mRNA D61380, protein BAA09603). DJ-1 is a ubiquitous cytoplasmic and nuclear oncogene also known as PARK7 (90-92). DJ-1 was initially identified by Nagakubo and colleagues in a yeast two hybrid screen for c-myc binding partners (93). Although a portion of the DJ-1 cDNA was identified as a putative c-myc binding protein in this assay, they ultimately determined that DJ-1 does not interact with c-myc. Instead, it was determined to be a

false positive because only a small non-coding region of DJ-1 interacted with the c-myc fusion protein (93). Although it did not interact with c-myc, the group was still interested in the DJ-1 cDNA because it was previously uncharacterized. They determined that increased DJ-1 expression is capable of transforming NIH-3T3 cells either alone or, to a greater extent, in conjunction with c-myc or H-ras over-expression, thus giving DJ-1 the oncogene moniker (93). Since this initial discovery and characterization, DJ-1 has been associated with multiple signaling pathways and human diseases, as well as being characterized in multiple model systems (90-92, 94-99).

The crystal structure of DJ-1 was determined by several groups, revealing that the mature protein exists as an obligate dimer (Figure 9) (100, 101). However, even the elucidation of the structure and analysis of the protein sequence was unable to determine the function of DJ-1. There were no known protein domains that were identified in the human DJ-1 sequence. Rather, the protein sequence and structure resembled domains required for thiamine synthesis and chaperone activity in bacteria (100-102). Since there were no exact matches for known protein domains, determination of the crystal structure seemed to raise more questions than it answered by providing a potential role for DJ-1 as a protein chaperone.

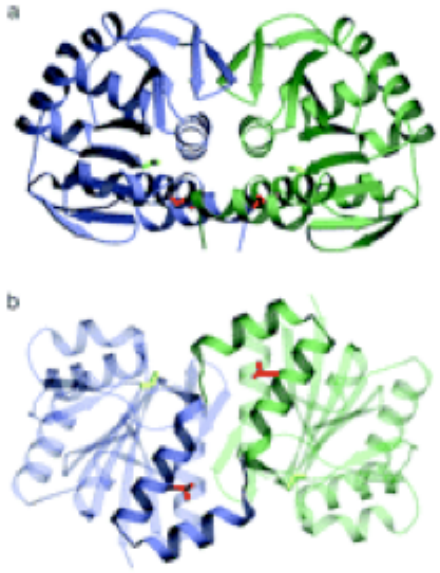

Figure 9: Crystal Structure of Human DJ-1. DJ-1 is an obligate dimer. One monomer is shown in blue and the second in green. Bottom view is rotated 90 degrees from the top view. Leucine 166 which is mutated in Parkinson's disease is shown in red. Figure modified from (100).

Since the initial discovery, over-expression of DJ-1 has been associated with a number of human diseases including Parkinson's disease (90, 92) and carcinomas of the lung, breast, and prostate (95, 99). In Parkinson's disease research, DJ-1 is referred to as PARK7. Many research groups study the role of DJ-1 in Parkinson's disease, and have discovered multiple functions that may contribute to disease onset and progression. Bonifati and associates were among the first to link DJ-1 to autosomal recessive early on-set Parkinson's (91) (103). Mapping of the DJ-1 (PARK7) locus in several genetically isolated families with this form of Parkinson's revealed the L166P DJ-1 mutation (103).

Bonifati and others determined that this mutation destabilized the protein leading to rapid turnover by the proteasome and affected oligomerization and sub-cellular localization (91) (90) (104) (105). Further, Yokota and colleagues determined that down regulation of DJ-1 in neuronal cells increased cell death from oxidative stress, ER stress, and inhibition of the proteasome, but not by pro-apoptotic stimulation (105). Cell death from hydrogen peroxide treatment was rescued by wild-type DJ-1 but not by the L166P mutant DJ-1 (105). Additional research in neuroblastoma cell lines (106), Drosophila (107) (108) and DJ-1 mutant mice (109) (110) confirmed the role of DJ-1 in oxidative stress and in normal function of dopaminergic neurons. Taira and co-workers demonstrated that DJ-1 expression increased after hydrogen peroxide treatment and that treatment caused a shift in the isoelectric point of DJ-1 (106). Oxidative damage to DJ-1 has been reported in the brains of sporadic Parkinson's disease and Alzheimer's disease patients (111). Ten isoforms of DJ-1 were identified in Parkinson's and Alzheimer's patients with isoelectric points ranging from 5.5 to 8.4 (111).

Although mutations in DJ-1 were associated with Parkinson's disease and oxidative stress, the role of DJ-1 in degeneration of dopaminergic neurons was unclear until the interaction between DJ-1 and protein-associated splicing factor (PSF) was discovered (112). DJ-1 inhibited the transcriptional-silencing activity of PSF and wild-type DJ-1 prevented PSF-induced neuronal apoptosis, but mutated DJ-1 was less effective (112). Zhong and colleagues demonstrated that down-regulating DJ-1 expression using siRNA decreased tyrosine hydroxylase expression (113). Tyrosine hydroxylase (TH) is an enzyme critical in the synthesis of dopamine, a pathway targeted

in the treatment regimen for Parkinson's patients. Chromatin immunoprecipitation assays determined that DJ-1 bound and transcriptionally-activated the promoter region of TH. However, they did not perform gel-shifts to confirm a direct interaction between DJ-1 and the TH promoter, indicating the interaction could be indirect. Further, they showed that DJ-1 inhibited the sumoylation of PSF and PSF-induced inhibition of TH, providing a second mechanism for DJ-1 regulation of TH (113). These results identified a novel function for DJ-1 as a transcription factor. Proteomics suggested that DJ-1 might act a transcription factor since it is a dimer, but until recently, there were no known DJ-1 regulated genes.

In addition to Parkinson's disease, DJ-1 has been implicated in adenocarcinomas of the lung, breast, and prostate (95, 99). Increased DJ-1 expression in lung cancer correlates with poor clinical prognosis (95). Further, increased expression of DJ-1 in breast cancer is associated with decreased expression of the tumor suppressor PTEN, (95). Despite the oncogenic properties of DJ-1, its functional significance in prostate cancer development and progression is not well understood. The importance of PTEN in PCa is well documented (27, 30, 114-117) and although it is likely that DJ-1 antagonizes PTEN in prostate cancer as in breast cancer, this interaction has not yet been defined in prostate. Another potential link between DJ-1 and prostate cancer was reported by Takahashi and colleagues who determined that DJ-1 positively regulates AR (98). They demonstrated that DJ-1 bound the AR-binding-region of PIASx-alpha, a known co-repressor of AR, thereby releasing and allowing AR to become transcriptionally active (98). Further, Niki and associates demonstrated a second mechanism for activation of

AR by DJ-1. They showed that DJ-1 bound and sequestered DJ-1-Binding-Protein also resulting in activation of AR (118). One recent study investigating the role of AR in the activation of TH found that DJ-1 inhibited, rather than activated, AR in a neuronal cell line, which suggests that the function of DJ-1 likely varies between cell-types (119). These data indicated that DJ-1 could function as a co-activator or a co-repressor of AR in PCa. Since the role of AR co-regulators in AIPC has been established, this provided a potential role for DJ-1 in androgen-independent disease. Despite the diverse DJ-1 literature however, there was a lack of research pertaining to the importance of DJ-1 in PCa, on the transcriptional regulation of DJ-1, downstream targets, and DJ-1 binding proteins.

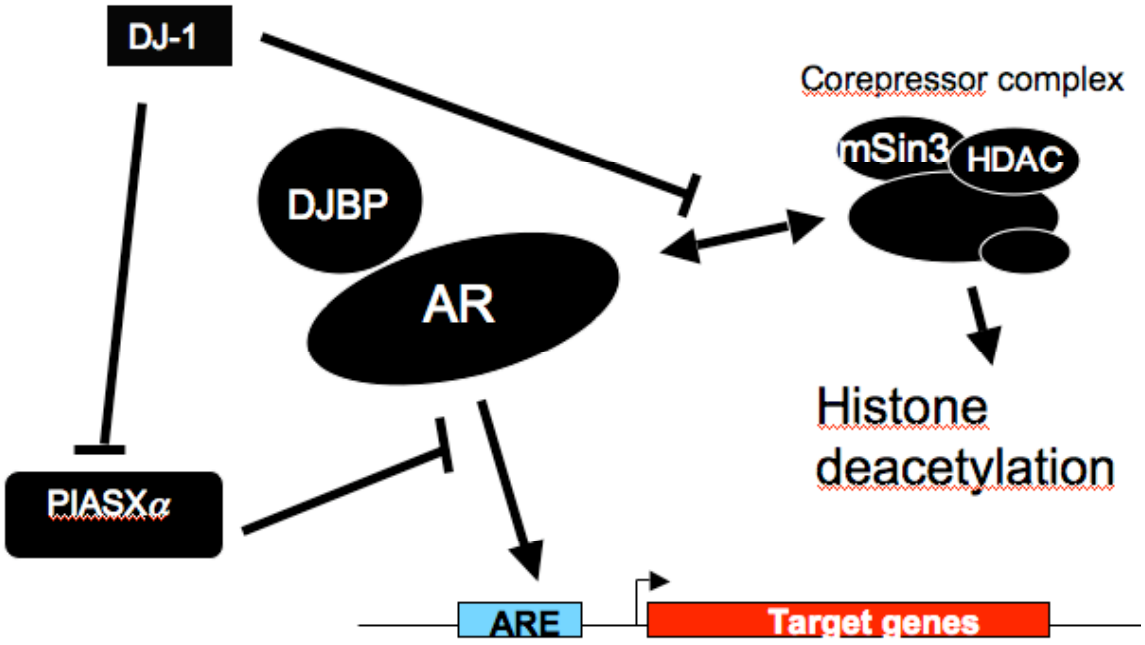

Figure 10: DJ-1 Indirectly Activates AR. DJ-1 binds and inhibits PIASx-alpha preventing it from binding AR. DJ-1 also binds DJ-1 Binding Protein (DJBP) and a multi-protein HDAC co-repressor complex resulting in AR activation. Figure modified from (98).

CHAPTER II

MATERIALS AND METHODS

Construction of Viral Constructs

The androgen responsive 5'-flanking region [(-244/-96)(-286/+28) bp] of the rat PB gene designated ARR_2PB was linked to the chloramphenicol acetyl transferase (CAT) reporter gene (120) and subcloned into the XhoI/BglII restriction sites of pAdBN (AdenoQuest Quantum Biotechnology, Montreal, Canada) to create pPB-CAT/Ad. Viral particles were generated in 293 cells according to the manufacturer's protocol and titrated in LNCaP cells. Only those clones which resulted in high levels of CAT gene expression in response to androgen treatment were selected and amplified for the HPE cell TIGR assay. The negative control plasmid contained a promoterless CAT gene (pCAT/Ad).

To generate DJ-1 shRNA, appropriate oligos were designed using the online tools at www.Genscript.com. Briefly, the full-length human DJ-1 cDNA sequence was inserted into the online system which generates several potential hairpin sequences using a proprietary algorithim. One of these sequences was chosen by comparing the generated sequences to published reports for known DJ-1 siRNA/shRNA sequences that had been effective. Once an oligo was chosen, a control shRNA sequenced was generated by scrambling the DJ-1 shRNA sequence to generate a non-targeting shRNA. (performed by Genscript online tools) The control sequence was checked for potential off-target effects by BLASTing the sequence against the human genome (performed through Genscript

website). The oligonucleotides contained overhangs complimentary to BamHI and XhoI sites to be used to clone the oligos into pRNATi/Lenti plasmid (Genescript). Oligos were ordered from www.IDT.com and PAGE purified. To anneal the oligos and generate double-stranded products, 1ug of each oligo was combined in a total volume of 20 ul IX SSC and heated at 95°C for 10 minutes and then incubated at room-temperature for one hour. The annealed oligos were then cloned into the pRNATi/Lenti plasmid (Genescript). Oligos for DJ-1 shRNA were: top strand – 5'-GATCCCGTCTCAGAGTAGGTGTAATGACTTGAT-3' and bottom strand – 5'-TCGAGTTGGAAAAAATCTCAGAGTAGGTGTAAT-3'. Scrambled (non-targeting) control shRNA oligos were: top strand – 5'-GATCCCGTACCAATACTACCATTCGAGTTTGAT-3' and bottom strand – 5'-TCGAGTTGGAAAAAAGTACCAATACTACCATTC-3'. Plasmids were transfected into 293FT cells (Invitrogen) to generate lentiviral particles according to manufacturer's protocols. Viral supernatant was used to infect LNCaP-TET-ON cells which were obtained from Dr. Renjie Jin in the Matusik laboratory at Vanderbilt. Infected cells were isolated by FACS sorting for GFP positive cells, and grown to confluency. DJ-1 was knocked down by treating cells with the indicated dose of doxycycline for 24 hours.

HPE Cell Culture

A total of 40, two to four millimeter (mm^3) specimens were obtained from radical retropubic prostatectomy, with 30 specimens composed of histologically normal, non-tumor tissue and 10 specimens composed of 5 to 95 % PCa (Gleason Score 3+3). Since one or two specimens were obtained per patient, the 40 specimens represent 28

individuals. Two to four mm^3 prostatic tissue fragments were just sufficient to generate HPE cells to perform the bioassay and isolate protein and RNA for a limited number of Westerns and RT-PCR reactions presented in this study. Primary HPE cells were isolated and cultured according to the method of Hayward and colleagues (121). Briefly, punch biopsies of prostate tissue were minced, tissue fragments were plated on Primaria plates (Falcon, Phoenix, AR) and HPE cells were cultured in epithelial cell selective medium (RPMI 1640 medium supplemented with 2.5 % charcoal stripped, heat-inactivated FBS, 20 mM HEPES buffer, 100 units/ml penicillin, 100 μg/ml streptomycin, 0.25 μg/ml amphotericin B, 50 μg/ml gentamycin, 56 μg/ml bovine pituitary extract, 1x insulin-transferrin-selenium, 10 ng/ml epidermal growth factor, and 50 ng/ml cholera toxin) and maintained in 5 % CO_2 at 37^o C. The medium was changed every 2 to 4 days and HPE cells from individual prostatectomy specimens were maintained and passaged for a maximum of 4 passages.

TIGR (transiently infected gene reporter) assay

The LNCaP and PC-3 human prostate cancer cell lines were purchased from the American Type Culture Collection (Rockville, MD) and served as controls in this study. Cells were plated in 24-well plates at a density of 10^5cells/well and upon reaching 80% confluence, were infected with 10^8 plaque forming units (pfu) adenoviral particles containing pCAT/Ad or pPB-CAT/Ad and treated with anti-androgen (flutamide, 10^{-5} M) or androgen (10^{-8} M R1881) with/without flutamide (10^{-5} M) in the presence of 2.5% charcoal-stripped fetal bovine serum. The concentration of 10^{-5} M flutamide was selected since it inhibited greater than 99.5% of androgen-induced activity in LNCaP cells

. Forty eight hours later, cells were harvested, lysed in passive lysis buffer (Promega, Madison, WI), protein concentrations were determined using the Bio-Rad Protein Assay and 20 μg protein per sample were used to determine CAT activity as described previously (122). At least three separate experiments (each treatment in triplicate) were carried out.

The length of time required to transfect primary HPE cells was determined by utilizing adenoviral particles containing pCMV-EGFP. HPE cells were faintly green 3 days post infection and EGFP expression increased up to 4 days when intensity stabilized and did not change thereafter (data not shown). Therefore, 4 days post infection was selected as the time point to harvest HPE cells and determine reporter gene activity. The TIGR assay was carried out as described above. Since prostatectomy material was rate limiting (only two to four mm^3), each of the 40 assays was performed one to two times and each treatment group was analyzed in quadruplicate.

Western Blot Analysis

HPE cell proteins were isolated according to TRI REAGENT™ protocol (Sigma, St. Louis, MO). Protein concentrations were determined by the Bradford Protein Assay (Bio-Rad). Thirty micrograms of total protein were separated on precast 4-12 % NuPAGE® Novex polyacrylamide gels (Invitrogen, Carlsbad, CA) and transferred onto Hybond™ ECL™ Nitrocellulose membranes (Amersham Pharmacia Biotech, Uppsala, Sweden). Only 50 ng LNCaP protein was loaded per lane, since LNCaP AR concentrations were higher (see Figure 4C, real-time RT-PCR data) and did not facilitate

the longer exposure time required to visualize the HPE AR. After blocking with 5 % Skim Milk (BD, Sparks, MD) membranes were incubated with a 1:1000 dilution of rabbit polyclonal anti-AR antibody (Santa Cruz Biotechnology, Santa Cruz, CA), washed and subjected to 1:10,000 dilution of horseradish peroxidase linked anti-rabbit IgG (Amersham Pharmacia Biotech, Uppsala, Sweden). Proteins were visualized by ECLplus Solution (Amersham Pharmacia Biotech, Uppsala, Sweden) and exposure to Hyperfilm™ ECL™ (Amersham Pharmacia Biotech, Uppsala, Sweden) for 1 to 2 minutes. For subsequent β-actin detection, the membrane was stripped [100 mM 2-mercaptoethanol, 2 % SDS, 62.5 mM Tris-HCl for 30 min at 70^{o}C], washed, blocked, and subjected to immunodetection as outlined above utilizing rabbit polyclonal anti-actin (1:200 dilution) as primary antibody (Santa Cruz Biotechnology, Santa Cruz, CA).

For DJ-1 analysis, 20 μg total protein was separated on precast Ready gel 4-20% polyacrylamide (BioRad) and transferred onto PVDF membrane (BioRad). Nonspecific binding and washes were performed as described above and membranes were incubated with 0.5 μg/μl of mouse anti-DJ-1 antibody (Stressgen Biotechnologies Corp., San Diego, CA) and simultaneously probed with 1:5,000 dilution of mouse anti-beta-actin antibody (Sigma), washed, and then incubated with 1:10,000 dilution of horseradish peroxidase linked anti-mouse IgG (Amersham Pharmacia Biotech, Uppsala, Sweden). Proteins were visualized as described above.

For Western analysis in Chapter IV the following antibodies were used: 1:1000 dilution of goat anti-DJ-1 antibody was used (Abcam, Cambridge, MA), 1:1000 dilution

of rabbit anti-AR (N-20) antibody (Santa Cruz Biotechnology, Santa Cruz, CA), 1:5000 dilution mouse anti-GAPDH (Imgenex, San Diego, CA), 1:1000 dilution mouse anti-Rho A (Santa Cruz Biotechnology, Santa Cruz, CA), 1:1000 dilution (in 2% BSA) of mouse anti-Histone H1 (Abcam, Cambridge, MA). Membranes were washed and subjected to 1:5000 dilution of horseradish peroxidase (HRP) linked anti-goat IgG (Santa Cruz Biotechnology, Santa Cruz, CA), 1:10,000 dilution of HRP-anti-rabbit IgG, or 1:10,000 HRP-anti-mouse IgG (Amersham Pharmacia Biotech, Uppsala, Sweden). Proteins were visualized as described above.

Reverse transcriptase-polymerase chain reaction (RT-PCR)

Total cellular RNA from primary HPE cultures, LNCaP, and DU-145 cell lines was extracted using TRI® Reagent (Sigma, St. Louis, MO) according to the manufacturer's instructions. Two μg total RNA for all cell lines was utilized to generate cDNA (RT-PCR Access System, Promega, Madison, WI) and the cDNA was subjected to PCR analysis with gene specific primers for AR, PSA, and 18S for 35 cycles as indicated below. The PCR products were analyzed by electrophoresis on 1.5% agarose gels.

Table 1: RT-PCR primer pairs. Forward primer is listed on top, followed by reverse primer. All primer pairs target human sequence unless otherwise specified.

Gene Name	Primers	Product Length (bp)	Annealing Temp. (^{O}C)
AR	5'-AGCCCCACTGAGGAGACAACC-3' 5'-ATCAGGGGCGAAGTAGAGCAT-3'	350	60
PSA	5'-CCTCACACCTAAGGACAAAGG-3' 5'-CATTGAACCAGAGGAGTTCTTG-3'	414	60
18S	5'-CAAGAACGAAAGTCGGAGGTTC-3' 5'-CTGTGATGCCCTTAGATGTCC-3'	488	60
DJ-1	(DJ1Cf) 5'-ATGGCTTCAAAAAGAGCTCTGG-3' (DJ1CR) human 5'-CTAGTCTTTAAGAACAAGTGGA-3' (mDJ1R) mouse 5'-CTAGTCTTTGAGAACAAGCGGT -3'	569	56
FKBP9	5'-GTACTTCTGATGGATATTTGG-3' 5'-GTTGTGGAAGTCGATCACAT-3'	670	50
P-cadherin	5'-GATGCCATCTACACCTACAAT-3' 5-CATGATAAGGTAGGTGGCAC-3'	380	50
PLOD-1	5'-TTCAAGCGCTCAGCTCAGTTC-3' 5—CTTGAGCACGACCTCATCCA-3'	530	54

Real-time RT-PCR analysis

AR concentrations in cultured HPE cells were determined by real-time RT-PCR, utilizing 2 μg HPE total RNA to generate cDNA which was subsequently used in PCR reactions with the primers described above [icycler iQ Real-Time PCR Detection System (Bio-Rad, Hercules, CA)]. LNCaP cells (2 μg total RNA) served as a positive control. The AR standard curve was generated using serial dilutions of the human $pSVAR_0$ expression vector. The human 18S gene was subcloned into pGEM-T easy (Promega, Madison, WI) and served as an internal standard. PCR amplification was performed using SYBR Green PCR Core Reagent (Applied Biosystems, Foster City, CA), followed by analysis of melting curves to validate the real-time RT-PCR data and agarose gel electrophoresis of an aliquot from each RT-PCR product to monitor purity of the specific

RT-PCR product. AR concentrations (in μM) were determined and standardized to the 18S product from the same sample.

DJ-1 expression in CD-1 and 12T-7f mice was determined using 2ug total pooled RNA that was used for generation of cDNA as described (123). cDNA was used for subsequent real-time RT-PCR using DJ-1 primers: for mouse DJ-1 amplification, DJ1CF primer + mDJ1-R primers were used, while human DJ-1 is amplified with DJ1CF and DJ1CR primers. DJ-1 expression was normalized to 18S rRNA as described above. The standard curve was generated using serial dilutions of full-length human DJ-1-TEasy plasmid.

AR mutational analysis

The HPE AR was screened for potential somatic mutations. PCR amplification of six targeted areas in which most of the prostate cancer somatic mutations co-localize [2 in the AR-NTD [aa 54-92; 253-282;] and 4 in the AR-HBD [aa 654-689; 688-721; 723-738; 867-917] was performed on genomic DNA. The following primer pairs were designed to encompass the targeted areas.

Table 2: Primers Used in AR Mutational Analysis Forward primer listed on top, followed by reverse primer. Exonic/Intronic location and amino acids are given.

Target Name	Primers	Primer Location	Amino Acid Range	Annealing Temp. (^{O}C)
AR-I	5' CTT TCC AGA ATC TGT TCC AGA G 3' 5' CCT CAT CCA GGA CCA GGT AGC C 3'	Exon Exon	Leu54 to Ser92	55
AR-II	5' GTG TGG AGG CGT TGG AGC AT 3' 5' GAA CCT TTG CAT TCG GCC AA 3'	Exon Exon	Leu253 to Pro282	48
AR-IV	5' ACC AGC CCC ACT GAG GAG ACA A 3' 5' TGC AAA GGA GTC GGG CTG GT 3'	Exon Exon	Thr654 to Asn689	62
AR-V4	5' AGG TGT AGT GTG TGC TGG AC 3' 5' CCA CTT CCC TTT TCC TTA CC 3'	Exon Intron	Asp688 to Pro721	53
AR-V5	5' TAC CCA GAC TGA CCA CTG CC 3' 5' AAA CAC CAT GAG CCC CAT CC 3'	Intron Exon	Phe723 to Ser738	61
AR-VI	5' GAG GCC ACC TCC TTG TCA ACC CTG 3' 5' GGG GTG GGG AAA TAG GGT TT 3'	Intron Intron	Ile867 to End917	53

The PCR products were sequenced utilizing an Applied Biosystems ABI Prism 377 DNA Sequencer at the Norris Cancer Center Genomics Core facility (UCS/Norris, LA) and the resulting data aligned to the AR sequence (124) using Sequence Navigator software.

Electron microscopy

HPE cells cultured in 6 well culture plates were fixed in 2% glutaraldehyde in PBS for 5 minutes at room temperature. Cells were scraped, pelleted and further fixed for 60 minutes at room temperature. The pellets were processed for electron microscopy by standard techniques and thin and semi-thin sections were cut and stained with uranyl acetate and lead citrate and photographed on a Joel X100 microscope.

Two-Dimensional gel electrophoresis and mass spectrometry

Samples were individually solubilized in lysis buffer (7M urea, 2M thiourea, 4% CHAPS, 30 mM Tris, 5 mM magnesium acetate) prior to labeling with 200 picomoles of either Cy2, Cy3 or Cy5 (Amersham Biosciences, Piscataway, NJ) for 30 min on ice in the dark. Reactions were quenched with 2 µl of 10 mM lysine for 10 min on ice in the dark, combined and added to an equal volume of 2x rehydration buffer (7M urea, 2M thiourea, 4% CHAPS, 4 mg/mL DTT) supplemented with 0.5% IPG (Immobilized pH gradient) buffer 4-7. Combined samples (Cy2/3/5) were co-resolved by standard 2D gel electrophoresis using an IPGphor first-dimension isoelectric focusing unit and 24 cm 4-7 immobilized pH gradient (IPG) strips (Amersham Biosciences, Piscataway, NJ), followed by second-dimension 12% SDS-PAGE using an Ettan DALT 12 unit (Amersham Biosciences, Piscataway, NJ). The samples were reduced and alkylated with 1% DTT and 2.5% iodoacetamide in equilibration buffer (6M Urea, 30% glycerol, 2% SDS, 50mM Tris pH 8.8) between the first- and second-dimensional separations. Second-dimension SDS PAGE gels were hand-cast using low-fluorescence glass plates, with one glass plate pre-silanized (bind-silane, Amersham Biosciences, Piscataway, NJ) to affix the polymerized gel to only one of the glass plates.

CyDye-specific images were acquired using mutually-exclusive excitation/emission wavelengths using 2D 2920 Master Imager (Amersham Biosciences, Piscataway, NJ). Individual protein spot-features were co-detected and analyzed using DeCyder Differential In-gel Analysis software (Amersham Biosciences, Piscataway, NJ), where individual spot volume ratios were calculated for each protein-pairs. Two standard

deviations of the mean, calculated from a modeled normal distribution of all spot volume ratios, was used to identify those protein spot features that exhibited significant abundance changes within the 95th percent confidence level.

The 2D gels were subsequently stained with Sypro Ruby (Molecular Probes, Eugene, OR) according to the manufacturer's instructions, to allow for accurate robotic protein excision. Proteins of interest were robotically excised and processed for digestion in-gel with trypsin protease (Promega) using Ettan Spot Picker and Digester workstations (Amersham Biosciences, Piscataway, NJ) Peptides were reconstituted in 10 µl of 0.1% triflouroacetic acid, and manually de-salted/concentrated into 2 µl of 60% acetonitrile, 0.1% triflouroacetµic acid using C18 ziptip pipette tips (Millipore, Billerica, MA). The peptide eluate (0.5 µl) was applied to a sample target and overlaid with 0.5 µl of α-cyano 4-hydroxycinnamic acid matrix (10 mg/ml in 60% acetonitrile, 0.1% triflouroacetic acid). Matrix-assisted laser desorption/ionization, time-of-flight (MALDI-TOF) mass spectrometry was performed on a Voyager 4700 (Applied Biosystems, Foster City, CA). Peptide mass maps were acquired in reflectron mode averaging 2000 laser shots per spectrum, and internally calibrated to within 20 ppm mass accuracy using trypsin autolytic peptides (*m/z* = 842.51, 1045.56 and 2211.10). Ions specific for each sample (discrete from background and trypsin-derived ions) were used to interrogate human sequences entered in the SWISS-PROT and NCBInr databases using the MASCOT (www.matrixscience.com) and ProFound (prowl.rockefeller.edu) database search algorithms, respectively. Protein identifications from MALDI-TOF peptide mass maps are based on the masses of the tryptic peptides (125-127). Searches were performed

without constraining protein molecular weight or isoelectric point, and allowed for carbamidomethylation of cysteine, partial oxidation of methionine residues, and one missed trypsin cleavage.

Northern Blot Analysis

LNCaP cells were cultured in normal growth media (RPMI 1640, 10% FBS, 1X penicillin/streptomycin, 0.25% glucose, 1mM Na Pyruvate) until 70% confluent when media was changed for growth media containing 10% charcoal-stripped FBS for overnight. The next day, cells were treated with 10^{-8}M DHT, 10^{-5}M OH-Flutamide, 10^{-5}M Casodex, or ethanol (vehicle control) for the following times: 15 minutes, 30 minutes, 45 minutes, 1, 2, 4, 8, 12, 16, or 24 hours. Cells were harvested in 1 ml Trizol (Invitrogen) and RNA was extracted following manufacturer's instructions. 20 micrograms of total RNA was loaded per lane on a 1% formaldehyde-agarose gel and transferred overnight in 6X SSC by upward capillary transfer to positively charged nylon membrane. For probe synthesis, full length human DJ-1 cDNA was cloned into pGEM-Teasy (Promega). The plasmid was linearized with Sac II (NEB) and single stranded antisense RNA probes for DJ-1 were transcribed *in vitro* using Megascript SP6 RNA Polymerase transcription kit (Ambion). To label the probe, the reaction was supplemented with 3000 Ci/mmol alpha-P^{32}-UTP (Amersham Biosciences). The membrane was hybridized overnight with 10^6 counts in buffer containing (0.2M $NaPO_4$, 7% SDS, 100 μg/ml sheared herring sperm DNA, and 2X Denhardt's solution (Sigma)) at 65 degrees. The membrane was washed in 2X SSC, 1X SSC, and 0.5X SSC containing 0.1%SDS and then exposed overnight to a phosphor imager.

Cyclohexamide Assay

LNCaP cells were cultured to 70-80% confluency in normal growth media as described above when media was changed to media containing 10% charcoal stripped FBS for overnight after which cells were pretreated with one of the following: 10^{-8}M DHT, 10^{-5}M OH-Flutamide, or an equal volume of 100% ethanol (vehicle control) 30 minutes before the addition of 75 μg/ml cycloheximide for the following times: 24 hours, 48 hours, and 72 hours. Cells were harvested in 300 μl of lysis buffer (25mM HEPES [pH 7.5], 5 mM $MgCl_2$, 300 mM NaCl, 1 mM EDTA, 0.2 mM EGTA, 1mM DTT, 10% glycerol, 1% TritonX 100, 0.1% Na-deoxycholate, 0.1% SDS, 20 mM p-nitrophenylphosphate, 20 mM β-glycerolphosphate, 2 mM Na-pyrophosphate, 1 mM PMSF, 10 μg/ml Aprotinin, and 10 μg/ml Leupeptin), briefly sonicated, and clarified by centrifugation. Twenty μg total protein was separated on a denaturing 12% acrylamide gel, transferred to PVDF membrane and DJ-1 and GAPDH were visualized as described above.

Yeast Two-Hybrid Assay

Yeast Two-Hybrid Assay was performed using the Matchmaker System (Clontech, Mountain View, CA) following manufacturer's protocols. A cDNA library was generated from primary Human Prostate Epithelial cells that exhibited AR activation via TIGR assay (128) were harvested, total RNA was extracted (Trizol, Invitrogen, Carlsbad, CA) and used for reverse-transcriptase PCR using Oligo dT primers. cDNAs were cloned into the pGADT7 plasmid (Clontech, Mountain View, CA) where they were expressed as fusion proteins to the GAL4 Activation Domain. For the bait protein, full-

length human DJ-1 cDNA was cloned into the pGBKT7 plasmid and expressed as a fusion to GAL4 DNA Binding Domain. Plasmids were transformed into AH109 yeast strain and positive clones were selected on high stringency dropout plates (-Leu/-Trp/-His/-Ade) containing X-alpha-Galactose. Plasmid DNA was extracted, transformed into DH5-alpha competent *E. Coli,* and sequenced using T7 promoter.

Cell Culture and Transfection of LNCaP and LAPC4 Cell Lines

The LNCaP human prostate carcinoma cell line was obtained from American Type Culture Collection (Manassas, VA). LNCaP cells were cultured as described (128). The LAPC4 human prostate carcinoma cell line was a gift from Dr. Charles Sawyers (Memorial Sloan-Kettering Cancer Center, New York). LAPC4 cells were cultured in IMDM media (Gibco, Carlsbad, CA) containing 10% FBS, 2 mM L-Glutamine, with 1X Penicillin/Streptomycin.

Immunoprecipitation

Cells were lysed in 300 μl cold lysis buffer (1% Triton X-100, 150 mM NaCl, 10 mM $NaHPO_4$ pH 7.2, 5 mM NaF, 2 mM EDTA, 1X HALT Protease Inhibitor cocktail (Pierce Biotechnology. Rockford, IL)) in the cold room and allowed to rock for 15-20 minutes. Lysates were cleared by centrifugation and 400-500 micrograms of total protein was immunoprecipitated overnight at 4°C using 10μg rabbit anti-AR antibody or 5μg mouse anti-HA antibody (Santa Cruz Biotechnology, Santa Cruz, CA). Complexes were pulled down using ImmunoPure™ Immobilized Protein G beads (Pierce Biotechnology,

Rockford, IL) Immunoprecipitates were washed 4 times in 1X PBS, re-suspended in 1X Lammeli buffer and subjected Western analysis.

Luciferase Assays

LAPC4 cells were plated in 24-well plates (Falcon, Phoenix, AZ) and allowed to attach overnight. Cells were transfected with androgen-responsive luciferase reporter, ARR_2PB-luciferase. Firefly luciferase is driven by the androgen-responsive region of the rat probasin promoter similar to the ARR_2PB-CAT reporter (128, 129). Media was changed to IMDM containing 10% charcoal-stripped FBS, 2 mM L-Glutamine, 1X Penicilin/Streptomycin, and supplemented with 10^{-9}M DHT. 48 hours post-transfection, cells were lysed in 1X Passive Lysis Buffer (Promega, Madison, WI) and frozen at -80°C until subsequent luciferase assay. Lysate was cleared by centrifugation and protein concentration was determined as described above. 20μl of lysate was loaded into 96-well plates (Corning, Corning, NY) and luciferase activity was determined using the Luciferase Assay System (Promega, Madison, WI) and a LUMIstar luminometer (BMG Lab. Technologies, Inc. Durham, NC). Firefly luciferase activity was normalized to protein concentration and expressed as fold change over non-transfected controls. Each bar represents the mean of at least three replicates +/- SEM and each experiment was repeated at least twice.

Nuclear and Cytoplasmic Extracts

Cells were plated in 6-well plates (Falcon, Phoenix, AZ) and allowed to attach overnight. On the second day, cells were washed in Hank's buffer and changed to media containing 10% charcoal-stripped FBS. On the third day, media was again replaced for fresh media containing 10% charcoal-stripped FBS and the following treatments: ethanol (vehicle control), 10^{-8}M DHT (LNCaP), 10^{-9}M DHT (LAPC4), 10^{-5}M OH-flutamide (LNCaP), 10^{-6}M OH-flutamide (LAPC4), 10^{-5}M bicalutamide (LNCaP), or 10^{-6}M bicalutamide (LAPC4). Optimal concentrations of androgens and anti-androgens for LNCaP cells were experimentally determined previously (128) while concentrations for LAPC4 cells were communicated from Dr. Sawyers' lab. 24 hours after treatment, cells were harvested by trypsinization, washed in PBS, and lysed for cytoplasmic and nuclear fractions using the NEPER Kit and HALT Protease Inhibitors according to manufacturer's protocol.

Immunofluorescence and Confocal Microscopy

Prostate specimen fragments were formalin-fixed and paraffin-blocked. Tissue sections (5 microns) were deparaffinized and antigen retrieval was performed by immersing the slides in citric buffer (pH 6.0), microwaving for 10 min and allowing the slides to cool to room temperature in the buffer. The slides were washed twice in distilled water prior to immunohistochemical analysis. For cultured HPE cells, the cells were harvested by trypsinization and allowed to attach to glass slides (VWR) overnight at 37°C. Slides were fixed in 4% paraformaldehyde/phosphate buffed saline (PBS) for 15 min, washed three times in PBS, permeabilized on ice in PBS + 0.1% Triton X-100 for

5 min and blocked in PBS with 3% BSA and 3% donkey serum for 30 min at room temperature. Slides were incubated with rabbit polyclonal antibody against human p63 (Santa Cruz), mouse monoclonal antibody against human CK8 or CK18 (Sigma), rabbit polyclonal antibody against human AR, goat polyclonal antibody against human PSA (Santa Cruz), monoclonal mouse anti-human Adipophilin or CD59 for 1 h at room temperature, and subsequently incubated with Alexa Fluor 594 and/or Alexa Fluor 488-conjugated donkey anti-rabbit, mouse or goat secondary antibody (Molecular Probes) for 1 h at room temperature. The slides were washed in PBS and mounted using Vectashield mounting medium containing 4,6-diamidino-2-phenylindole (DAPI) to counter-stain nuclei (Vector Laboratories). Images were captured with a Zeiss fluorescence microscope equipped with a digital camera. To demonstrate specificity of staining, either the primary antisera or secondary antibodies were omitted from control slides.

LNCaP and LAPC4 cells were harvested by trypsinization and allowed to attach to glass chamber slides (Lab-Tek Products Naperville, IL) overnight at 37°C. Cells were treated as described in nuclear/cytoplasmic extract section. 24 hours after treatment, slides were fixed, permeabilized, and blocked as described above. Slides were incubated with 1:1000 dilution anti-DJ-1, 1:500 dilution (for LNCaP) or 1:100 dilution (for LAPC4) anti-AR, and 1:2500 dilution of mouse anti-SC-35 (Sigma, St. Louis, MO) antibody overnight at 4°C, and subsequently incubated with Alexa Fluor 594-conjugated donkey anti-rabbit, Alexa Fluor 488-conjugated donkey anti-goat, and Alexa Fluor 654-conjugated donkey anti-mouse secondary antibody (Molecular Probes, Eugene, OR) for 1 h at room temperature. The slides were washed in PBS and mounted in 50% glycerol

and imaged with a Zeiss LSM510 Meta Laser Scanning microscope. Stacks were acquired with LSM510 software, Z-projections and merged images were made with NIH ImageJ. All confocal images were acquired with a Plan-Apochromat 63x/1.4 oil DIC objective at the following settings: wavelength 488nm 5%, 543 nm 37%, 633 nm 10%; filters: Ch2-1: BP5050-550, Ch3-2:BP 560-615; and ChS1-3: 649-756 with a pinhole of 281 micrometers. Images have identical microscope settings between treatment groups. Image brightness/contrast was not altered between treatment groups so intensity comparisons could be made. Quantification and images of co-localization were obtained using Metamorph^{TM} software.

Human Tissue Arrays and Immunohistochemistry

Tissue microarrays (TMA) were generated using H&E slides from 112 radical prostatectomy specimens (from 1989 to 2003) obtained from the Vancouver General Hospital. Benign and cancer sites were identified and marked in donor paraffin blocks using matching H&E reference slides. TMA was constructed using a manual tissue micro-arrayer (Beecher Instruments, Silver Springs, MD). Each marked block for benign and cancer was sampled 4 times with a core diameter of 0.6 mm arrayed in rectangular pattern with 1 mm between the centers of each core creating a quadruplicate TMA layout and ordered by histopathology and tumor Gleason grade. The Gleason TMA contains 336 tissue cores representing 84 patients. The second TMA represents patients who received either no androgen deprivation therapy (ADT), less than 3 months ADT, 3-6 months ADT, or more than 6 months ADT. These patients received with mono- or combination therapy with the LHRH antagonists Lupron or Zoladex, and the anti-

androgens flutamide or cyproterone acetate. The second TMA was generated in a similar manner and tissue cores were arranged based upon treatment group. The ADT TMA contains 294 cores representing 98 patients. DJ-1 immunohostochemistry was performed using 1:1000 dilution of goat anti-DJ-1 antibody (Abcam, Cambridge, MA) and visualized using DAB and standard techniques.

Hormones

DHT is commercially available and was purchased from Sigma. OH-flutamide was purchased from LKT Laboratories, Inc. (St. Paul, MN). bicalutamide was provided by Astrazeneca, Inc. (Alderley Park, Macclesfield, Cheshire, SK10 4TG, UK).

Plasmids and siRNA

DJ-1 was cloned into pCruz-HA plasmid (Santa Cruz Biotechnology, Santa Cruz, CA) and transiently transfected into LAPC4 cells using Lipofectamine 2000 and following manufacturer's protocol (Invitrogen, Carlsbad, CA). Cells expressing N-terminal HA-tagged DJ-1 were selected using 400 μg/ml G418. Western Blot confirmed expression of tagged DJ-1. To knockdown DJ-1 expression, pooled siGENOME SMARTpool siRNAs (Dharmacon catalog #M-005984-00 Lafayette, CO) directed against DJ-1 were transfected (200 picomoles/well of 6 well plate) into LAPC4 cells using Lipofectamie 2000. Cells were harvested 48 hours post-transfection for Western Blot or luciferase assay. To ensure specificity of the chosen siRNA pool, a pool of nonspecific siRNAs (200 picomoles/well of 6 well plate) was used as a control (Dharmacon Non-targeting siRNA #1 catalog # D-001210-01).

Statistical Analysis

For the cell lines, statistical analyses were performed on at least three separate experiments (in triplicate or quadruplicate) and represent the mean +/- SD. For HPE CAT assays, measurements were carried out in quadruplicate and represent the mean +/- SD. These assays were performed up to two times per specimen depending on the size of the prostatectomy specimen acquired from Surgical Pathology.

For luciferase assays and real-time RT-PCR, bars represent mean values +/- SEM. P-values were determined using Student's t-test and each experiment was repeated at least twice.

CHAPTER III

ANDROGEN AND ANTI-ANDROGEN TREATMENT MODULATES AR ACTIVITY AND DJ-1 STABILITY

Introduction

Currently, there are no markers that identify patients who may exhibit adverse responses to ADT. The agonistic effects of anti-androgens have been extensively studied in prostate cancer cell lines such as LNCaP and DU-145 as well as in cell lines derived from African green monkey kidney such as COS-1, COS-7 and CV-1. However, these cell lines are far removed from the patient and do not represent the early changes that occur while the disease is primarily organ confined. The TIGR (Transiently Infected Gene Reporter) assay was specifically developed to analyze the effects of androgen and anti-androgen treatment on the endogenous AR by culturing primary HPE cells directly from patient biopsy specimens.

Primary HPE cells were grown out of biopsy specimens from radical retropubic prostatectomy samples as described (121, 128). Once luminal epithelial cells were isolated, they were infected with an androgen-responsive reporter gene. The androgen-responsive 5'-flanking region [(-244/-96)(-286/+28) bp] of the rat Probasin (PB) gene designated ARR_2PB was linked to the chloramphenicol acetyl transferase (CAT) reporter gene (120) and subcloned into the pAdBN plasmid (AdenoQuest Quantum Biotechnology, Montreal, Canada) to create pPB-CAT/Ad. After HPE cells were infected with this plasmid, endogenous AR activity was determined following androgen and anti-androgen treatment.

We determined that treatment with the anti-androgen flutamide increased CAT reporter gene activity in 2/10 (20%) of tumor and 12/30 (40%) of non-tumor HPE cell cultures derived from radical prostatectomy specimens. This agonistic activity occurred in the absence of any apparent AR mutations. Interestingly, flutamide treatment appeared to increase DJ-1 levels through protein stabilization in a similar manner to that for AR (130). DJ-1 functions as an indirect positive modulator of AR activity by allowing AR to become transcriptionally active (98). The stabilization of AR and DJ-1 may provide HPE cells with a transcriptional advantage that permits them to progress further along the pathway of prostate carcinogenesis during ADT.

Results

HPE Cells are Morphologically and Phenotypically Epithelial

Histologically, benign human prostatic glands are composed of a layer of differentiated secretory luminal cells and a small subpopulation of neuroendocrine cells surrounded by a layer of basal epithelial cells (3, 4). Human biopsy fragments from 30 non-tumor and 10 PCa (Gleason Score 3+3) prostatectomy specimens were placed into cell culture under conditions favoring epithelial cell growth as described above. HPE cells were passaged for further analysis while the remaining tissue fragments were harvested after two weeks for immunohistochemical analysis. A representative immunohistological analysis of benign prostate glands in radical prostatectomy specimens before and after culture is shown in Figure 1. Before culture, hematoxylin and eosin (H&E) analysis

clearly indicated that the basal cell layer was circumferentially intact, surrounding a stratified or pseudostratified layer of secretory luminal epithelial cells (Figure 11A). This histology was confirmed by double immunofluorescence staining with p63 (a basal epithelial cell marker) and cytokeratins 8 and 18 (luminal epithelial cell markers, Figure 11 B). Both luminal and stromal cells expressed AR, with luminal cells also expressing PSA (Figure 11C). In contrast, basal cell hyperplasia was evident after 2 weeks in culture (Figure 11D) and this was again confirmed by double immunofluorescence staining with p63, CK8 and CK18 (Figure 11E). AR expression was observed in both stromal and epithelial cells and often appeared more strongly expressed in hyperplastic basal epithelial compared to luminal epithelial cells. Low PSA expression was evident in luminal epithelial cells (Figure 11 F).

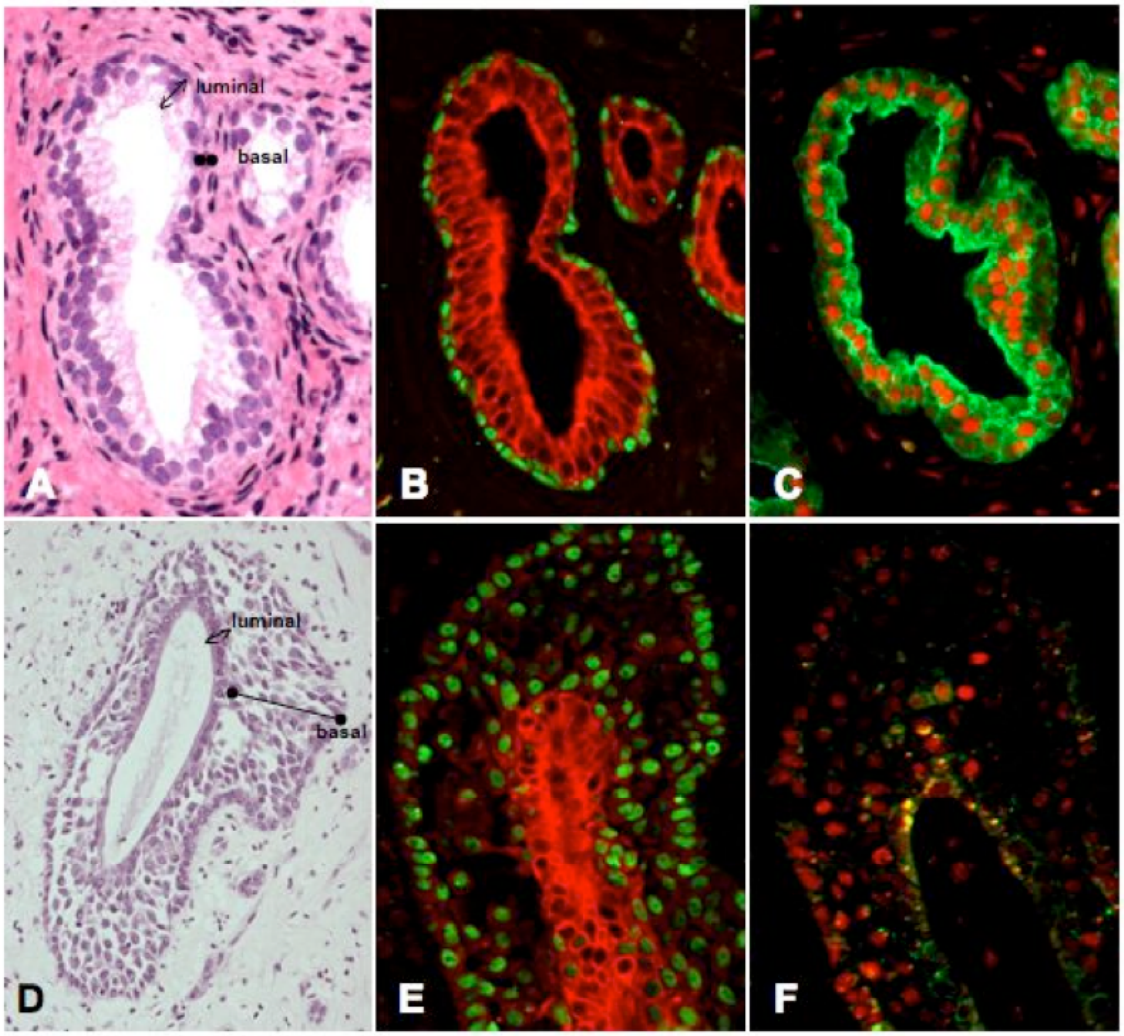

Figure 11: Immunohistochemical analysis of benign prostate glands in radical prostatectomy specimens before and after 2 weeks in culture. *A to C represent the tissue fragments before culture and D to F represent the tissue fragments after culture.* (**A) and (D).** Hematoxylin and Eosin stain; basal epithelial cell layer (●—●); luminal epithelial cell layer (↔). **(B) and (E).** Basal epithelial cell marker p63 (green); Luminal epithelial cell markers CK8 or CK18 (red). **(C) and (F).** Tissue sections were stained using rabbit polyclonal antibody against human AR or goat polyclonal antibody against human PSA. AR (red); PSA (green).

Cultured HPE cells were double-stained with immunofluorescence antibodies to CK8/CK18 and p63 to determine which cell type was predominant in the bioassay. Initially, 100% of the cells were p63 positive, indicating that they were basal epithelial

cells (data not shown). With passage number, the number of CK8/CK18 positive cells increased and the number of p63 positive cells decreased, suggesting that they had undergone differentiation. Recently, Dalrymple *et al* reported that the level of calcium in tissue culture media affects the population of cells that grow out of cultured tissue fragments (131). They report that high calcium containing medium selects against p63 positive basal cells allowing luminal epithelial cells to predominate. We commonly see basal cell proliferation in tissue fragments and as the first cells to grow out of the tissue *in vitro*, however determining whether the loss of p63 positive cells with passage number was due to differentiation or selection was beyond the scope of this project.

The TIGR assays were performed at passage 3 (unless otherwise stated) since this number of passages was required to generate sufficient cells for the TIGR assay. Six separate areas per slide were analyzed and the number of CK8/CK18- and p63-expressing cells tabulated (Figure 12A-C). Surprisingly, nearly 100% of HPE cells expressed CK8/CK18 and 56% of HPE cells co-expressed p63, suggesting that by passage 3, basal epithelial cells had differentiated into cells with more luminal epithelial cell characteristics (Figure 12C). Further analysis indicated that all HPE cells expressed AR and that this expression was primarily nuclear (Figure 12D) whether DHT or the synthetic androgen R1881 were present or absent in the cell culture medium.

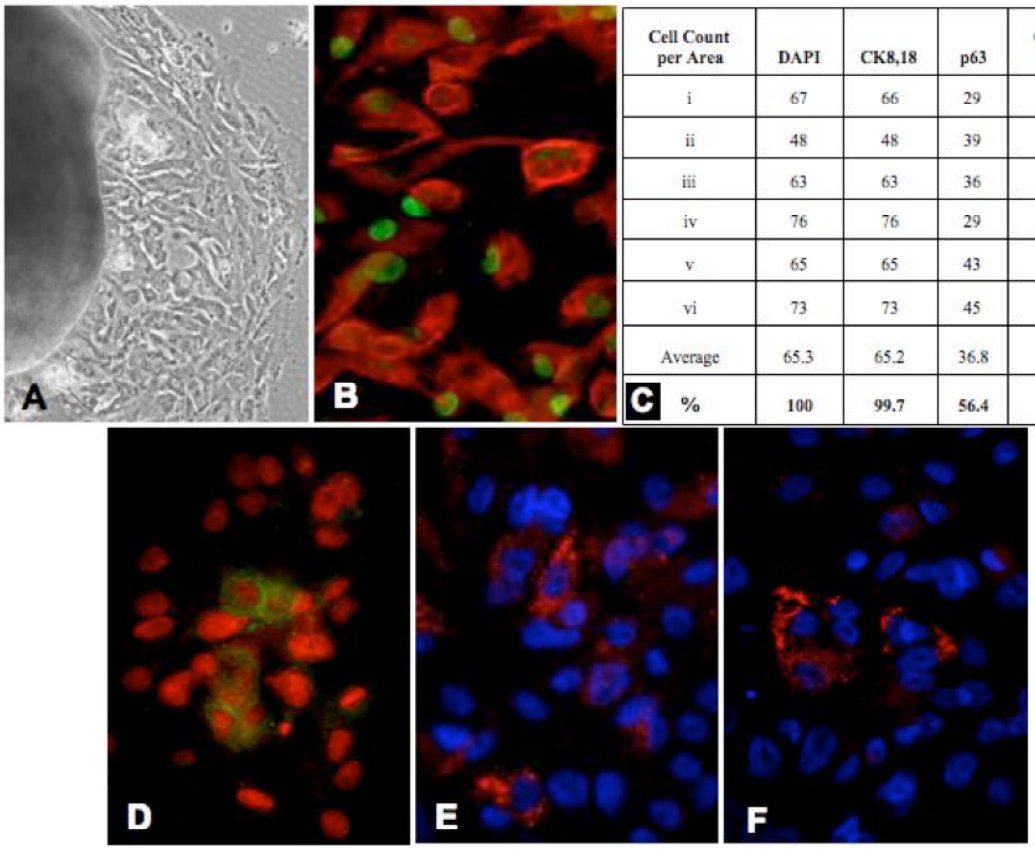

Cell Count per Area	DAPI	CK8,18	p63	CK8,18 +p63
i	67	66	29	29
ii	48	48	39	39
iii	63	63	36	36
iv	76	76	29	29
v	65	65	43	43
vi	73	73	45	45
Average	65.3	65.2	36.8	36.8
%	100	99.7	56.4	56.3

Figure 12: Immunohistochemical analysis of cultured HPE cells. HPE Cells were allowed to attach to glass slides and were stained using rabbit polyclonal antibody against human p63, mouse monoclonal antibody against human CK8 or CK18, rabbit polyclonal antibody against human AR, goat polyclonal antibody against human PSA, and monoclonal mouse anti-human adipophilin or CD59. **(A)** Cultured HPE cells derived from prostatectomy fragments in organ culture. **(B)** Expression of p63 (green) or CK8/CK18 (red) at passage 3. **(C)** The table summarizes a representative experiment (HPE 10072, passage 3). Six separate areas (i through vi) per section were analyzed for the number of p63 and CK8/CK18 positive cells. The DAPI stain represented the number of nuclei and therefore, the number of cells per area. Therefore, it was set at 100%. **(D)** Expression of AR (red) and PSA (green) at passage 3. **(E)** Adipophilin (red) expression in primary cultured HPE cells at passage 3. Nuclei were counterstained with 4,6-diamidino-2-phenylindole (DAPI) (blue). **(F)** CD59 expression (red) in primary cultured cells at passage 3. Nuclei were counterstained with DAPI (blue).

In short-term culture, HPE cells maintained a secretory phenotype. Immunofluorescence analysis indicated that within a subpopulation of HPE cells, PSA staining appeared typically granular within the cytoplasm (Figure 12D). This pattern of expression was similar to that seen in other culture systems (132). Adipophilin, a protein component of lipid storage droplets, is associated with cellular differentiation and secretion (133, 134). Immunoreactivity to adipophilin was localized in vacuolar, intracellular compartments of HPE cells, consistent with lipid droplets (Figure 12E). Prostasomes are stored in membrane-bound storage vesicles in prostatic acinar epithelial cells and secreted through exocytosis or diacytosis into the glandular lumen (132). HPE CD59 immunolocalization determined extracellular, granular and intracellular granular staining as seen in prostasomes (Figure 12F). Thus HPE cells in short term culture were primarily prostatic epithelial cells which synthesized AR and limited PSA and maintained a secretory phenotype as seen by prostasome and adipophilin production.

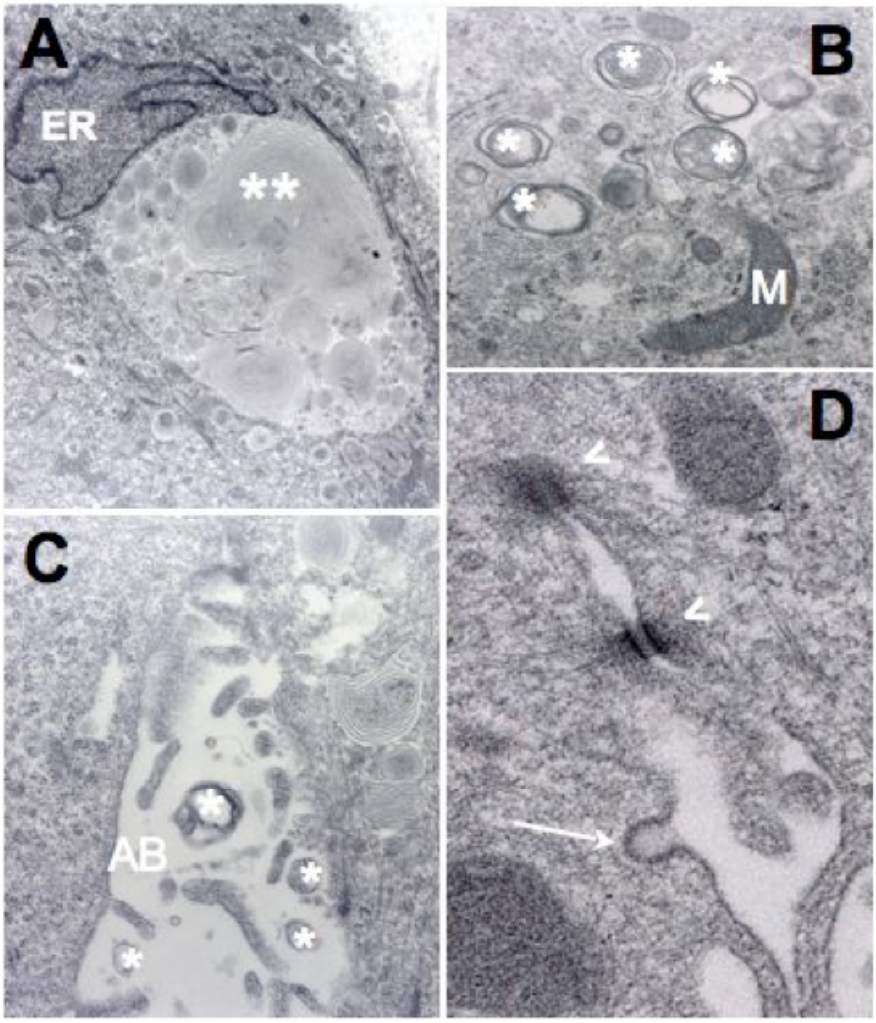

Figure 13: Ultrastructural analyses of HPE cells. HPE cells were analyzed by electron microscopy. (A) Large secretory body (**) filled with multiple tightly packed concentric membrane lamellae. **(B)** Smaller secretory bodies (*) containing loosely organized membranes. **(C)** Numerous secretory granules (*) released at the apical brush borders between 2 adjacent HPE cells. **(D)** Desmosomes containing attachment plaques with tonofilaments radiating from these plagues (<) and brush border vesicle (→).

Electron microscopy (EM) analysis of HPE cells further demonstrated their epithelial cell characteristics. HPE cells contained numerous larger and smaller secretory bodies filled with multiple tightly packed concentric membrane sheets or lamellae (Figure 13A). Smaller secretory bodies contained loosely organized membranes, suggesting that

these represented an early stage in lamellar body formation (Figure 13B). Of particular interest was that HPE cells did not lose their brush borders which are essential for the processes of exo- and endocytosis. Secretions appeared to be released at the apical brush borders as seen by the numerous secretory granules between two adjacent cells (Figure 13C). Brush border vesicles were also observed (Figure 13D). Neighboring epithelial cells are characteristically connected through desmosomes which form focal points of cell-cell contact to provide resilience and tensile strength to the epithelial monolayer. Desmosomes, containing characteristic attachment plaques with tonofilaments radiating from these plagues, formed between adjacent HPE cells (Figure 13D).

HPE Cells Express Endogenous AR

To analyze the responsiveness of HPE cells to androgen and anti-androgen treatment, it was essential that HPE cells express AR. Immunohistochemical analysis indicated that HPE cells expressed AR and this was confirmed by Western blot analysis (Figure 14A), RT-PCR (Figure 14B), and real-time (RT)-PCR (Figure 14C). Since AR protein levels in LNCaP cells were greater compared to those in HPE cells, only 50 ng LNCaP protein was run as a positive control. DU-145 cells provided a negative AR control. Two μg total RNA for HPE and LNCaP cells were analyzed by real-time RT-PCR analysis. As predicted, AR levels were greatest in LNCaP cells at $1.5x10^{-20}$ μM (Figure 14C). In comparison, AR mRNA levels in HPE cell cultures (from 7 different representative individuals) ranged from $8.3x10^{-22}$ μM to $1.44x10^{-22}$ μM. All HPE cells cultured to date have expressed AR, although HPE AR levels were 18 to 104-fold lower than those measured in LNCaP cells. Variability of AR expression is a common

occurrence in cultured primary HPE cells as well as commercially available, immortalized, prostate cancer cell lines (131, 132, 135). Importantly however, most prostate adenocarcinomas express AR both in the androgen-responsive and the androgen-independent stages of the disease; thus, the study of AR in all stages of prostate cancer progression is important (48, 62, 64-66, 88). Since all HPE cell cultures express endogenous AR, they can be utilized in TIGR assays to characterize the responsiveness of primary HPE cells cultured from prostatectomy specimens to androgen and anti-androgen treatment.

PSA expression is variable in primary cultured prostate epithelial cells (132). This was confirmed in our HPE cell cultures where PSA expression was observed in one of seven representative HPE cell cultures derived from tumor specimens (Figure 14B). The status of AR affects PSA expression, so it is expected for AR negative cells to lose PSA. The reason for PSA and AR expression variability remains largely unclear, although culture conditions likely play a role. In order to efficiently grow HPE cells out of tissue fragments, androgens must be omitted from the media. Inclusion of androgens prevents cell outgrowth from the tissue fragment greatly limiting cell number. Another important consideration that partially explains AR variability in the 1980's literature to that of today, is improved sensitivity of techniques used. Initially, detection of AR protein was difficult due to lack of antibodies. Further, detection of extremely low mRNA species was not possible before the advent of RT-PCR. Another aspect of cell culture which likely affects expression of differentiation markers is the change in morphology, from a tall columnar phenotype adapted to secrete markers into a lumen to a squamous

phenotype adapted to cover a tissue culture plate which a cell likely perceives as a wound (136). These points highlight the importance of culture conditions and specific starting material for establishing primary cell cultures or maintaining existing lines.

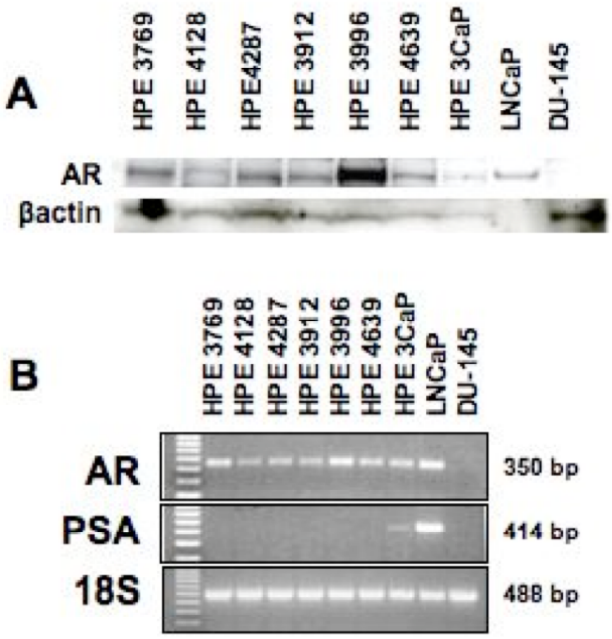

C

sample	[AR] µM
HPE 3769	1.93×10^{-22}
HPE 4128	1.44×10^{-22}
HPE 4287	3.07×10^{-22}
HPE 3912	1.78×10^{-22}
HPE 3996	8.30×10^{-22}
HPE 4639	3.10×10^{-22}
HPE 3CaP	3.30×10^{-22}
LNCaP	1.51×10^{-20}

Figure 14: Primary HPE cells express AR. HPE primary cultures from 7 representative patients were analyzed for AR expression. (A) Western blot analyses for AR. DU-145 prostate cancer cells served as a negative control. Thirty micrograms of HPE or DU145 protein was loaded per lane. Please note that due to the greater AR concentration in LNCaP compared to HPE cells, only 50 ng/lane LNCaP protein was loaded as a positive control for the purpose of identifying the band corresponding to AR. **(B)** RT-PCR for AR and PSA for the same HPE samples as in 4A. DU-145 cells served as negative controls for AR and PSA expression. Two µg total RNA were analyzed in each RT-PCR reaction. **(C)** Real-time RT-PCR analyses of AR levels in HPE cells. LNCaP served as a positive control.

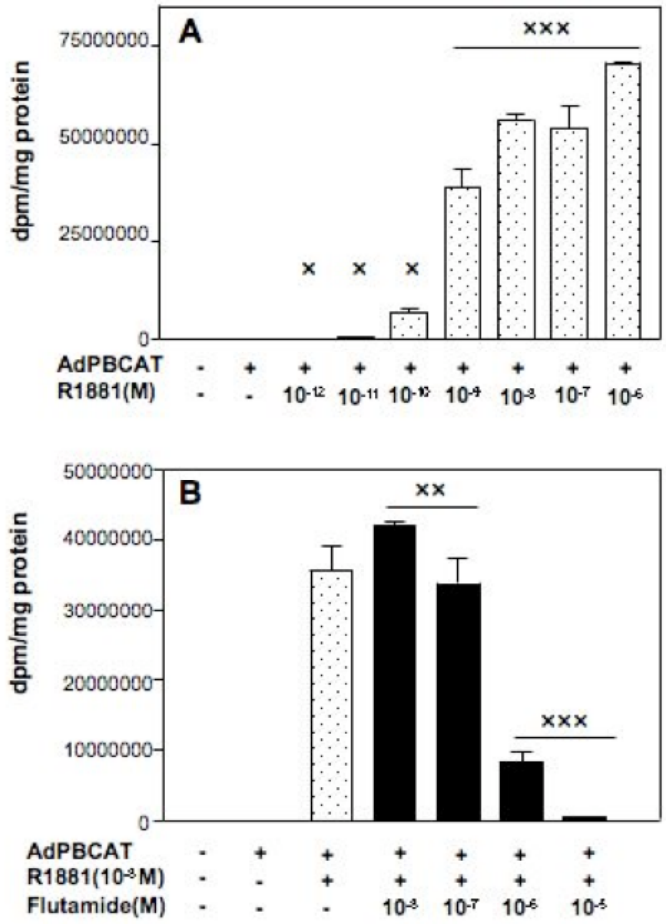

Figure 15: Androgen and anti-androgen activity in LNCaP cells. LNCaP cells were infected with 10^8 pfu ARR_2PB-CAT/AdBN viral particles. (**A)** Cells were treated with increasing concentrations of R1881 (10^{-12} to 10^{-6}M) to determine the effect of androgen treatment on CAT gene expression. Error bars +/- SD. To generate p values, pPB-CAT/Ad and R1881 treatments were compared to pPB-CAT/Ad alone. ×, $p>0.05$; ××, $p<0.05$; ×××, $p<0.001$. **(B)** LNCaP cells were treated with10^{-8} M DHT and increasing concentrations of the anti-androgen flutamide (10^{-8} to 10^{-5}M) To generate p values, pPB-CAT/Ad, R1881, and flutamide treated samples were compared to pPB-CAT/Ad and R1881 treated sample. ×, $p>0.05$; ××, $p<0.05$; ×××, $p<0.001$.

AR-regulated Transcription is Activated by flutamide in a Subgroup of HPE cells

ADT is still one of the most common strategies for treating prostate cancer. The goal of the TIGR assay was to characterize the response of endogenous AR to androgen and anti-androgen treatment to determine whether anti-androgen could stimulate AR-regulated transcription. To achieve this, primary HPE cells were infected with adenoviral particles containing the CAT reporter gene linked to the prostate-specific probasin promoter (pPB-CAT/Ad) (120). Initially, all adenoviral particles were titrated and characterized in the androgen-dependent LNCaP human prostate cancer cell line. No difference in basal CAT activity was seen with/without pPB-CAT/Ad, determining that these adenoviral particles had no intrinsic biological activity in the absence of androgen (Figure 15A). In the presence of pPB-CAT/Ad and increasing concentrations of R1881, near maximal CAT activity was observed at 10^{-8} M R1881 and greater than >99.5% of this activity was inhibited at 10^{-5} M flutamide (Figure 15B). Once the adenoviral particles were characterized in LNCaP cells, they were used to compare AR activity in primary HPE cells. Due to high levels of endogenous AR in LNCaP cells as compared to HPE cells (Figure 14), the absolute value of CAT activity was much lower in HPE cells (Figure 16) than that in LNCaP cells (Figure 15). Therefore, the absolute values between these cells could not be compared directly; instead they were grouped based upon the pattern of activity in response to hormonal treatment.

The responses of HPE cells to androgen and anti-androgen treatment separated into four groups. In the first group, androgen treatment induced CAT gene expression 11,000-fold and this activity could be blocked nearly 100% by the addition of flutamide,

implying that anti-androgen activity was antagonistic on AR-regulated transcription (Figure 16A). Thus, these HPE cells were designated as androgen responsive/flutamide suppressed (AR/FS).

In a second group of HPE cells (Figure 16B), basal CAT gene expression increased 195-fold in the absence of hormonal treatment. This observation was surprising since CAT activity did not increase above basal levels in LNCaP, PC-3 or AR/FS HPE cells under similar culture conditions. Flutamide treatment was still antagonistic, resulting in the partial suppression (57%) of this basal activity, suggesting that the increase in CAT activity was, at least in part, due to transactivation of the AR signaling pathway. Furthermore, the addition of 10^{-8} M R1881 had little effect; however the addition of flutamide alone still inhibited 52% of CAT activity in the presence of androgen. These HPE cells were therefore designated as androgen independent/flutamide suppressed (AI/FS).

In group 3 (Figure 16C), elevated CAT activity (42-fold) was again observed in the absence of hormonal treatment and this activity was not increased by the addition of androgen, suggesting that these HPE cells produced factors which could stimulate AR-regulated transcription. Furthermore, flutamide treatment was agonistic, increasing CAT activity a further 2.2-fold and in combination with androgen, an additional 4-fold, indicating that the effects of androgen and anti-androgen treatment on AR-regulated CAT gene expression were additive. Since androgen treatment alone had little effect and flutamide activated AR-regulated transcription (through an androgen responsive

promoter) in the absence and presence of androgen, these HPE cells were designated as androgen independent/flutamide activated (AI/FA).

In Group 4 (Figure 16D), increased levels of CAT activity (12-fold) were determined in the absence of androgen and the addition of androgen or flutamide did no t alter this activity. Thus, these HPE cells were categorized as non-responsive (NR) to androgen or anti-androgen treatment. Table 3 summarizes the response of HPE cells to androgen or anti-androgen treatment.

Table 3: Summary of the Agonist and Antagonist Activities of Flutamide on Androgen Receptor-Induced Signaling in the TIGR assay. A total of 40 primary HPE cell cultures were analyzed in this study. Ten specimens were PCa tissue (Gleason score 3+3) and 30 specimens were non-tumor tissue obtained from areas adjacent to the PCa lesion. This table summarizes the data obtained from the TIGR assays.

HPE cell response	Description of response to androgen and antiandrogen treatment	Gleason score 3+3	non-tumor tissue
AR/FS	- **A**ndrogen **R**esponsive/**F**lutamide **S**uppressed - androgen treatment induces CAT activity - flutamide inhibits androgen-induced CAT activity	0/10	4/30
AI/FS	- **A**ndrogen **I**ndependent/**F**lutamide **S**uppressed - androgen treatment does not induce CAT activity - flutamide inhibits AR-regulated CAT activity	7/10	10/30
AI/FA	- **A**ndrogen **I**ndependent/**F**lutamide **A**ctivated - androgen treatment does not induce CAT activity - flutamide is agonistic, promoting AR-regulated CAT activity	2/10	12/30
NR	- **N**on-**R**esponsive - androgen or flutamide treatment do not induce or inhibit CAT reporter gene expression	1/10	4/30

HPE cells from passage 2 were compared with those from passage 4 (derived from the same specimen) to determine whether passage number influenced response to flutamide treatment. As seen in Figure 17, the agonistic activity of flutamide induced CAT gene expression at both passage 2 (3.5-fold) and passage 4 (2-fold), indicating that the response to anti-androgen treatment was not dependent on passage number. Furthermore, HPE cells cultured from the transitional zone (TZ) responded in a similar manner to flutamide (2.6-fold increase) as those from the peripheral zone (PZ). The same response, whether flutamide activation or flutamide suppression, was observed in 60% of TIGR assays where PZ and TZ HPE cells were derived from the same prostate, suggesting that the antagonist or agonist activity of flutamide on AR-regulated transcription appeared to be an inherent response of HPE cells within that prostate.

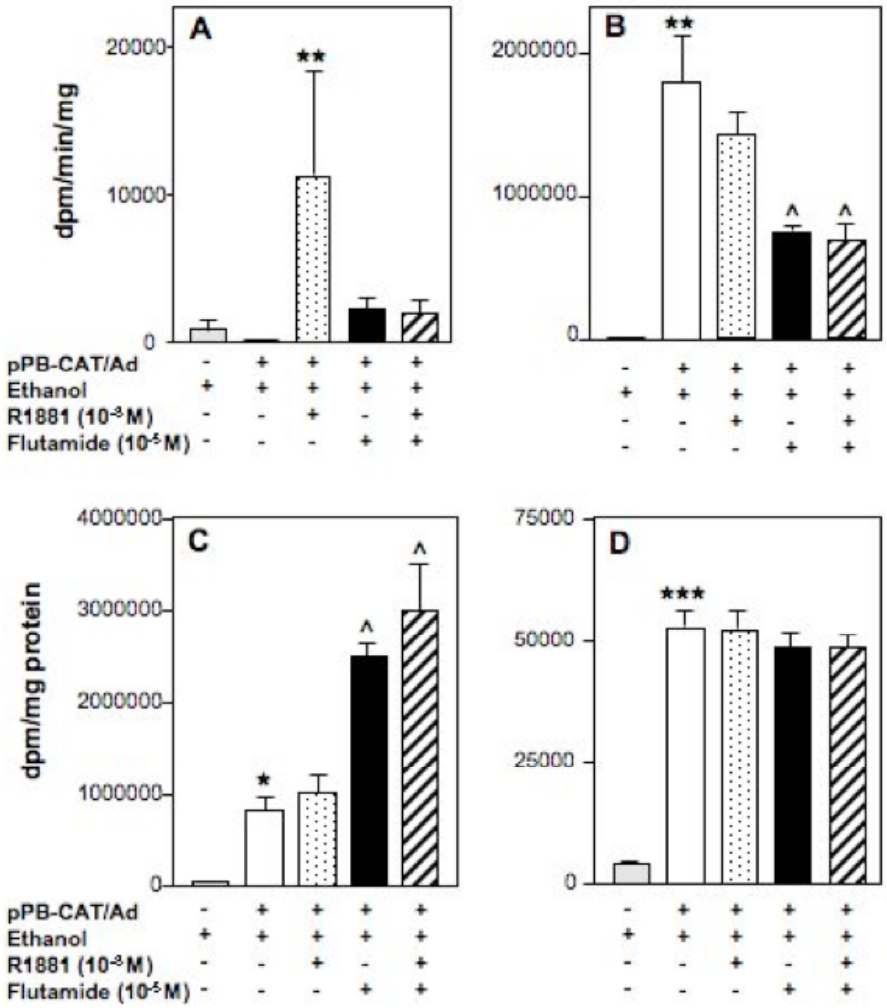

Figure 16: Androgen and anti-androgen activity in HPE cells. 1 x 10^5 HPE cells/well were plated in quadruplicate in 24 well plates and the cells were infected with 10^8 pfu pPB-CAT/Ad viral particles. The cells were treated with ethanol, 10^{-8}M R1881, or with 10^{-5}M flutamide as indicated and CAT activity was determined as described previously [23]. Error bars, +/- SD. The asterisk indicates p values of pPB-CAT/Ad and ethanol compared to ethanol alone. *, $p<0.007$; **, $p<0.001$; *** $p<0.0001$. The ^ symbol indicates p values of pPB-CAT/Ad and R1881 or flutamide treatment compared with pPB-CAT/Ad and ethanol treatment. ^, $p<0.016$.

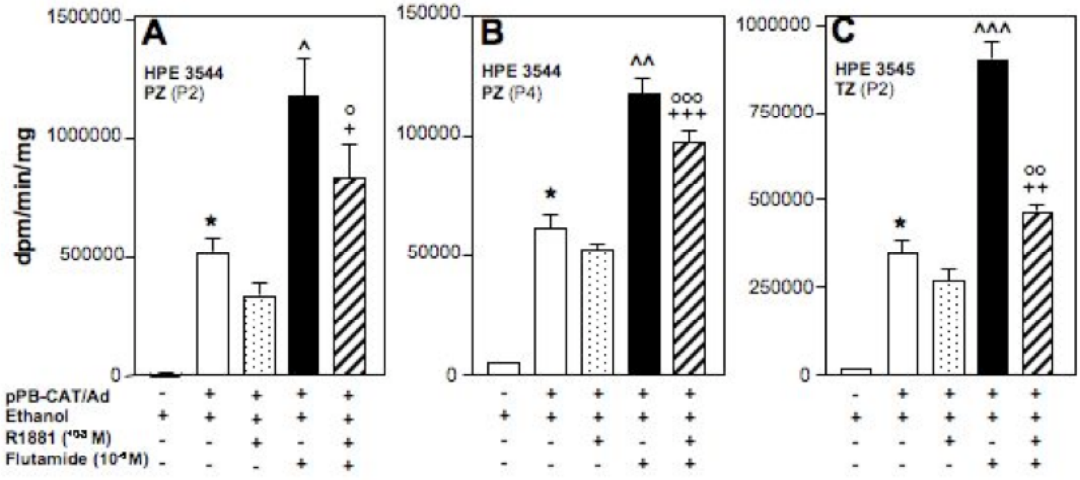

Figure 17: Comparison of HPE cells cultured from different passage numbers or prostate regions to androgen and anti-androgen treatment. HPE cells from passage 2 (P2) were compared with those from passage 4 (P4) (derived from the same prostatectomy specimen) or from peripheral (PZ) or transitional (TZ) zones of the prostate to determine whether passage number or location influenced response to flutamide treatment. CAT assays were performed as describes elsewhere [23]. **(A)** HPE cells from P2 were plated in quadruplicate at 1 x10^5 HPE cells/well, infected with 10^8 pfu pPB-CAT/Ad viral particles and treated with 10^{-8}M R1881 or with 10^{-5}M flutamide as indicated. **(B)** HPE cells from P4. **(C)** HPE cells from the prostate TZ. Error bars, +/- SD values. The asterisk indicates p values of pPB-CAT/Ad and ethanol compared to ethanol alone. *, $p<0.0001$. The ^ symbol indicates p values of pPB-CAT/Ad and flutamide treatment compared with pPB-CAT/Ad and ethanol. ^, $p< 0.007$; ^^. $p<0.0006$; ^^^, $p<0.0001$. The + symbol indicates p values of pPB-CAT/Ad, R1881 and flutamide treatment compared with pPB-CAT/Ad and ethanol. +, $p<0.09$; ++, $p<0.02$; +++, $p<0.003$. The ○ symbol indicates p values of pPB-CAT/Ad, R1881 and flutamide treatment compared with pPB-CAT/Ad and R1881. ○, $p<0.019$; ○○, $p<0.001$; ○○○, $p<0.0002$.

Mutational analysis of AR in HPE cells where AR-regulated signaling was activated by flutamide

AR mutations may allow transactivation of AR signaling through other steroid hormones and ligands such as corticoids and flutamide (72, 137). Thus, AR in AI/FA HPE cells was analyzed for somatic mutations. Genomic DNA was extracted from cultured HPE cells and PCR amplification was performed on six targeted areas in which most of the prostate cancer somatic mutations co-localized. These areas include 2 in the AR-NTD [amino acids (aa) 54-92; 253-282;] and 4 in the AR-HBD [aa 654-689; 688-721; 723-738; 867-917] (67). No point mutations, insertions or deletions in these 6 areas were identified. These observations do not exclude the possibility that mutations could have been present outside of these common regions.

Identification of DJ-1 in HPE cells treated with flutamide

Difference gel electrophoresis was used to flag DJ-1 as a protein that underwent a change in expression level upon hormonal treatment. Briefly, HPE cells were treated with ethanol, 10^{-8} M R1881, or 10^{-5} M flutamide, harvested and lysed as described in materials and methods. One hundred μg of each whole cell lysate was labeled with Cy2, Cy3, or Cy5 respectively, recombined and subjected to 2D gel electrophoresis (Figure 18A). The resulting 2D gel was visualized under the appropriate wavelengths and protein spots that increased with flutamide treatment relative to the ethanol control (Figure 18B) were excised, treated with trypsin, and analyzed by mass spectrometry (Figure 18C). DJ-1, a positive regulator of AR activation (98), was identified as increasing 1.44-fold (44%) with flutamide treatment. The ion signals at m/z = 1158.62, 1286.70, 1707.79, 1920.99, and 2584.36 were used to identify DJ-1 using a peptide mass mapping strategy (Materials and

Methods), yielding statistically-significant search scores, 37% protein coverage, and a database-predicted MW and isoelectric point (20,100 kDa and 6.3 pI) that were consistent with the gel region. This preliminary finding was validated in the following experiments.

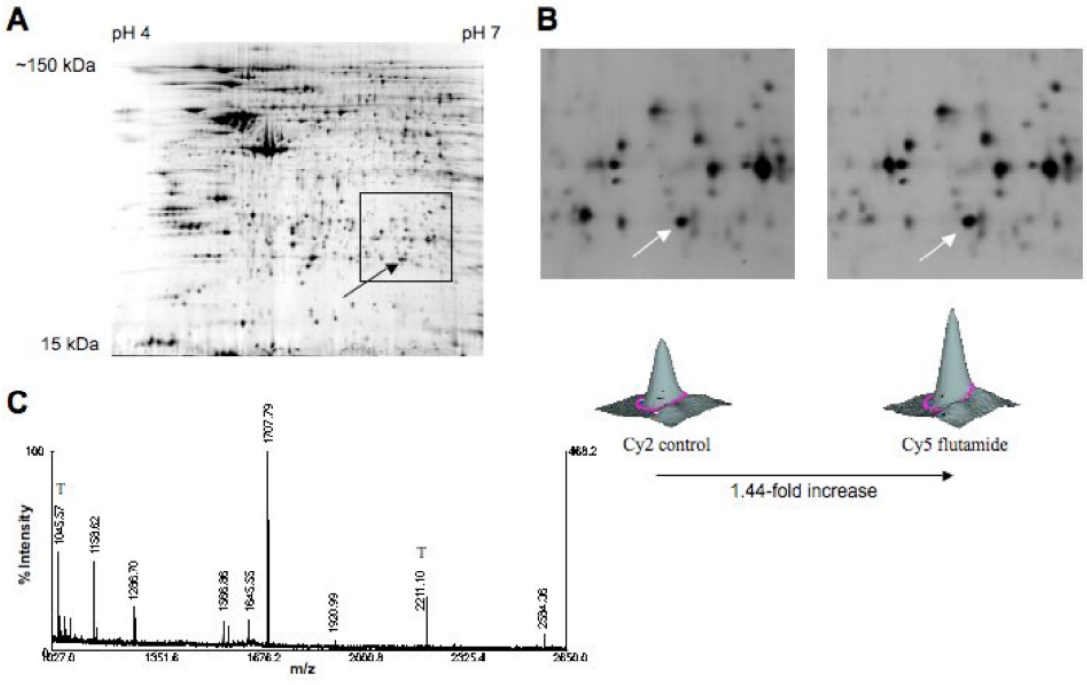

Figure 18: Identification of DJ-1, a flutamide-regulated protein, in HPE cells. **(A)** Total protein stain image of the 2D-gel used for the difference gel electrophoresis analysis, wherein separately-labeled total protein extracts from HPE cells treated with ethanol, R1881, or flutamide were co-resolved. The arrow indicates the protein spot-of-interest that was determined to be DJ-1. **(B)** The boxed region from panel A is enlarged and Cy2 and Cy5 are individually imaged to show the increase in protein expression between the ethanol and flutamide treated samples. Below each gel is a graphical representation of increase in protein levels**. (C)** Protein profile of the tryptic peptides which identified the protein as DJ-1.

Flutamide and androgen regulate DJ-1 and AR expression

Due to limited tissue fragments and the short lifespan of HPE cells in culture, it was important to identify an immortalized cell line expressing DJ-1 to confirm the primary culture data. Therefore LNCaP, PC-3, DU-145, and NIH-3T3 cells were analyzed for DJ-1 expression (data not shown). Although all cell lines tested expressed DJ-1, LNCaP cells were selected since they also expressed endogenous AR which could be transactivated by hydroxyflutamide (OHF), albeit through a T877A substitution mutation. LNCaP cells were deprived of androgens and treated with different activators of transcriptional regulation including 10^{-8}M DHT, 10^{-8}M R1881, 10^{-5} hydroxyflutamide (OHF), 10^{-5} M Forskolin, or 10^{-6}M TPA, for 48 hours. The vehicle (ethanol) served as a control. Forskolin and TPA were included to determine whether DJ-1 expression was modulated by other transcriptional regulators such as adenylate cyclase or AP1 respectively. Western blot analysis demonstrated that DJ-1 protein levels increased up to 6-fold with R1881 and OHF treatment (Figure 19A). DJ-1 expression also increased in LNCaP cells that were deprived of androgens for 24 hours (CSS) and then returned to media containing 10% FBS (CSS+FBS). Forskolin and TPA treatment had limited effect, increasing DJ-1 expression only 2-fold (Figure 19B). Thus, DJ-1 expression appeared to be primarily modulated by R1881 or OHF treatment. AR expression also increased or decreased in parallel with DJ-1 in all treatment groups.

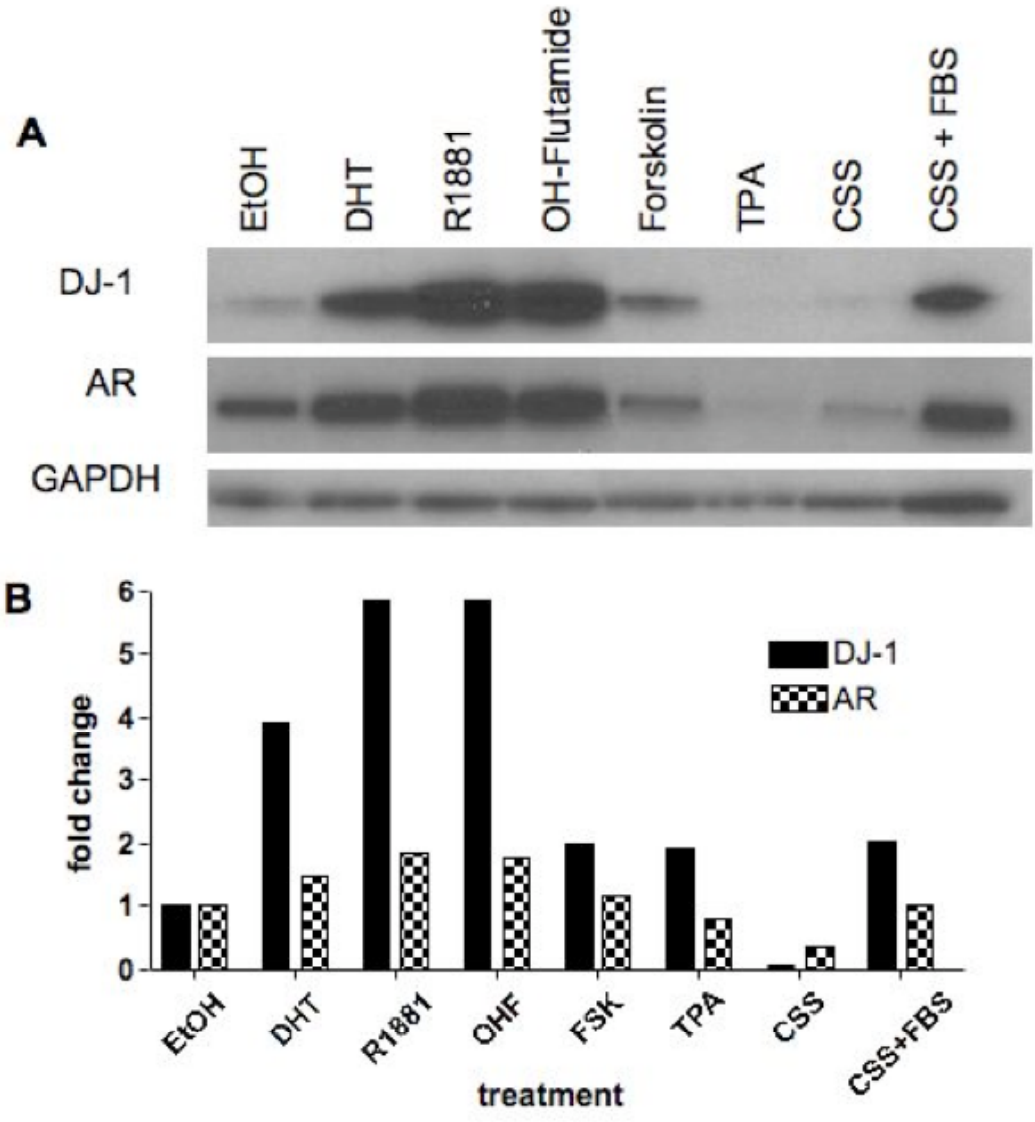

Figure 19: Androgens and anti-androgens increase protein levels of DJ-1 and AR. (A) LNCaP cells were grown to 70% confluency and changed to media containing 10% charcoal stripped fetal calf serum (CSS). After 24 hours of androgen depletion, cells were treated with the indicated agents for 48 hours. CSS alone served as a negative control (lane 7), while CSS for 24 hours followed by 24 hours with 10% FBS served as a positive control (lane 8). **(B)** AR and DJ-1 protein levels are represented as a histogram after normalization to GAPDH loading control.

DJ-1 protein is stabilized in response to androgen and anti-androgen treatment

LNCaP cells were treated with ethanol, 10^{-8} M DHT, or 10^{-5} M OHF for 24 hours, total RNA was extracted and Northern blot analysis was performed to determine whether the increase in DJ-1 protein levels was due to increased DJ-1 gene transcription. A riboprobe to full-length human DJ-1 was labeled with ^{32}P. Unlabeled antisense RNA served as a negative control and DJ-1 plasmid as a positive control. No change in DJ-1 mRNA levels was observed at all time points tested (Figure 20A).

Since androgen and anti-androgen treatment did not appear to regulate DJ-1 gene expression, LNCaP cells were treated with the translation inhibitor cyclohexamide (CHX) to test whether hormone treatment stabilized DJ-1 protein. After 30 minutes of pretreatment with ethanol, DHT, or OHF, CHX was added and cells were harvested at 24, 48, and 72 hours and processed for Western blot analysis (Figure 20B and 20C). DJ-1 protein levels remained unchanged even up to 72 hours after OHF treatment whereas DJ-1 protein was reduced by 60% with ethanol treatment. DHT stabilized DJ-1 slightly as compared to ethanol control which correlates with the greater increase of DJ-1 following OHF treatment (Figure 19A). These results imply that the increase in DJ-1 protein levels is due to increased protein stability during androgen and anti-androgen treatment.

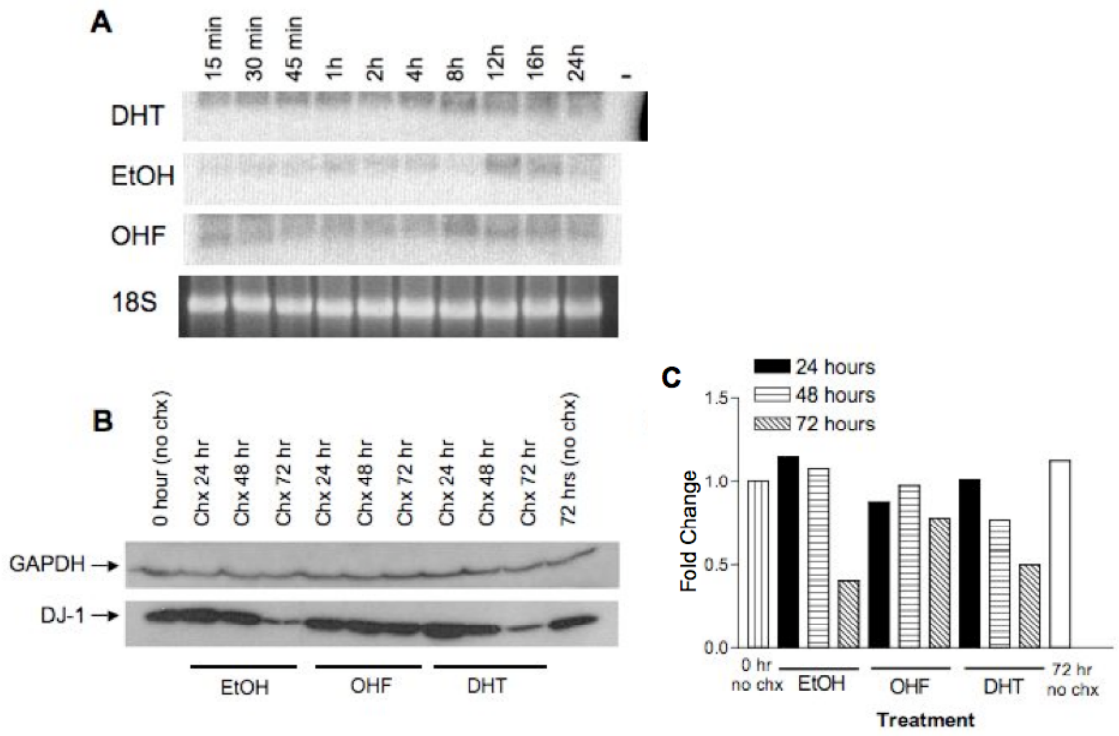

Figure 20: Increased DJ-1 Protein Expression after OH-Flutamide Treatment Results from Protein Stabilization. (A) Northern blot analysis of DJ-1 using total RNA from LNCaP cells. Cells were treated either with ethanol, DHT, or OH-Flutamide (OHF) for the amount of time indicated above each lane. DJ-1 plasmid was used as a positive control (+). Unlabeled antisense RNA was used as a negative control (-). **(B)** Cyclohexamide Stabilization Assay for DJ-1. LNCaP cells were again deprived of androgens and then were pretreated either with ethanol, DHT, or OHF for 30 minutes prior to treatment with cyclohexamide (CHX). Cells cultured in CSS media and were not treated with CHX serve as controls at 0 and 72 hours. **(C)** Densitometry shows that treatment with OHF stabilizes DJ-1 protein for 72 hours after addition of CHX, whereas approximately 50 % degrades with DHT treatment, and 60% by 72 hours in the EtOH treated sample. Values for DJ-1 were normalized to the GAPDH loading control.

Discussion

Anti-androgens such as flutamide and bicalutamide have been used in combination with ADT for PCa. The HPE TIGR assay was developed to study the effects of androgen and anti-androgen treatment in primary HPE cells since these cells most closely represent those from the patient. Unlike other PCa cell lines which were derived from metastatic lesions or from virally transformed cell cultures, HPE cells were cultured from biopsy material only up to passage 4 to capture the early responses of AR-regulated transcription to hormone therapy. These cells were typically epithelial and expressed prostatic secretory proteins. A further advantage of HPE cell cultures was that the assay measured endogenous AR responses to androgen and anti-androgen treatment. Endogenous AR activity was significantly lower than that observed in studies where exogenous AR was transfected into cells to promote high levels of reporter gene activity (138). The lower levels of CAT activity most likely reflect the physiological levels of AR-regulated signaling in the prostatic epithelium.

The most surprising observation was that flutamide promoted AR-regulated transcription in HPE cells derived from 2/10 (20%) tumor and 12/30 (40%) nontumorous biopsy specimens. These observations suggested that transcriptional activation by flutamide occurred in cells derived from histologically normal prostate tissue. Flutamide promotes androgen-independent transcriptional activation and proliferation through the well-characterized AR T877A substitution mutation in LNCaP cells (72, 137). This mutation was detected in 5 of 16 metastatic lesions obtained from patients who received combined androgen blockade with flutamide (69). We analyzed this region in the AR

from AI/FA HPE cells. No mutations, including the T877A mutation, were identified, demonstrating that the agonist activity of flutamide occurred through a wild-type AR (130). In a similar study, hydroxyflutamide treatment increased reporter gene activity in DU-145 transfected with wild-type AR. Our analysis does not eliminate the possibility that as yet unidentified mutations may have occurred outside the common areas analyzed.

Difference gel electrophoresis analysis of HPE cells identified the oncogene DJ-1 as a protein whose expression was increased by anti-androgen treatment. PIASxα [protein inhibitor of activated STAT (signal transducer and activator of transcription)] interacts with the DNA-binding domain/zinc finger region of AR and suppress AR-activated transcription (139). DJ-1 was identified as a PIASxα binding partner, interacting directly with the AR-binding region of PIASxα to remove it from AR and restore AR transcriptional activity (98).

In our study, DJ-1 protein levels increased in parallel with AR in response to flutamide as well as to R1881. In addition, DJ-1 protein levels were stabilized by flutamide similar to that observed for AR (130). Thus, it is possible that stabilization of AR and DJ-1 allowed flutamide to gain agonist activity. This mechanism may account, in part, for the anti-androgen withdrawal syndrome.

In addition to PIASxα, DJ-1 interacts with the death protein DAXX, sequestering it in the nucleus and inhibiting apoptosis signal-regulating kinase 1 activity to promote cell survival (94). DJ-1 binding protein (DJBP) binds to the DNA binding domain to AR

and negatively regulates AR by recruiting histone deacetylase complex, including HDAC1 and mSin3 (118). DJ-1 restores AR activity by interacting with DJBP (118). Thus, DJ-1 appears to play a major role in AR function.

The ARR_2PB promoter contains two androgen responsive regions, each containing two androgen receptor binding sites ARBS1 and ARBS2 (120). This reporter is exquisitely sensitive to androgen and anti-androgen treatment. Low/no CAT activity was observed in the untreated control groups in AR/FS HPE, LNCaP, and PC-3 cells. This was in contrast to HPE cells in the AI/FS, AI/FA, and NR groups which all demonstrated high basal levels of CAT activity in the absence of hormonal treatment. Flutamide could still suppress 57% of this activity, implying that this activity was, in part, promoted through the AR signaling pathway. Since this blockade was not 100%, it is possible that HPE cells produce factors in addition to DJ-1 that promote AR-regulated promoter activity in the absence of androgen.

Stabilization of AR and positive regulators such as DJ-1 may partially explain the progression from anti-androgens functioning as AR antagonists to agonists. This stabilization may provide the double-edged sword for cancer progression. Not only is AR protein itself stabilized, similar to the hypersensitivity hypothesis whereby increased levels of AR allow the cell to respond to extremely low androgen levels (48), but also DJ-1 and other AR co-regulators are stabilized which promote transcriptional activation of AR. Taken together these changes could provide the transcriptional advantage that allows hormone responsive cancers to escape ADT.

Our study using primary cultured HPE cells suggests that anti-androgens can become agonists by stabilizing DJ-1 and increasing DJ-1 and AR protein levels. The agonistic activity of flutamide was already observed in histologically normal HPE cells, suggesting that these cells had a transcriptional advantage for survival and that these changes may occur before the disease is clinically diagnosed. Thus, the HPE TIGR cell assay provides a mechanism for studying the early molecular changes which allow anti-androgens to acquire agonistic properties and highlights the importance of utilizing cells derived from radical prostatectomy specimens in determining these mechanisms.

CHAPTER IV

DJ-1 BINDS ANDROGEN RECEPTOR DIRECTLY AND MEDIATES ITS ACTIVITY IN HORMONALLY TREATED PROSTATE CANCER CELLS

Introduction

Multiple molecular events are involved in prostate cancer (PCa) initiation, growth, invasion, and metastasis. Despite the diverse etiology, there is at least one universal similarity to the disease – the requirement of androgens and AR for tumor progression (49, 140-145). Androgen deprivation therapy (ADT, also known as neo-adjuvant hormone therapy), is initially effective to treat prostate cancer and remains the most common treatment regimen for advanced disease. Although androgen deprivation therapy initially causes tumor regression, the eventual evolution of PCa from an androgen-dependent to an androgen-independent phenotype allows continuation of tumor progression (reviewed in (146)). There are many hypotheses for the development of androgen-independent prostate cancer. Some of these involve increased cellular proliferation/decreased apoptosis and, in some patients, increased serum prostate-specific antigen (PSA) corresponding with promiscuous or increased AR activity (48, 116).

We hypothesized that identification of proteins that increase following androgen deprivation therapy would modulate molecular changes that promote and/or maintain AIPC. To this end, we performed proteomic analysis of primary HPE cells after treatment with the anti-androgen flutamide (128). We identified DJ-1 as one protein that increased following flutamide treatment. Western blot analysis confirmed this result, demonstrating

that DJ-1 and AR protein levels increased following treatment with dihydrotestosterone (DHT), the synthetic androgen R1881, or the anti-androgen hydroxy-flutamide (OH-flutamide) in LNCaP cells. Blocking protein synthesis with cycloheximide revealed the increase in DJ-1 was due to increased protein stability (128). This indicates DJ-1 and AR expression are regulated by both androgens and anti-androgen therapy and could play a role in AIPC.

In order to elucidate the DJ-1 pathway in PCa, we sought to identify DJ-1 binding proteins in prostate epithelial cells. To address this, primary HPE cells were derived from a punch biopsy of human prostate and the androgen-responsiveness of these cells was determined using the TIGR assay as described (128). Briefly, this assay utilizes an androgen-responsive reporter to determine whether primary HPE cells are androgen responsive, androgen independent, or flutamide activated. Since we previously demonstrated that DJ-1 increases after flutamide treatment, we used flutamide activated HPE cells to generate a novel cDNA library. This library was screened using DJ-1 and identified AR as a DJ-1 binding partner. Previously, DJ-1 was thought to control AR activity through an indirect mechanism, although these studies were performed after transient transfection of AR and DJ-1 in non-prostate cell lines (98, 118). This is the first evidence that endogenous DJ-1 directly binds AR, and that the sub-cellular localization and protein-protein interaction is hormonally regulated. Further, we analyzed two prostate cancer tissue arrays providing the first large-scale expression analysis for DJ-1 in PCa. The first of the two arrays is arranged by Gleason pattern, and the second is arranged by length of time of ADT. DJ-1 immunohistochemical staining on these arrays

demonstrates for the first time that DJ-1 is expressed in benign as well as high Gleason pattern regions. Interestingly, DJ-1 expression increased significantly in patients receiving greater than 6 months of ADT, indicating that DJ-1 may contribute to the development of AIPC. Taken together, these data provide a new mechanism for regulation of AR in androgen independent prostate epithelial cells.

Results

DJ-1 Binds the Androgen Receptor

In order to identify DJ-1 binding partners in PCa we generated a cDNA library from primary human prostate epithelial cells where flutamide treatment activated AR signaling in an androgen-independent manner. This unique library was generated because our previous studies indicated that DJ-1 expression increased in HPE and LNCaP cells following anti-androgen treatment. Screening the flutamide-activated library allows identification of DJ-1 binding partners that may contribute to the development or maintenance of AIPC. Therefore, full length DJ-1 cDNA was used to screen the library and identified a region of AR (Figure 21B). The AR fragment contains a region of the N-terminal activation domain, the entire DNA Binding Domain, and a portion of the Ligand Binding Domain (Figure 21A).

The DJ-1:AR interaction was confirmed using AR immunoprecipitation (IP) in the LAPC4 cell line. These androgen-dependent cells were derived from a lymph node metastasis and retain wild-type AR and PSA expression, unlike most PCa cell lines that

have lost AR expression or have AR mutations (147). IP of endogenous AR pulls down DJ-1 (Figure 21C). The reciprocal IP was performed in LAPC4 cells expressing a N-terminal HA-tagged DJ-1. IP using anti-HA antibody co-immunoprecipitated HA tagged DJ-1, endogenous DJ-1, and AR. DJ-1 exists as an obligatory dimer (100). Therefore, we postulate that HA-DJ-1 binds endogenous DJ-1, explaining the precipitation of both tagged and un-tagged DJ-1 (Figure 21D).

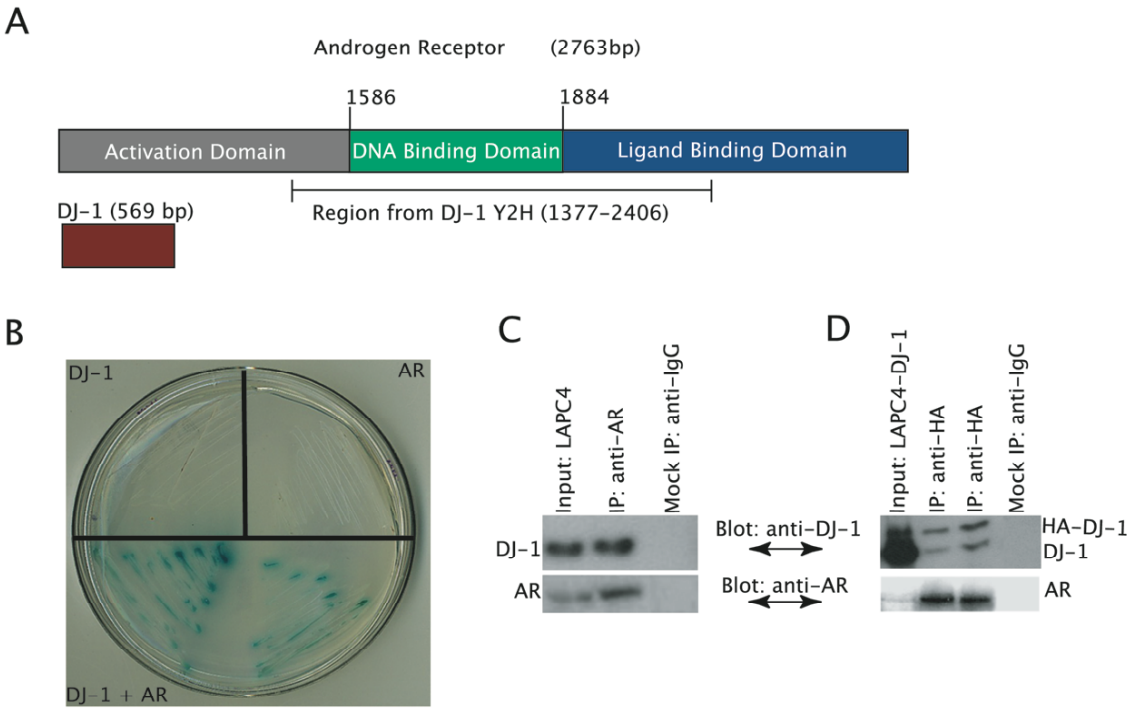

Figure 21: AR Binds DJ-1 in the Yeast Two-Hybrid System and LAPC4 Cell Line

A) The fragment of AR identified spans the C-terminal region of the Activation Domain, the DNA Binding Domain, and a portion of the Ligand Binding Domain. **B)** High stringency selection demonstrates that neither the bait (DJ-1) nor prey (AR) plasmid are capable of activating reporter genes individually, but the combination produces an interaction and activation of the reporters.

C) Immunoprecipitation (IP) of AR in LAPC4 cells pulls down DJ-1 confirming the interaction. **D)** Reciprocal IP was performed using LAPC4 cells that express HA-tagged DJ-1. Input lane contains total protein, mock IP was performed with anti-IgG antibody to demonstrate specificity.

Hormonal Treatment Increases The Interaction Between DJ-1 and AR

We performed IPs following hormonal treatment in LAPC4 and LNCaP cells to determine if these treatments regulated the DJ-1:AR interaction. LAPC4 and LNCaP cells were serum starved overnight and then treated with ethanol, 10^{-8}M DHT (LNCaP), 10^{-9}M DHT (LAPC4), 10^{-5}M OH-flutamide (LNCaP), 10^{-6}M OH-flutamide (LAPC4), 10^{-5}M bicalutamide (LNCaP), or 10^{-6}M bicalutamide (LAPC4) for 24 hours. In both LAPC4 and LNCaP cells, anti-androgen treatment with either OH-flutamide or bicalutamide increased the amount of DJ-1 bound to AR (Figure 22). DHT treatment appeared to increase the DJ-1:AR interaction in LNCaP cells more so than in LAPC4 cells (Figure 22).

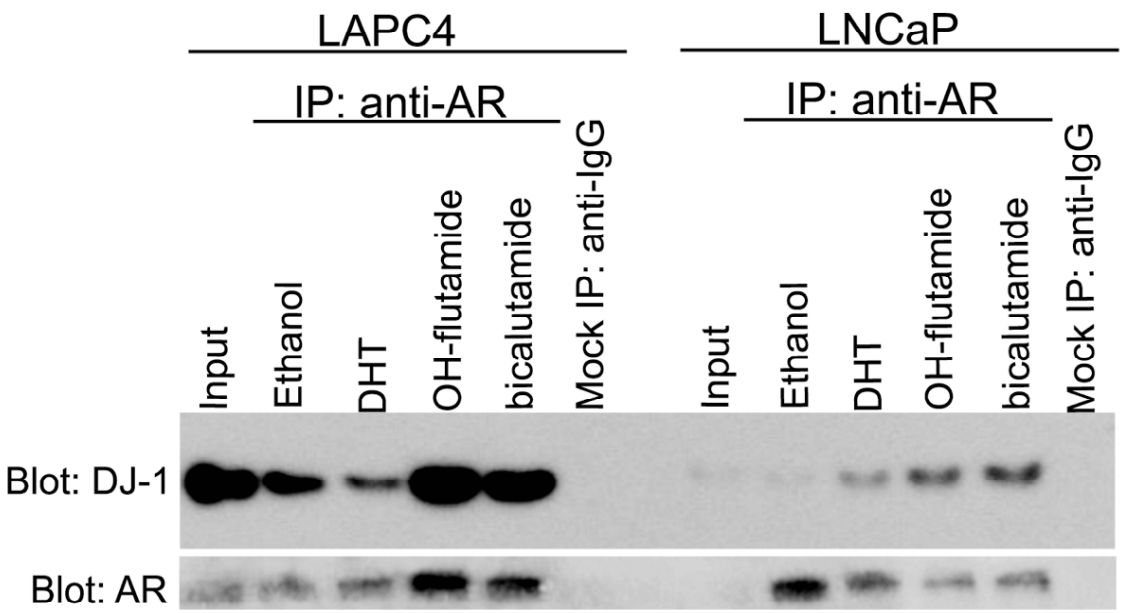

Figure 22: Hormonal Treatment Increases DJ-1:AR Interaction in LAPC4 and LNCaP Cell Lines
AR immunoprecipitation following treatment of LAPC4 and LNCaP cell lines with ethanol, DHT, OH-flutamide, and bicalutamide. Input lanes contain 5 micrograms of total protein lysate from DHT treated sample. Mock IP was performed with anti-IgG.

Androgen and Anti-Androgens Increase DJ-1 Nuclear Localization

In order to determine localization of DJ-1 in the prostate cancer cell lines LAPC4 and LNCaP, nuclear and cytoplasmic extracts were prepared. Cells were treated as described above. Twenty-four hours after treatment, cells were harvested and cytoplasmic and nuclear extracts were prepared using the NEPER kit (Pierce). Western Blot analysis of the resultant extracts revealed that DJ-1 is predominantly cytoplasmic, but both androgen (DHT) and anti-androgen (OH-flutamide and bicalutamide) treatment

increases DJ-1 expression in the nuclear fraction (Figure 23A). As expected, AR expression was very low in the absence of androgens, but when treated with DHT, AR expression is increased and predominantly nuclear (Figure 23A). Histone H1 and Rho A were used as nuclear and cytoplasmic controls, respectively, and to show equal loading between lanes (Figure 23A) (148). The same experiment was performed in LNCaP cells, where an increase in DJ-1 after hormonal treatment was previously documented (128). The LNCaP cell line also showed increased nuclear DJ-1 after hormonal treatment, with a greater increase in nuclear DJ-1 with DHT than in the LAPC4 cell line (Figure 23B). AR is predominantly nuclear in all treatment groups, consistent with previous reports (65, 149, 150). Histone H1 and Rho A demonstrate clear separation between the subcellular compartments (Figure 23B).

Immunofluorescence and confocal microscopy were used to confirm the presence of DJ-1 in both nuclear and cytoplasmic compartments. LAPC4 and LNCaP cells were plated on chamber slides, allowed to attach overnight, then treated in the same manner as cells used for nuclear/cytoplasmic extracts. Cells were stained for DJ-1, AR, and SC-35 and visualized with appropriate secondary antibodies. SC-35 is a nuclear speckle marker, and was included to identify sites of active transcription (151). As with nuclear and cytoplasmic extracts, DJ-1 (green) is predominantly cytoplasmic, but is also present in the nucleus in both LAPC4 and LNCaP cell lines (Figure 23C). AR (red) localization also confirms results from nuclear and cytoplasmic extracts, in that AR expression was low in the absence of androgens in LAPC4 cells, but driven to the nucleus upon treatment with DHT (Figure 23C). Further, AR positive nuclei were observed regardless of treatment in

LNCaP cells, confirming our observations from Western blot analyses (Figure 23C). The merged images show co-localization between DJ-1 and AR, indicated by yellow in merged images (Figure 23C, white arrows) but these areas appear distinct from nuclear speckles and active sites transcription (Figure 23C, white *). Low-magnification images of individual channels are shown in inset areas (Figure 23C).

Yellow pixels, from the LNCaP images in Figure 3C, were displayed alone and indicate DJ-1:AR co-localization increases following hormonal treatment (Figure 23D). White dashed lines outline nuclei (Figure 23D). Co-localization of DJ-1 and AR was quantified by determining the percentage of co-localized pixels per image (Figure 23D). DJ-1:AR co-localization was greatest with DHT treatment followed by OH-flutamide and then bicalutamide treatment. Each treatment demonstrated a distinct pattern. DHT and bicalutamide treatment resulted in similar co-localization throughout the nucleus, whereas DJ-1:AR with OH-flutamide treatment appeared to concentrate just within the nuclear perimeter. DJ-1:AR co-localization was not quantified in LAPC4 cells due to low AR levels except after DHT treatment.

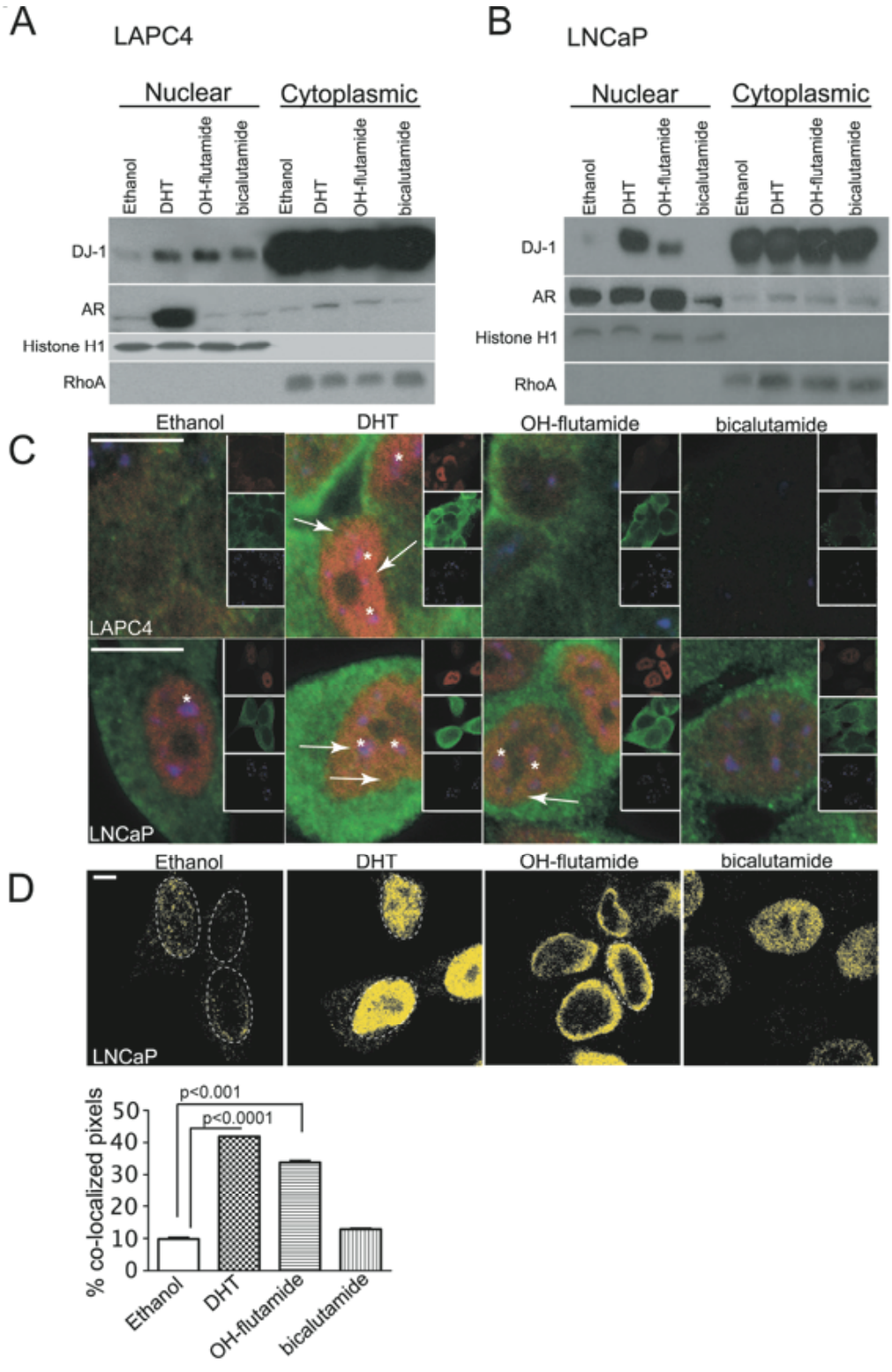
A
LAPC4
Nuclear
Cytoplasmic
Ethanol
DHT
OH-flutamide
bicalutamide
DJ-1
AR
Histone H1
RhoA
B
LNCaP
C
LAPC4
LNCaP
D
% co-localized pixels
p<0.001
p<0.0001
0
10
20
30
40
50

Figure 23: Androgens and Anti-androgens Increase DJ-1 Nuclear Localization in LAPC4 and LNCaP Cells

Nuclear and cytoplasmic extracts were prepared from **A)** LAPC4 cells and **B)** LNCaP cells indicated treatments. **C)** Immunofluorescence for DJ-1 (green), AR (red), and SC-35 (blue) in LAPC4 and LNCaP cells following treatment. Merged high-magnification images show co-localization between DJ-1 and AR (yellow spots) indicated by white arrows. Co-localization between AR and SC-35 (pink/purple spots) indicated by white asterisk mark active sites of transcription. Scale bar equals 5 microns. **D)** Images and quantification of co-localization between DJ-1 and AR. Yellow pixels indicate co-localization between DJ-1 and AR in LNCaP cells. White dashed lines outline several nuclei. The percent of pixels that co-localize between DJ-1 and AR channels was determined in multiple optical slices for each treatment in LNCaP cells and is represented as mean +/- SEM. Scale bar equals 5 microns.

DJ-1 Regulates AR Transcriptional Activity

We used an androgen-responsive luciferase reporter to determine how modulation of DJ-1 expression affected AR activity. A region of the probasin promoter, termed (ARR_2PB), containing two androgen responsive regions, was cloned upstream of the Firefly luciferase gene resulting in the ARR_2PB-luc reporter (128, 129). Over-expression of DJ-1 (HA-DJ-1 + luc) increased AR activity approximately 10-fold ($p<0.001$) compared to parental LAPC4 cells transfected with the luciferase reporter and to cells transfected with reporter and an empty plasmid control (Figure 24A). Western Blot analysis demonstrates that transfection with pCruz-HA-DJ-1 plasmid doubles the expression level of DJ-1, but does not change the expression level of AR (Figure 24B).

Similarly to over-expression, knockdown of DJ-1 expression influences AR regulated-transcription. Pooled siRNAs were co-transfected into LAPC4 cells along with

the ARR_2PB-luc reporter. Knockdown of DJ-1 expression decreased AR activity 5-10 fold compared to LAPC4 cells with reporter alone ($p<0.01$) (Figure 24C). The decrease in DJ-1 expression after transfection of siRNAs resulted in approximately 50% decrease in DJ-1 protein level compared to GAPDH loading control (Figure 24D). Transfection of nonspecific (NS) siRNA served as a control and did not change DJ-1 expression compared to nontransfected LAPC4 cells. Knockdown of DJ-1 did not change AR expression, indicating that AR expression is not regulated by DJ-1 (Figure 24D).

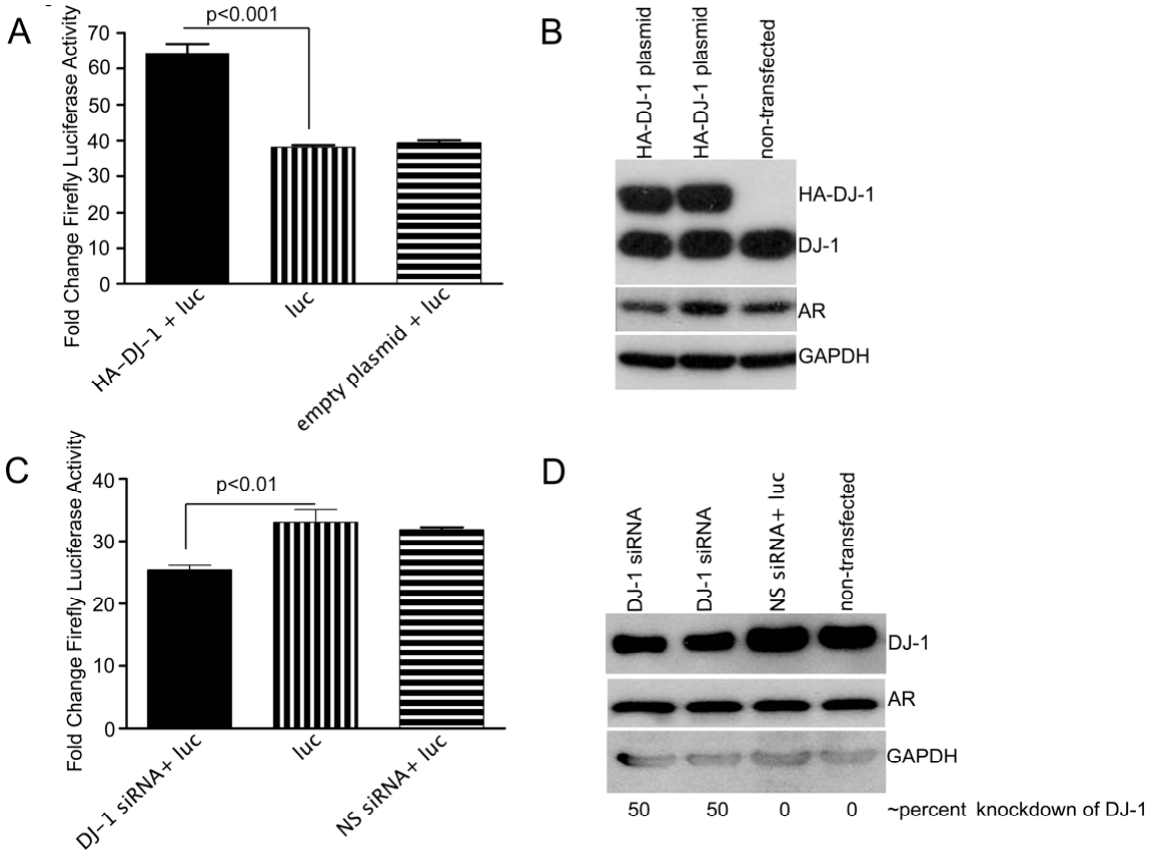

Figure 24: DJ-1 Regulates AR Transcriptional Activity in LAPC4 Cells

A) Overexpression of DJ-1 (HA-DJ-1) increases AR transcriptional activity using the ARR_2PB-luciferase (luc) reporter compared to reporter alone. Each bar represents the mean of three samples +/- SEM after normalization to protein concentration and expressed as fold change compared to nontransfected control. This experiment was repeated 3 times with the same result. **B)** Western blot of LAPC4 cells transfected with HA-DJ-1 plasmid compared to parental LAPC4 cells. AR expression level does not change with overexpression of DJ-1. GAPDH was included as a loading control. **C)** Knockdown of DJ-1 expression using siRNA decreases AR activity as compared to reporter alone. Nonspecific siRNA (NS) indicates that the effect is specific. Samples are presented in the same manner as in panel A. **D)** Western blot of LAPC4 cells transfected with siRNAs shows that DJ-1 siRNA decreases expression by 50%. AR expression does not change after knockdown of DJ-1. The percent knockdown of DJ-1 compared to NS siRNA was determined by densitometric analysis using ImageJ software.

DJ-1 Expression Does Not Increase With Gleason Pattern

Prostate samples from patients who underwent radical prostatectomy between 1989 to 2003 were obtained from Vancouver General Hospital. These patients received no treatment prior to surgery. The samples were grouped based upon Gleason score and arranged on the slide based upon predominant Gleason pattern for each tissue core in the following groups: Benign, Gleason 2, Gleason 3, Gleason 4, and Gleason 5. Figure 25A indicates the number of patients represented by each group.

DJ-1 immunohistochemical staining was performed on this array and quantitated based on intensity. Four areas per tissue core were evaluated using the following scale: "0" indicates no staining of any cells, "1" indicates a faint stain, "2" indicates a moderate intensity stain, and "3" indicates intense staining. DJ-1 was present in all 5 sample groups at moderate intensity, but no statistically significant change was observed, indicating that DJ-1 does not increase with Gleason pattern (Figure 25B). Figure 25C shows representative areas from each group at low and high magnifications (scale bars equal 20 microns). DJ-1 is predominantly expressed in luminal epithelial cells and is both cytoplasmic and nuclear.

A

Histopathology of Specimen	Number of Patients
Benign	7
Gleason 2	14
Gleason 3	21
Gleason 4	21
Gleason 5	21
Total	84

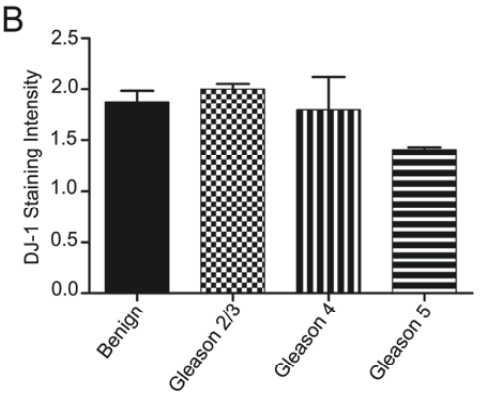

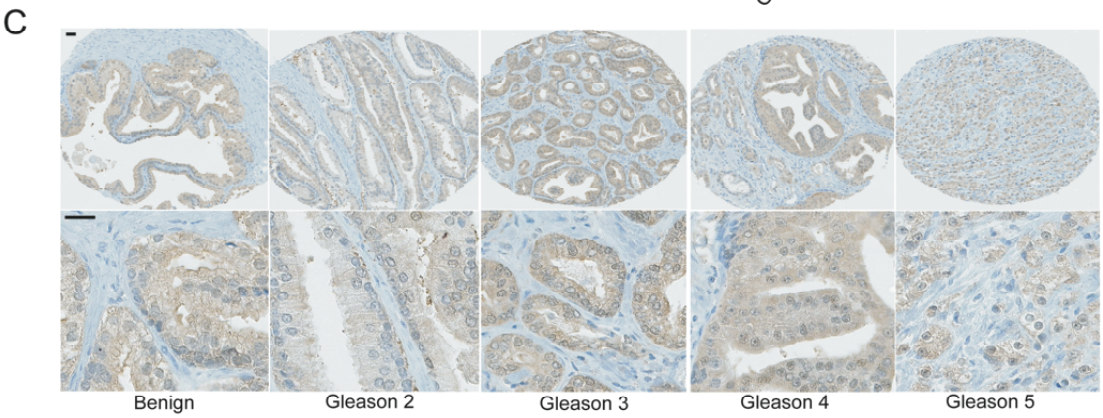

Figure 25: DJ-1 Expression Does Not Increase With Gleason Pattern
A) The number of patients represented per group on the TMA. **B)** Quantification of DJ-1 staining intensity on the Gleason TMA. Staining intensity was evaluated on a 4 point scale, with "0" indicating no positive cells, and "3" indicating intensely positive cells. DJ-1 is moderately expressed in all groups and does not increase with Gleason pattern. Bars represent mean +/- SEM. **C)** Representative immunohistochemistry images from each of the groups on the array at low and high magnification. DJ-1 is expressed predominantly in the luminal epithelial cells and is both cytoplasmic and nuclear. Scale bars equal 20 microns.

DJ-1 Expression Increases in Human Prostates with Androgen Deprivation Therapy (ADT):

The second tissue array was generated identically to the first. This array was composed of samples from patients who received either no ADT, less than 3 months ADT, 3-6 months ADT, or greater than 6 months ADT before undergoing radical prostatectomy surgery at Vancouver General Hospital. The samples were evaluated

histologically and arranged based upon duration of treatment. Figure 26A indicates the number of patients per group (unshaded boxes).

DJ-1 staining intensity was evaluated in the same manner as on the Gleason tissue array. DJ-1 expression increased significantly in the greater than 6 months ADT group as compared to the untreated group ($p<0.01$) (Figure 26B). Figure 26B shows representative tissue cores from each treatment group at low and high magnification (scale bars equal 20 microns). DJ-1 is expressed in both the cytoplasm and nuclei of luminal epithelial cells. The increase in the intensity of DJ-1 staining after prolonged ADT treatment suggests that DJ-1 may be involved in the emergence of AIPC as our previous data suggested.

A

Histopathology of Specimen	Number of Patients
Untreated	21
< 3months ADT	21
3-6 months ADT	28
> 6 months ADT	28
Total	98

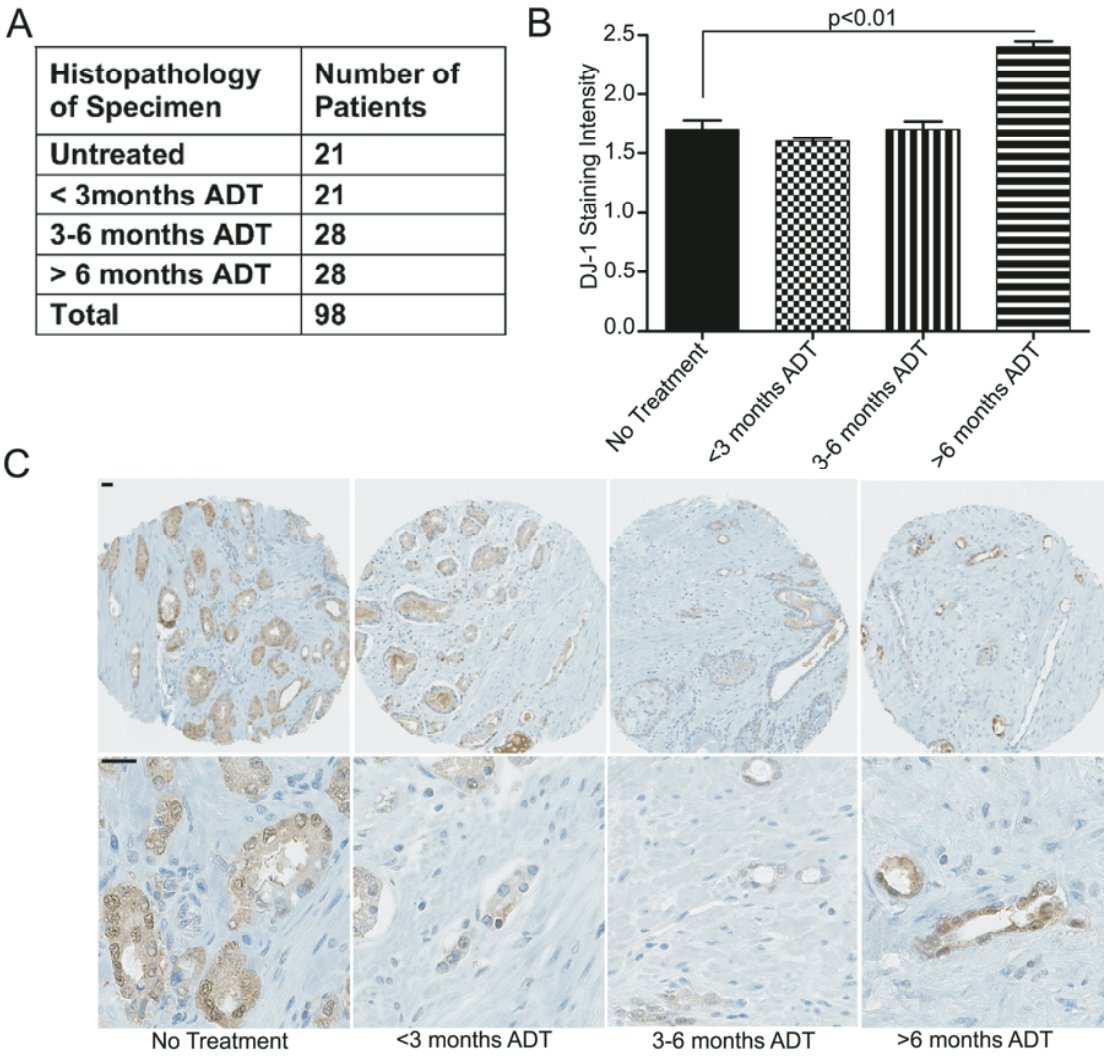

Figure 26: DJ-1 Expression Increases Following Prolonged Androgen Deprivation Therapy (ADT)

A) The number of patients represented per group on the TMA. **B)** Quantification of DJ-1 staining intensity on the ADT TMA. Samples are grouped by amount of time of ADT and DJ-1 staining intensity was evaluated on a 4 point scale, with "0" indicating no positive cells, and "3" indicating intensely positive cells. DJ-1 expression increases significantly in the greater than 6 months ADT group ($p<0.01$). Bars represent mean +/- SEM. **B)** Representative immunohistochemistry images from each of the groups on the array. Scale bars equal 20 microns.

Discussion

DJ-1 is a diverse signaling protein that appears to have multiple roles that may largely depend on cell type and cellular environment (91, 93-95, 97-99). DJ-1 was initially thought to activate AR through indirect mechanisms, for example, by interacting with the AR binding region of PIASx-alpha (Protein Inhibitor of Activated STAT-alpha) and preventing it from binding and inhibiting AR (98). However, it has also been reported that DJ-1 represses AR activity in the SK-N-BE(2)C neuroblastoma cell line (119). From these conflicting reports, it appears that DJ-1 regulation of AR may be cell type dependent. We demonstrate that DJ-1 directly interacts with AR and that DJ-1 functions as a positive regulator of AR signaling in two PCa cell lines, possibly through multiple mechanisms.

Direct interaction between DJ-1 and AR was determined using a yeast two-hybrid screen of a cDNA library generated from flutamide-activated HPE cells (Figure 21). The interaction was confirmed in LAPC4 cells via co-IP showing that the endogenous proteins interact (Figure 21C-D). Multiple yeast two-hybrid screens have been performed to identify DJ-1 binding partners, but AR has never been reported among them (94, 96-98, 118). DJ-1 was shown to interact with the apoptotic protein Daxx when a human brain cDNA library was screened using this technique. This interaction was confirmed and demonstrated to prevent cellular apoptosis following apoptotic stimuli in neuronal cells (94). DJ-1 interacts with PIASx-alpha and DJ-1 Binding Protein (DJBP) (98, 118). Both of these proteins are co-repressors of AR. DJ-1 was shown to interact with both proteins in mammalian cells resulting in increased AR transcriptional activity. Our

screen did not identify DJBP or PIASx-alpha, however, this may be due to differences in the cDNA libraries and cell lines used. Previous studies were performed in COS and 293 cells and relied on transient transfection into these AR negative cell lines, while our experiments were carried out with prostate cell lines and largely examined endogenous proteins.

We demonstrate that the DJ-1:AR interaction is hormonally regulated in both LNCaP and LAPC4 cell lines. Specifically, anti-androgen treatment increases the DJ-1:AR interaction in both cell lines to a greater extent than DHT (Figure 22). Immunofluorescence also demonstrates that hormonal treatment increases the co-localization between DJ-1 and AR in LNCaP cells (Figure 23C and D). Co-localization was not quantified from immunofluorescent images in LAPC4 cells due to low AR levels except after DHT treatment.

Further, both androgens and anti-androgens increased nuclear localization of DJ-1, providing a potential mechanism for DJ-1 regulation of AR in the nucleus. Interestingly, increased nuclear DJ-1 is observed after androgen and anti-androgen treatment in both LAPC4 and LNCaP cell lines (Figure 23A-C). Nuclear/cytoplasmic extracts and immunofluorescence demonstrate the increase in DJ-1 and AR expression (Figure 23A-C) and co-localization (Figure 23D) following treatment. In LAPC4 cells, DHT, OH-flutamide, and bicalutamide treatment result in approximately equal levels of nuclear DJ-1 (Figure 23A). However, in LNCaP cells, DHT treatment results in higher levels of nuclear DJ-1 than either OH-flutamide or bicalutamide (Figure 23B-D).

Additionally, DHT and bicalutamide treatment resulted in DJ-1:AR co-localization throughout the nucleus, whereas DJ-1:AR appeared to concentrate just inside the nuclear perimeter after OH-flutamide treatment. These differences may be due to the well characterized AR T877A substitution mutation in LNCaP cells (137) (72) (84). This mutation allows flutamide to exhibit agonist activity, however, since this mutation causes an AR conformational change, it could inhibit the interaction with DJ-1. Alternatively, the differences between the LNCaP and LAPC4 cells may be due to differences in signaling pathways between the cell lines. For example, DJ-1 has been shown to antagonize the tumor suppressor, PTEN (95). LNCaP cells lack functional PTEN (30) while the PTEN pathway is intact in the LAPC4 cell line (27). Since the exact role of DJ-1 in the PTEN pathway remains unclear, it is possible that loss or inactivation of members of this pathway alter the function of DJ-1.

Modulation of DJ-1 expression regulates AR transcriptional activity in LAPC4 cells suggesting that over-expression of DJ-1 could facilitate AR activation in the absence of androgens (Figure 24A and C). We previously identified DJ-1 as a protein which is up-regulated with anti-androgen treatment in primary HPE and LNCaP cells. Currently, TMA analysis of DJ-1 expression demonstrates that DJ-1 does not change with Gleason pattern, but increases significantly after 6 months of ADT (Figures 25 and 26). This correlates with our previous data and is the first reported large scale evaluation of DJ-1 expression in PCa. Additionally, the importance of this study should be emphasized, due to the difficulty in obtaining tissue samples from patients who received ADT prior to surgery. However, the current study did not evaluate DJ-1 staining intensity in relation to

the patient's overall PCa risk which is determined by clinical parameters such as PSA and total Gleason score. This is a potential future direction as well as determining whether DJ-1 staining intensity correlates with PCa recurrence or time-to-recurrence.

Current and previous data demonstrate that anti-androgens stabilize DJ-1, increase nuclear localization, and increase the interaction between DJ-1 and AR. Further, DJ-1 expression increases in patients who received more than 6 months ADT providing clinical evidence that DJ-1 is involved in AIPC. Taken together, these data demonstrate that DJ-1 is a novel AR binding protein that may be part of a group of genes regulated by anti-androgens. Factors, such as DJ-1, that are regulated by anti-androgens may increase following anti-androgen therapy to activate AR in the absence of androgens. Future studies are needed to identify other anti-androgen regulated genes and to better understand the role they play in PCa progression and activation of AR signaling in the absence of ligand.

CHAPTER V

ADDITIONAL STUDIES TO DETERMINE THE FUNCTION OF DJ-1

Introduction

The following sections provide additional data that was generated during the course of the DJ-1 study. These observations could potentially be developed into studies that investigate the regulation of DJ-1 expression and function in prostate cancer. Furthermore, the yeast two-hybrid system identified other putative DJ-1 binding proteins which could provide novel insights into the role of DJ-1 in prostate cancer.

DJ-1 Promoter

One unexplored area of the DJ-1 field is transcriptional regulation of this multi-functional protein. A 2kb region of the human DJ-1 promoter was entered into the NCBI database (accession number AB045294) but has not been characterized fully. The transcription initiation site was identified and it was determined that DJ-1 expression is dependent on the Sp-1 transcription factor in HeLa cell extracts (152). However, other transcription factor binding sites were not identified. We performed sequence analysis to identify potential transcription factor binding sites that are known to be important in PCa. We included the consensus binding sites for AR, Androgen Responsive Elements (ARE), AP-1, Foxa1, and NF-1 in the initial search of the promoter sequence.

Prostate Cell Lines

Over the last several decades, multiple PCa cell lines have been generated. These cell lines vary between site of origin and molecular characteristics. For example, some cells retain AR expression, but most lose AR and PSA expression after being cultured *in vitro*. Further, some cell lines will grow in a mouse host, while others either do not grow, or grow so quickly that *in vivo* studies are difficult. Each cell line has pros and cons depending on the question under study, and for these reasons most labs have multiple cell lines that are used for experiments. DU145 cells were one of the first PCa cell lines generated and are still used today. DU145 cells originated from a brain metastasis and were first published in 1977 (135, 153). Several years later, the LNCaP and PC3 cell lines were generated from a lymph node and brain metastasis, respectively (135, 153-155). While DU145 and PC3 cells do not express AR at the protein level, LNCaP cells were unique at the time because they retained AR expression (153, 154) (155). Further study of the LNCaP cell line revealed that although they are AR-positive and androgen-responsive, they harbor a well characterized mutation in the ligand binding domain, T877A, which was discussed previously (Chapters III and IV) (72, 73, 135, 137, 156). Since the late-seventies and early-eighties, many more PCa cell lines have been derived. The LAPC4 cell line is a more recent addition to the available PCa cell lines. This cell line was discussed previously (Chapter IV) and has been used in recent years by several groups studying AR. LAPC4 is one of the few PCa cell lines that is androgen-dependent and expresses wild-type AR (135, 147). Our lab utilizes the above PCa cell lines as well

as several other non-prostate cell lines that were screened for DJ-1 expression. Table 3 summarizes some of the important characteristics of these cell lines.

Table 4: Cell Lines That Express DJ-1.

Cell Line	Site of origin	Year published	AR status	Androgen Regulation	References
DU145	PCa brain metastasis	1977	(-)	Androgen-independent	(153, 154)
PC3	PCa bone metastasis	1978	(-)	Androgen-independent	(155)
LNCaP	PCa lymph node metastasis	1980	(+) T887A	Androgen-responsive	(157, 158)
LAPC4	PCa lymph node metastasis	1997	(+) wild-type	Androgen-dependent	(147)
BPH-1	Benign prostate	1995	(-)	Androgen-independent	(159)
HPET	Primary PCa tumor	2007	(-)	Androgen-independent	(160)
HeLa	Cervical cancer	1951	(-)	Androgen-independent	
HeLa AR	Cervical cancer		(+) exogenous	Androgen-independent, androgen-responsive	(161)
NIH-3T3	Mouse fibroblast	1969	(-)	Androgen-independent	(162)

Mouse Prostate and Lady Mouse Model for Prostate Cancer

Although far from identical, the mouse prostate and urogenital system is similar enough to humans to make it a convenient model system. Both species have prostates surrounding the urethra that function similarly to contribute fluid to semen. After birth,

mouse epithelial/stromal cellular differentiation occurs in the first 2-3 weeks when distinct populations of secretory luminal epithelial cells, basal epithelial cells, and stromal cells are formed (5). Briefly, in addition to cellular differentiation, branching morphogenesis occurs after birth whereby the prostatic ducts proliferate at the distal tips. During branching morphogenesis, the once solid epithelial cords branch to form the complex network of glands (reviewed in (5)). By 5 weeks of age prostatic differentiation is complete, resulting in the adult mouse prostate and mice are sexually mature at 6 weeks of age. Unlike human prostate, the adult mouse prostate is composed of multiple lobes – the dorsal (DP), lateral (LP), ventral (VP), and anterior (AP). The dorsal and lateral lobes are connected and surround the urethra (Figure 27) and are sometimes experimentally examined as a single lobe which is referred to as the dorso-lateral prostate or DLP. Due to lobe-specifc patterns of branching, each lobe has a distinct shape (Figure 27). In addition to shape, there are differences in gene expression, morphology, epithelial-infolding, and secretory-activity between prostatic lobes (5).

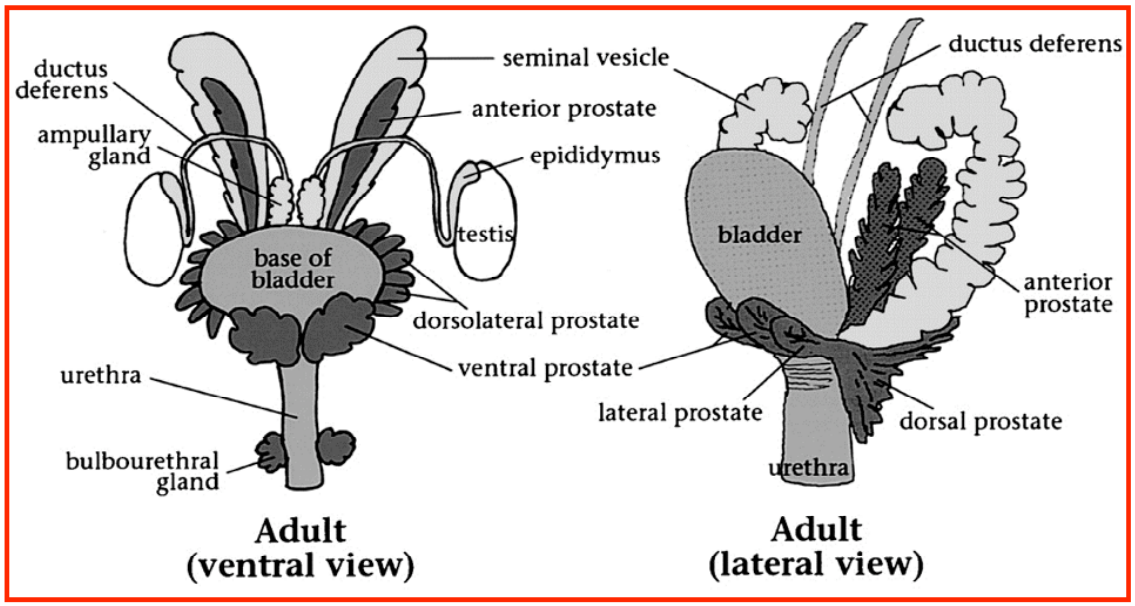

Figure 27: Urogenital System of the Adult Male Mouse Two views are shown. The four lobes of the prostate are shown which are located adjacent to the bladder and surrounding the urethra. Other male urogenital glands include the seminal vesicles, ductus deferens, ampullary gland, epididymus, testis, and bulbourethral gland. Figure from (50).

There are multiple mouse models available to study human PCa progression (reviewed in (115)). Due to the heterogeneous nature and multi-step progression of PCa, it has been difficult to generate a single mouse model that covers all aspects of disease progression. Many PCa models have been generated by over-expression, loss, or mutation of a single gene, but another widely studied series of models was generated by the introduction of the Simian Virus 40 (SV40). The Large-T and small t-antigens are the two most studied viral proteins that compose SV40. Although each protein has multiple functions, a major function of Large-T is inactivation of the tumor suppressors p53 (163) and Rb (164) in order to promoter viral replication and cellular transformation (165).

Small-t antigen has mitogenic activity that facilitates transformation such as activation of the Wnt and MAP Kinase pathways (165).

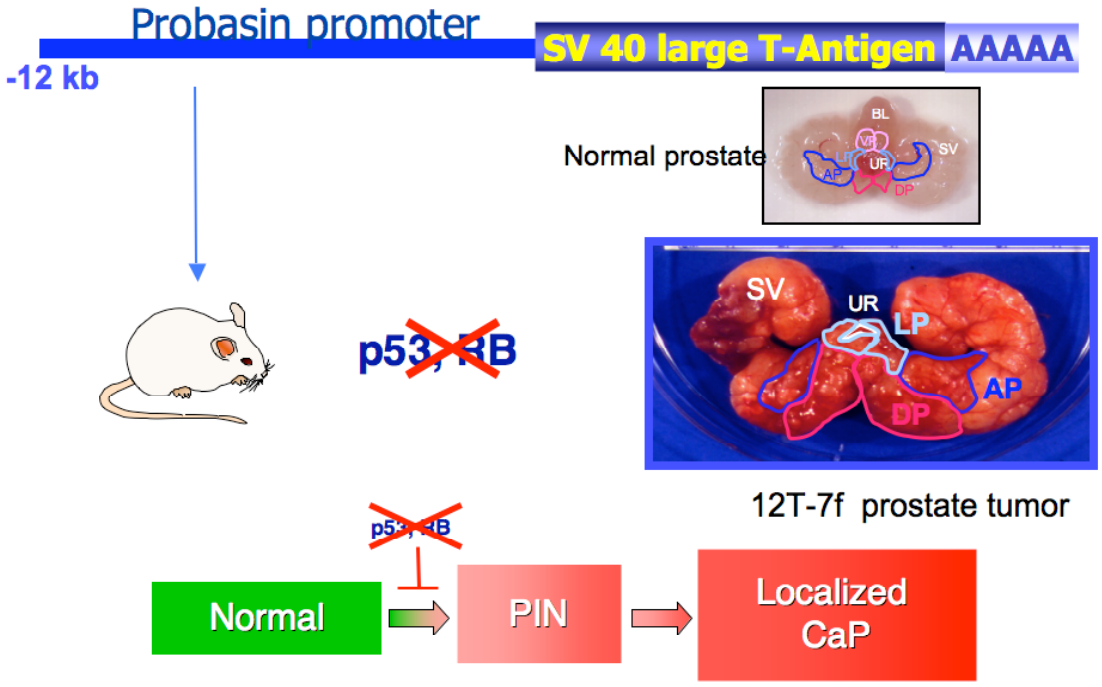

Figure 28 The Lady Mouse Model for Prostate Cancer Progression The large probasin promoter targets the SV40 Large-T antigen to the mouse prostate resulting in inhibition of p53 and Rb and development of localized PCa. The normal mouse prostate and a transgenic prostate are shown with different prostatic lobes and urogenital organs identified. BL=bladder, UR= urethra, AP =anterior prostate, VP=ventral prostate, LP=lateral prostate, DP=dorsal prostate, SV=seminal vesicles .

Several mouse models have been generated using the SV40 Large-T and small-t antigens. The Lady model was generated by targeting the Large-T antigen to the CD-1 mouse prostate using the probasin promoter (LPB-TAg) (Figure 28) (166, 167). Multiple LPB-TAg lines were generated and characterized (166), but this project utilized only the 12T-7f line. The 12T-7f transgenic line has been extensively characterized and the prostates of these mice develop multifocal lesions that express TAg. 12T-7f tumors progress to resemble human low-grade PIN (LGPIN), marked by areas with mild nuclear atypia, and later progress to more pronounced nuclear atypia which resembles human high-grade PIN (166). These tumors do not metastasize to distant sites, although localized invasion has been reported (166). Figure 28 demonstrates the size of the 12T-7f tumors as compared to age-matched wild-type prostate, indicating the location of seminal vesicles (SV), AP, DP, LP, VP, urethra (UR), and bladder (BL). These tumors are androgen-dependent demonstrated by tumor regression following castration, and exogenous androgen treatment that causes tumor re-growth (166). Although these tumors remain androgen-dependent today and the molecular characteristics are similar to those originally reported, there have been noticeable changes to the line over time. Multiple labs have seen an increase in tumor on-set and more rapid tumor growth. For example, when the line was originally characterized, male mice would routinely live past 20 weeks of age before the tumor-burden was life threatening, but today, tumor growth has increased and mice are euthanized at 15 weeks of age before they succumb to tumor-burden due to bladder and bowel obstruction (unpublished observations, Kasper and Matusik laboratories). The reasons behind this increase in tumor growth are unknown, but could be due epigenetic events. For the purposes of this study, it should be noted that

all 12T-7f male mice have large prostate tumors by 10-11 weeks of age, while the prostates of mice younger than 6 weeks are closer to phenotypically normal prostates.

Yeast Two-Hybrid System to Identify DJ-1 Binding Partners

The MatchMaker™ System from Clontech was used to identify novel DJ-1 binding partners in PCa. This screen was described previously (Chapters II and IV). Full-length DJ-1 was used to screen a cDNA library generated from flutamide-activated primary HPE cells. AR was identified as a novel DJ-1 binding partner, which was confirmed and became the major focus of this research project because of the essential role of AR and androgen signaling in PCa (Chapter IV). In addition to AR, 18 other genes were identified as putative DJ-1 binding partners. There is a lack of information on the DJ-1 signaling pathway in PCa, and future research is required to verify the interaction between DJ-1 and these potential binding partners to better elucidate the DJ-1 signaling pathway.

Results

Transcriptional Regulation of DJ-1

Currently there is no published literature on factors that transcriptionally regulate DJ-1. We performed a sequence-based analysis of the human DJ-1 promoter region (NCBI accession number AB045294) using the web-based programs, Transcription Factor Search (TF SEARCH) (http://www.cbrc.jp/research/db/TFSEARCH.html) and

Basic Local Alignment Search Tool (BLAST) (http://www.ncbi.nlm.nih.gov/BLAST/), in order to determine putative transcription factor binding sites. Using these programs, we identified multiple putative binding sites, but no exact matches to consensus sequence binding sites. Imperfect sites include AP-1 (binding sites also known as phorbol 12-O-tetradecanoate-13-acetate (TPA) response elments), NF1, HNF-alpha, and multiple Androgen Recognition Elements (ARE)/Androgen Receptor Binding Sites (ARBS). Figure 29 illustrates the 2119 base pairs of the DJ-1 promoter examined. The percent homology is indicated for potential binding site. The top sequence is the consensus binding site and the bottom sequence is the DJ-1 promoter. Identical pairing is indicated in red. These potential binding sites were of interest for a number of reasons. AP-1 is a well known transcription factor that is composed of Jun and Fos (168) and is involved in multiple aspects of tumor progression including proliferation and inflammation (169) (168). Nuclear Factor-1 (NF-1) is part of a heterogeneous family of transcription factors that range in size and function (170-174). We included the well-conserved NF-1 binding site in this analysis because it has been shown to regulate milk proteins in mammary gland and is associated with hormonal regulation (170, 175, 176). Since mammary tissue is hormonally regulated through nuclear receptor action, there are many parallels to hormonal regulation and signaling cross-talk between breast and prostate (177, 178). FoxA1 is also known as hepatocyte nuclear factor 3 alpha, and is a member of the forkhead class of DNA-binding proteins. FoxA1 and other Fox proteins were originally described in development of endodermally derived tissues and in the regulation of liver-specific transcripts such as albumin (179). A member of our group discovered that FoxA1 is required for AR-mediated gene activation and that FoxA binding sites flank

AREs in the promoter region of PSA and probasin (180). Further, FoxA1 was expressed in human adenocarcinoma regardless of Gleason score, while FoxA2 was found only in neuroendocrine PCa (181). FoxA consensus binding sites were included in this analysis because at the time it was unknown whether DJ-1 was an androgen regulated gene. If FoxA binding sites flanked AREs as in PSA and probasin, it would add confidence that the sites were functional.

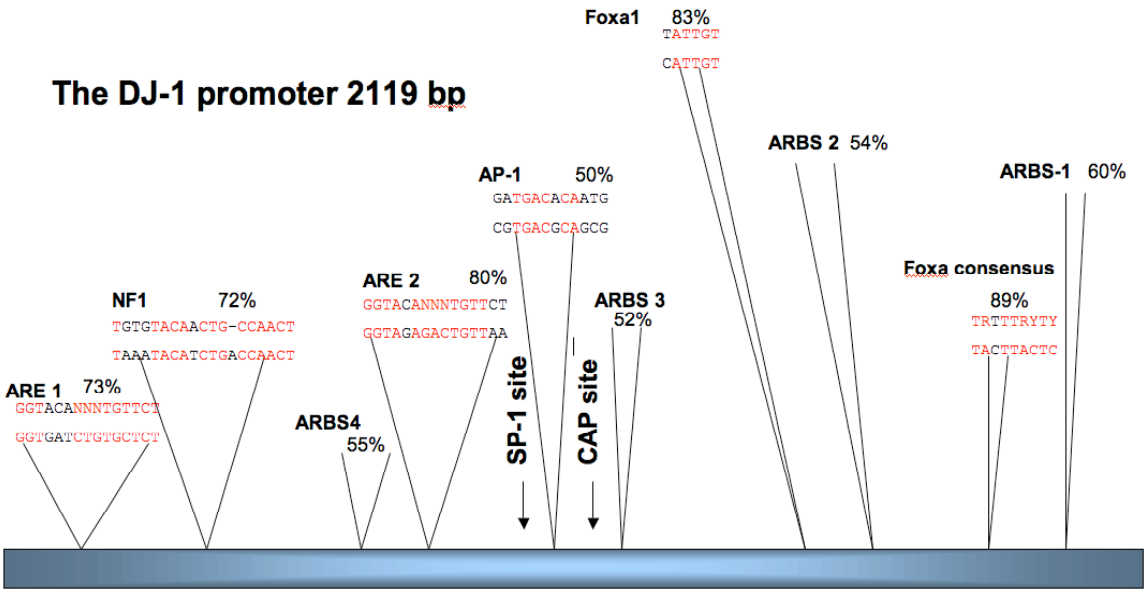

Figure 29: The Human DJ-1 Promoter Potential transcription factor binding sites were identified based upon sequence similarity. The percent homology is shown for each site. Top line of sequence is the consensus/published site and the bottom line is the DJ-1 sequence. Identical base pair matches are in red. Known Sp-1 and CAP sites are listed.

In order to determine whether any of the putative sites are functional, we planned to make truncations of the DJ-1 promoter region and clone the fragments upstream of the luciferase reporter. These reporter plasmids would be used to determine which region of the promoter was required for activity. Once identified, the region of interest could be used for band-shift assays with the appropriate purified transcription factors to determine an interaction. Transfection assays would be utilized to determine the effects of these transcriptional regulators on DJ-1 expression. However, due to difficulties cloning the region of the DJ-1 promoter, and a change in the direction of the project, these experiments were not completed.

Characterization of DJ-1 Expression in Prostate Cancer Model Systems

Expression in human PCa cell lines

Initially, there was little information on the expression pattern of DJ-1 in model systems for PCa including established human PCa cell lines and mouse models. Our lab uses a variety of cell lines, and it was important to determine the DJ-1 expression pattern in these cell lines.

The cell lines commonly used in our laboratory include: NIH 3T3, LNCaP, DU145, PC3, BPH1, LAPC4, HeLa, HeLa AR, and HPET (primary HPE cells immortalized with human Telomerase Reverse Transcriptase (hTERT)). Total protein was extracted from each of these cell lines at low and high confluency and used for Western Blot. This experiment revealed that DJ-1 is expressed in all cell lines currently

available to our laboratory and that increased confluency appeared to increase DJ-1 expression (Figure 30). Human beta-actin was used as a loading control, but after this experiment we determined that the levels of beta-actin vary between cell lines and is not a suitable loading control for this type of experiment. Nevertheless, we demonstrate that DJ-1 is widely expressed in available cell lines.

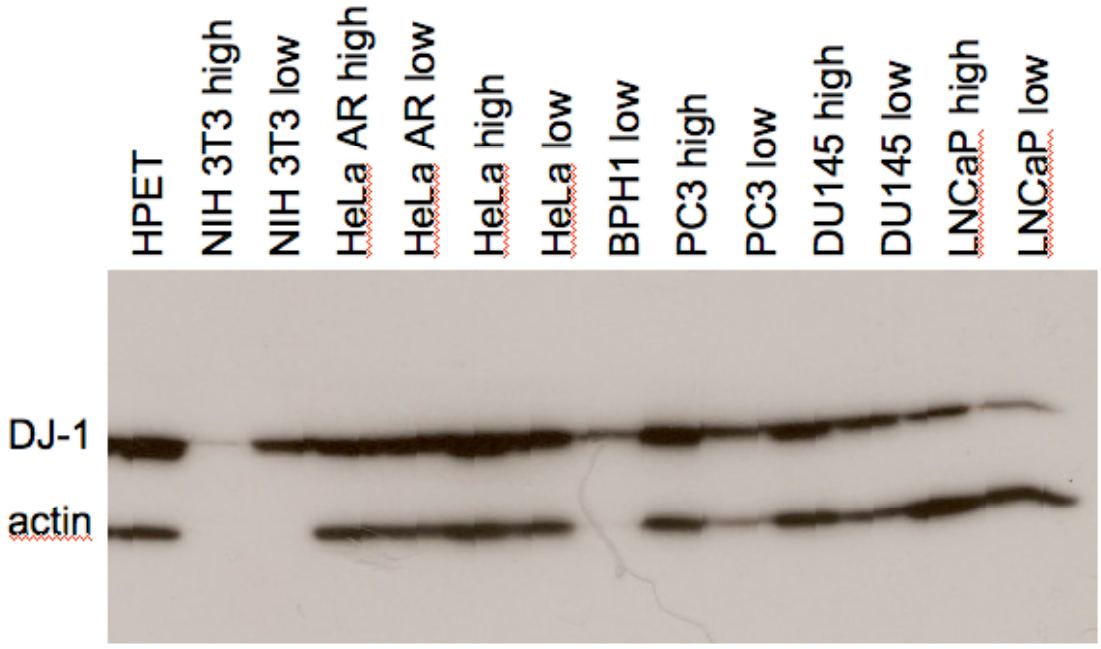

Figure 30: DJ-1 Expression in Available Cell Lines Western blot for DJ-1 expression in cell lines at high and low confluency. Human beta-actin used as a loading control.

Over-expression of DJ-1 Does Not Affect Growth or Motility of LNCaP and DU145 Cells

Based upon previous published data identifying DJ-1 as an oncogene, we over-expressed DJ-1 in the LNCaP and DU145 cell lines using the ViraPower lentiviral

expression system (Invitrogen). Increased expression of DJ-1 transformed both cell lines to some degree, as seen by formation of small colonies (Figure 31), However, it did not alter motility or proliferation in either cell line (data not shown). This experiment was repeated using a higher multiplicity of infection (MOI) in an attempt to over-express DJ-1 by 50 and 100 fold the endogenous level. This experiment was performed in LNCaP cells since they express endogenous AR. For an unknown reason, the transgene was expressed, but not at 50 or 100 fold as expected (Figure 32). This could be due to toxicity from using this level of virus, and only those cells infected with less DJ-1 virus survived. Even though these cells did not express higher levels of DJ-1 than observed with the initial experiments, proliferation assays were performed, but showed no difference between vector control and DJ-1 over-expressing cells. These experiments imply that in LNCaP cells DJ-1 could potentially function as an oncogene to transform cells, but that DJ-1 does not play a role in cell migration or invasion.

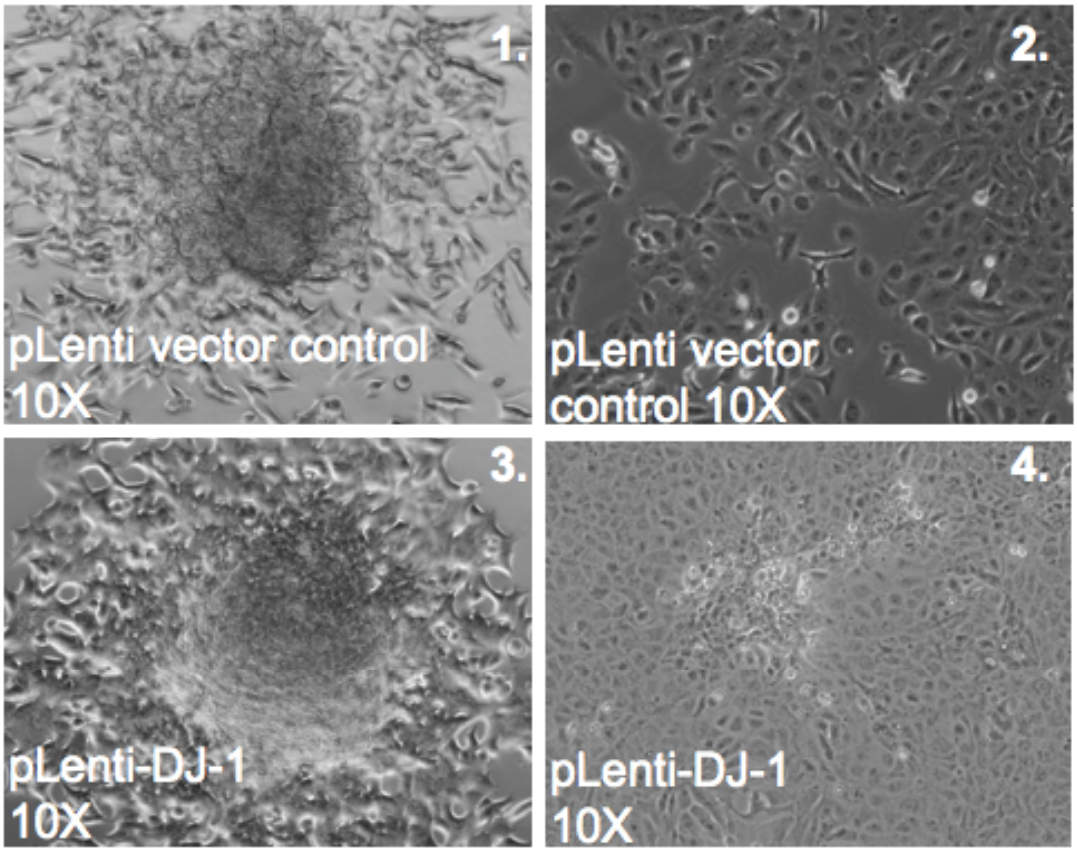

Figure 31: Over-expression of DJ-1 Causes Colony Formation in LNCaP and DU145 cells. Overexpression of DJ-1 in LNCaP and DU145 cells causes colony formation consistent with published reports in NIH 3T3 cells (93).

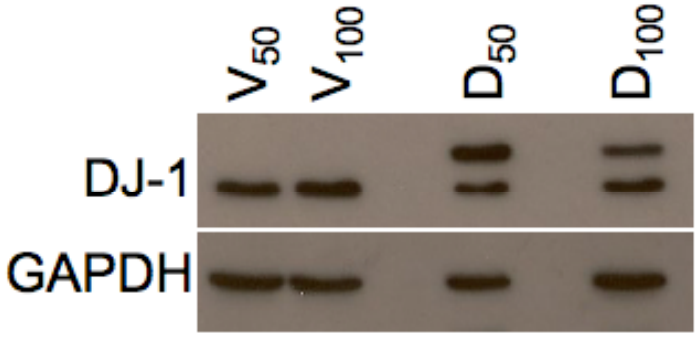

Figure 32: Expression of V5-tagged DJ-1 in LNCaP cells. LNCaP cells were infected at 50 and 100 MOI concentration of virus with either an empty vector (V_{50} and V_{100}) or V5-DJ-1 plasmid (D_{50} and D_{100}). Anti-DJ-1 antibody recognizes both tagged and un-tagged DJ-1.

Development of a Tetracycline (TET) Inducible DJ-1 shRNA Cell Line

DJ-1 is a highly conserved ubiquitiously expressed protein. Throughout the course of this research project, a DJ-1 negative cell line or tissue could not be found. Therefore, we sought to generate a human prostate cancer cell line that stably expressed a shRNA targeted against DJ-1. These cells could then be xenografted into SCID mice and compared to the parental cell line to determine the effect of DJ-1 on tumor growth *in vivo*.

LNCaP TET-ON cells that stably express the Tetracycline Repressor and Tetracycline Operon were obtained from Dr. Renjie Jin in Dr. Robert Matusik's laboratory at Vanderbilt. A viral mediated TET-inducible DJ-1 shRNA plasmid was purchased from Genscript. Figure 33 illustrates the features of this plasmid. When LNCaP TET-ON cells are infected with the TET-inducible DJ-1 shRNA plasmid, and treated with doxycycline, shRNA expression is induced, and DJ-1 expression should be knocked-down. After infection, cells expressing the DJ-1 shRNA plasmid were FACS sorted using the GFP marker. These cells were then treated with doxycycline (Dox) to induce shRNA expression, harvested, and analyzed by Western Blot. Treatment with 10 ug/ml doxycyline knocked-down DJ-1 expression to approximately 50% of the non-targeting control shRNA. AR expression did not change with modulation of DJ-1, which is consistent with previous data (Figure 34 and Figure 24, chapter IV). Although these cells were not used further in the present study, they are an available tool for future DJ-1 research.

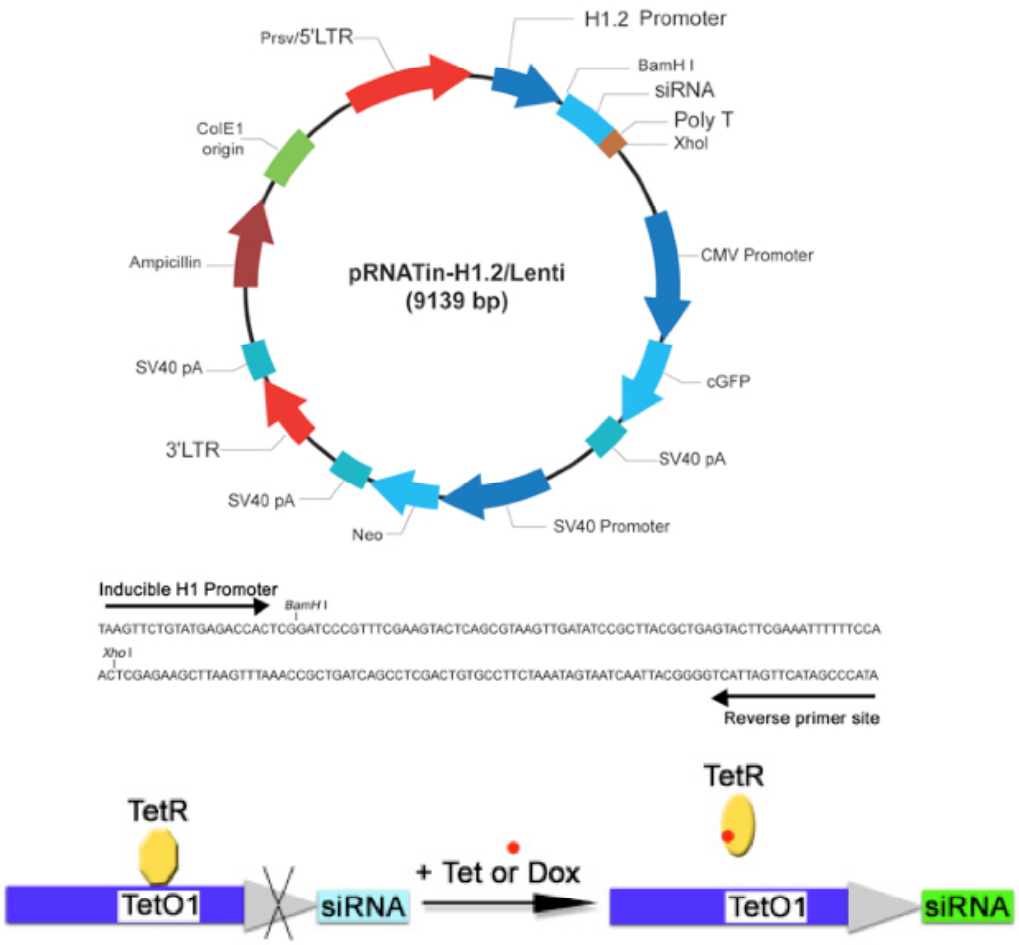

Figure 33: Tetracycline-inducible shRNA system. A Tet-inducible shRNA plasmid purchased from Genescript and a cartoon describing the Tet-inducible expression system.

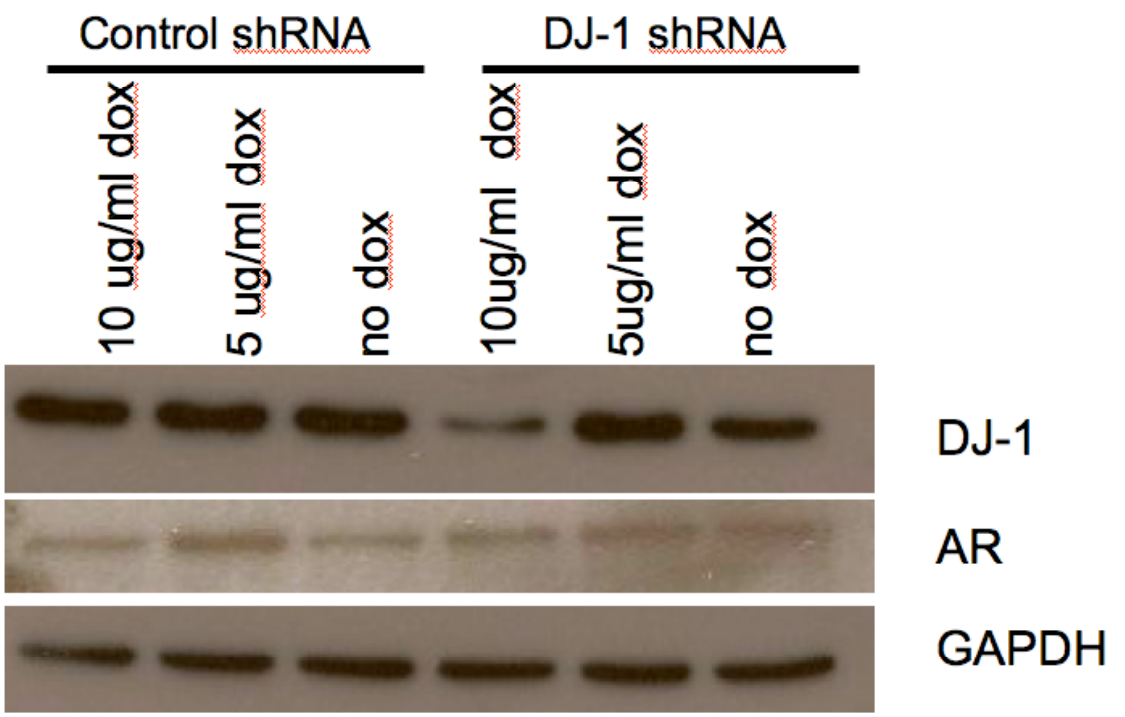

Figure 34: Knockdown of DJ-1 Using a Tet-Inducible shRNA in LNCaP Cells LNCaP TET-ON cells were stably infected with a cassette for either an inducible control shRNA or inducible DJ-1 shRNA. Cells were treated with two concentrations of doxycycline (dox) to induce shRNA expression. DJ-1 expression decreases following a high dose of dox, while AR is unchanged. GAPDH loading contol.

Expression in CD-1 and 12T-7f mice

To determine whether DJ-1 was expressed in mouse prostate, total RNA was extracted from 6 week and 15 week wild-type (CD-1) and LADY 12T-7f dorsal prostates, reverse transcribed, and used for RT-PCR. cDNA from LNCaP cells was used as a positive control for the PCR reaction. DJ-1 was expressed at the mRNA level at both time points in CD-1 and 12T-7f mice (Figure 35). Western Blot of total protein from 3 and 15 week CD-1 dorsal prostates and 13 week 12T-7f mice confirmed this expression at the protein level (Figure 35). In addition to dorsal prostates, the NeoTAg 1 and 2 cell

lines were included in this analysis. These cell lines were generated and obtained from Dr. Yongquing Wang in the Matusik laboratory at Vanderbilt. The NeoTAg cell lines were derived from the 12T-7f prostate tumors and have been previously described (182). As expected, DJ-1 is expressed in these mouse PCa cell lines as well as in the primary 12T-7f tumors.

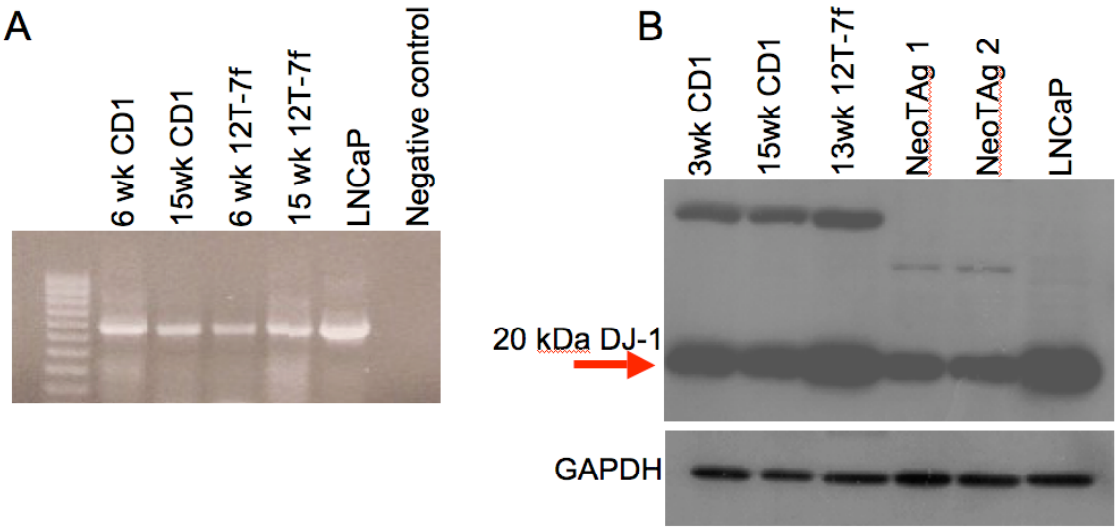

Figure 35: DJ-1 Expression in Mouse Dorsal Prostates and Cell Lines. A) RT-PCR shows that DJ-1 is expressed in wild-type and 12T-7f prostates. **B)** Western blot analysis confirms DJ-1 expression and demonstrated an increase in 12T-7f dorsal prostate. NeoTAg 1 and 2 are cell lines that are derived from 12T-7f prostate tumors. LNCaP human PCa cell line was used as a positive control. The larger bands at 80 and 50 kDa have not been observed in human cells or tissues and may represent mouse-specific post-translationally modified forms of DJ-1.

In order to complete the expression profile for DJ-1 in both developing prostate and in tumorigenesis, total RNA was extracted from dorsal prostates CD-1 and 12T-7f mice at 2, 3, 4, 5, 6, 10, and 15 weeks of age. Each sample represents a pool of total RNA from the individual age group as described (123). cDNA was prepared and used for

quantitative realtime RT-PCR. DJ-1 was expressed at all ages in both CD-1 and 12T-7f mice (Figure 36). Interestingly, DJ-1 expression is higher at all ages in the 12T-7f mice. Further, DJ-1 expression peaks at 3-4 weeks in both wild-type and 12T-7f mice during prostate differentiation and at 15 weeks in the 12T-7f tumors.

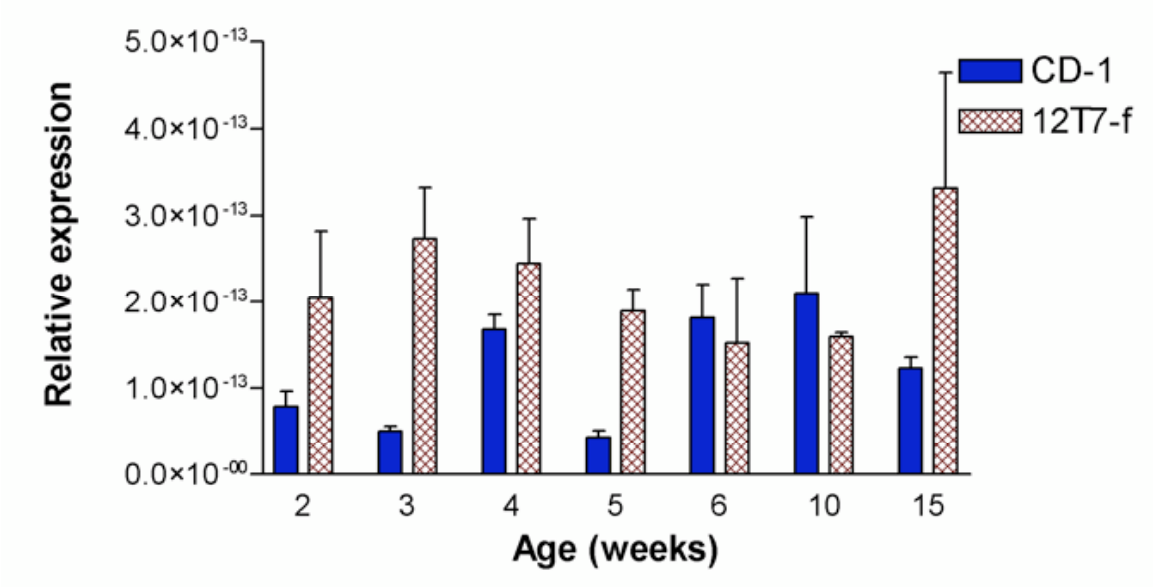

Figure 36: Real-time RT-PCR Analysis of DJ-1 Expression in CD-1 and 12T-7f Mouse Dorsal Prostates. Realtime RT-PCR analysis of DJ-1 expression at different aged CD-1 and 12T-7f mice. DJ-1 relative expression was determined by normalization to 18S rRNA control. CD-1 solid blue bars, 12T-7f hatched bars. Each bar represents mean +/- SEM.

Immunohistochemical analysis of 3- and 15-week CD-1 and 15-week 12T-7f dorsal prostates confirmed the real-time RT-PCR results indicating that DJ-1 expression was higher in 12T-7f tumors than in wild-type adult prostate (Figure 37). Additionally, DJ-1 subcellular localization changes from predominantly cytoplasmic in the 3-week old CD-1 dorsal prostate to nuclear in the 15-week adult growth-quiescent prostate. DJ-1

was highly expressed and mainly cytoplasmic in the adult 12T-7f prostate. Additional experiments determined that DJ-1 was cytoplasmic regardless of age in the 12T-7f mice (data not shown).

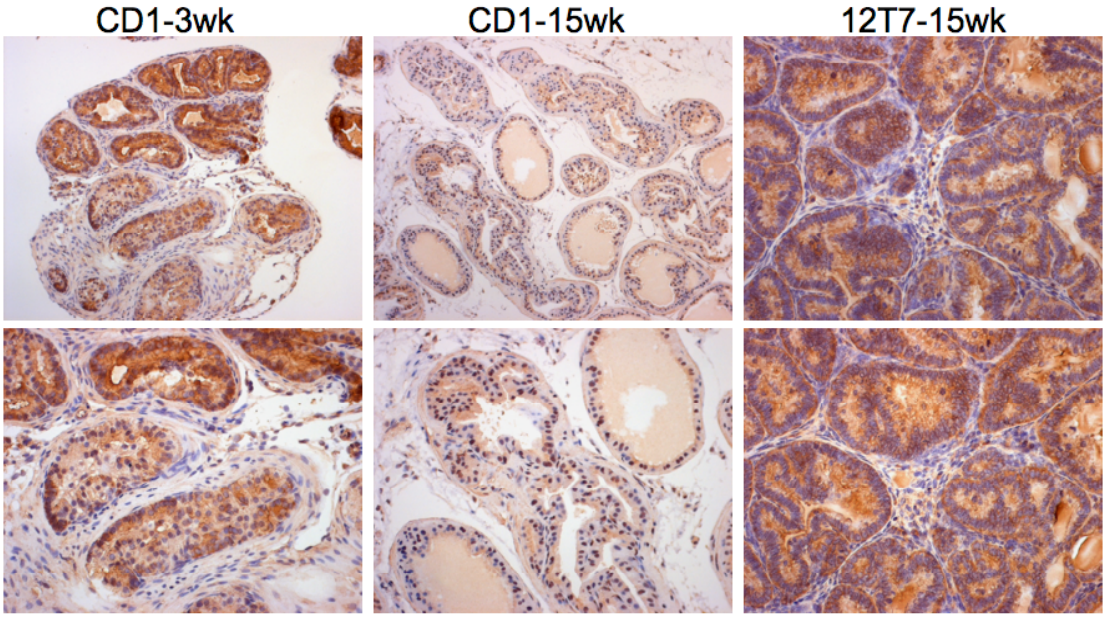

Figure 37: Immunohistochemical Analysis of DJ-1 Expression and Subcellular Localization in CD1 and 12T-7f Mouse Dorsal Prostates. Immunohistochemical staining for DJ-1 on dorsal CD1 and 12T-7f prostate lobes shows increased DJ-1 expression in the 3 wk developing prostate and in the 12T-7f prostate tumors. Subcellular DJ-1 localization changes from predominantly cytoplasmic in the 3 wk CD-1 prostate to predominantly nuclear in the 15 wk adult prostate. Interestingly DJ-1 is predominantly cytoplasmic regardless of age in 12T-7f prostates. Low (top) and high (bottom) magnifications for each sample are shown.

Hormonal Regulation of DJ-1 Expression in 12T-7f Mice

Total RNA was extracted from the dorsal prostates of CD-1 and 12T-7f mice that had been surgically castrated for 1, 2, 4, or 12 weeks and used for realtime RT-PCR analysis of DJ-1 expression. After castration, DJ-1 expression is maintained in both CD-1 and 12T-7f mice (Figure 38). DJ-1 expression peaked after 2 weeks of castration in the 12T-7f prostates, and returned to basal levels by 4 weeks post-castration. Error bars represent the mean +/-SEM between samples from different mice. For intact mice and the 12-week post-castration sample, there are no error bars because only one sample was available. However, this experiment was repeated twice with the same trend.

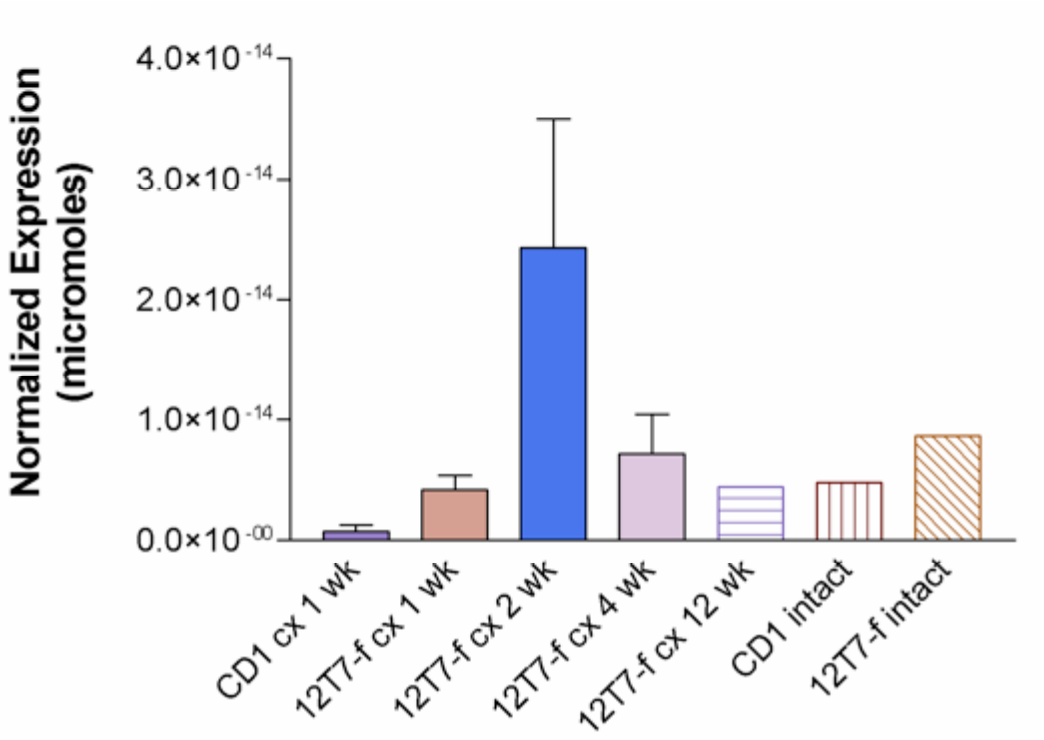

Figure 38: Real-time RT-PCR Analysis of DJ-1 Expression After Castration in CD-1 and 12T-7f Dorsal Prostates Real-time RT-PCR analysis of DJ-1 expression in the dorsal prostates post-castration. Sample and time after castration is indicated on the x-axis. Relative DJ-1 expression afer normalization to 18S rRNA in micromoles on the y-axis. DJ-1 expression increases in 12T-7f mice 2 weeks after castration before falling to basal levels at 4 weeks post-castration.

Table 5: Putative DJ-1 Binding Partners from Yeast Two-Hybrid Screen The gene name is listed along with NCBI protein accession number. The number of times the gene was represented in the screen is listed as the number of "clones" identified. The length of the exact alignment between the experimental sequence and the published sequence is listed in base pairs (bp). Any known interesting functions that might be relevant in PCa are listed on the right.

Gene	NCBI protein	clones	bp	Interesting Functions
Enolase 1	NP_001419	1	893	Tumor suppressor, perturbs cell proliferation by inhibtion of cyclinA and B1 (183)
Carcinoembryonic antigen-related cell adhesion molecule 5 (CEACAM5)	NP_004354	2	362	Cell adhesion; inhibition in colon cancer increases metastasis (184)
P-cadherin	NP_001784	8	823	Associated with aggressiveness in breast cancer (185)
NOL1/Sun domain member 5 (NSUN5)	NP_060514	1	647	Uncharacterized, has similarity to p120(NOL1)
Procollagen-lysine, 2-oxoglutarate 5-dioygenase 1 (PLOD-1)	NP_000293.2	1	211	Membrane-bound in endoplasmic reticulum; hydroxylation of collagen-like peptides
Carboxypeptidase D	NP_001295.2	1	829	metallopeptidase
Myosin 1C	NP_001074248	1	397	Non-conventional myosin isoform
Makorin 2	NP_054879.3	1	441	Uncharacterized ring-finger protein
Sirtuin 7	NP_057622.1	1	273	Unknown function, increased in breast cancer (186)
Ubiquitin-specific Protease 15	NP_006304.1	3	804	Degradation of ubiquitin
LDL related protein 1 (LDP1)/ApoE Receptor	NP_002323.1	1	466	Apolipoprotein E receptor
Solute Carrier Family 3, member 2 (SLC3A2)	NP_001012679.1	2	549	Membrane bound, regulates integrin-dependent signaling
Filamin B	NP_001448.2	1	232	Cell adhesion/Actin-binding protein
NADH-Ubiquinone Oxidoreductase Fe-S	NP_002487.1	1	797	unknown
FK506 BP9	NP_009201.2	1	397	unknown
Co-stimulatroy B7 molecule CD276	NP_001019907.1	1	468	Signaling
ADAM15	NP_003806	1	760	Cell adhesion, associated with aggressive prostate and breast cancer (187)
Plexin A1	NP_115618	1	801	Impairs chemotaxis (188)

Additional Putative DJ-1 Binding Partners in Prostate Cancer Epithelial Cells

After sequence analysis, multiple putative DJ-1 binding proteins were identified. In addition to AR, 18 other proteins were identified in the screen. Table 4 lists the genes identified, the NCBI accession number, the number of times identified in the screen, the length of the exact alignment with the published gene sequence in base pairs, and known functions of the protein. Several proteins were previously implicated in cancer. For example, inhibition of Carcinoembryonic antigen (CEA) in colon cancer inhibits apoptosis and increases metastasis (reviewed in (189)). ADAM 15 (A Disintegrin and Metallopeptidase 15) is a transmembrane glycoprotein that is involved in cell adhesion. ADAM 15 is over-expressed in breast and prostate adenocarcinoma and may play a role in metastasis (187). P-cadherin is another cell adhesion molecule that has been implicated in PCa. P-cadherin expression has been correlated with breast cancer aggressiveness (185). Other potential DJ-1 binding partners may be important in PCa, but have not been studied in prostate. PLOD 1 (Procollagen-lysine 1,2 oxoglutarate 5-dioxygenase 1) was identified as a potential AR binding protein in an independent yeast two hybrid screen performed in our laboratory (unpublished data). Currently, the role of PLOD 1 in PCa is unknown, but it could mediate AR signaling and form a heterotrimeric complex with DJ-1 and AR. Finally, there were several proteins identified that have not been characterized including Sirtuin and FK506 binding protein 9 (FKBP9). Interestingly, another protein in the FK506 binding protein family, FKBP52, is a heat-shock binding protein implicated in regulation of GR and AR. Male FKBP52 null mice exhibit dysgenic prostates and

ambiguous external genitalia. (190, 191). The FK506BP family is large and diverse, so it is unknown at this time whether FKBP9 plays a role in PCa or AR signaling.

Initial experiments were performed to determine the expression of several genes of interest from the yeast two hybrid screen. Genes were chosen based upon available reagents and interest to existing projects in the laboratory. Based upon these criteria, AR, PLOD-1, P-cadherin, and FKBP9 were examined. Expression profiles for these genes were determined in cell lines available in our lab. RT-PCR was performed using cDNA from the prostate derived LNCaP, DU145, BPH1, PC3 cell lines as well as the cervical cancer cell line HeLa AR. HeLa AR cells have a stably integrated human AR and have been used for many years to study AR signaling. Figure 39 shows that P-cadherin is expressed at the mRNA level in all cell lines tested. FKBP9 was present in all cell lines except LAPC4. PLOD-1 is expressed in all cell lines tested except for DU145. As expected, AR was expressed more highly in LNCaP, HeLa AR, and LAPC4 cells which express functional AR protein. PC3, DU145, and BPH1 cells were weakly positive at the mRNA level for AR, but these cell lines do not have functional protein (135). DJ-1 was a positive control since it was known to be expressed in all of the cell lines examined.

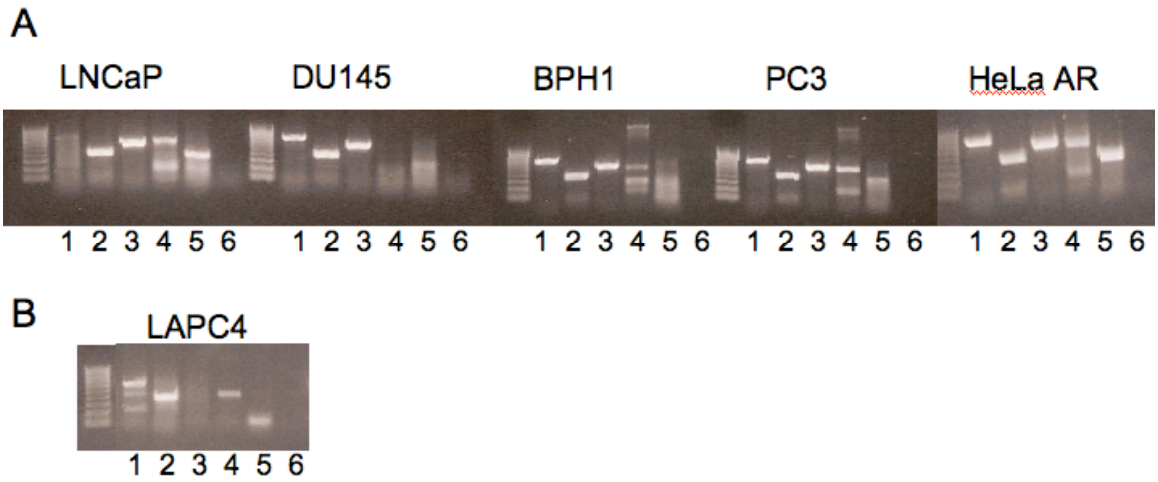

Figure 39: Expression of Genes of Interest From DJ-1 Yeast Two-Hybrid Screen RT-PCR of the indicated cell lines for several of the genes of interest. **A)** 1= FKBP9, 2=P-cadherin, 3=DJ-1, 4=PLOD-1 (upper band in LNCaP and HeLa AR cells is expected size), 5=AR, 6= negative control. B) Loading order is different than A. Here, 1=PLOD-1, 2=AR, 3=FKBP9, 4=P-cadherin, 5=PSA (control), 6= negative control. Annealing temperatures for some primer pairs are not optimized, which resulted in multiple bands.

After expression analysis was performed for the genes of interest, we wanted to determine whether modulation of expression of the genes of interest affected AR transcriptional activity since DJ-1 interacts with AR. To address this, commercial pooled siRNAs directed against PLOD-1 and FKBP9 were purchased from Dharmacon to knockdown expression of these genes and perform androgen-regulated luciferase assays (described in chapter IV). Initial transfections of siRNAs into LNCaP and HeLa AR cells demonstrated that both siRNA pools were moderately effective in knocking down PLOD-1 and FKBP9 at the mRNA level, but luciferase assays after down-regulation of PLOD-1 and FKBP9 showed very low AR activity, even in the positive control samples. For this reason, no conclusions can be drawn from this data (data not shown). At the time these experiments were performed, pooled siRNAs for P-cadherin were not available. These

experiments could be completed in the future to determine whether these are true DJ-1 binding partners and whether or not they affect AR transcriptional activity.

The list of putative DJ-1 binding partners is varied and includes proteins involved in cellular adhesion, signal transduction, and enzymatic reactions. Although the list of potential binding partners is diverse, this was expected based upon the heterogeneous DJ-1 literature. DJ-1 has been implicated in multiple diseases and signaling pathways. The interaction between DJ-1 and AR was confirmed (Chapter IV), but 19 other putative binding partners must be studied further. Future research should validate the potential binding partners and better define the precise role of DJ-1 in the pathways identified.

Discussion

Currently, there are still many aspects of the role of DJ-1 in PCa that are not understood. This project has provided information in multiple areas relating to DJ-1: potential transcriptional regulation of DJ-1, DJ-1 expression and regulation in PCa model systems, and additional putative binding partners.

Transcriptional regulation of DJ-1 is a completely novel area of research in the DJ-1 field. We used sequence analysis programs to identify potential transcrition factor binding sites in a 2kb region of the human DJ-1 promoter. This analysis identified multiple putative sites, but none with exact homology to the published binding site. Additional analysis is required to determine whether any of these putative sites are functional. Based upon data presented in previous chapters, however, it is unlikely that

the androgen receptor binding sites are functional. Specifically, the increase in DJ-1 expression after treatment with androgens and anti-androgens is due to protein stabilization rather than increased transcription of DJ-1 (Figure 20). Furthermore, treatment with TPA, which activates AP-1, did not increase DJ-1 protein levels in LNCaP cells. This result may indicate that DJ-1 is not regulated by the AP-1 transcription factor, however, AP-1 activation often requires other factors, so there is still a possibility that AP-1 regulates DJ-1. A complete analysis after TPA treatment was not performed, nor were additional experiments to confirm the NF-1 binding sites. Based upon the multiple roles of DJ-1 in different tissues, it is likely that transcriptional regulation varies between tissues, and that there are additional unidentified binding sites in the promoter region.

Multiple research groups have identified DJ-1 in different model systems and tissues. In accordance with this, we discovered that DJ-1 is widely expressed in PCa model systems. Using RT-PCR, Western Blotting analysis, and Immunohistochemistry, we showed that DJ-1 is expressed in multiple human and mouse cell lines as well as in normal mouse prostate and in the 12T-7f mouse model (Figures 30, 35-38). Quantitative realtime-RT-PCR determined that DJ-1 is expressed at higher levels in 12T-7f dorsal prostate as compared to wild-type prostate. Further, expression peaks during prostate differentiation and tumorigenesis, implying that DJ-1 is involved in both processes (Figure 36) corresponding to our data on DJ-1 in human PCa. Interestingly, DJ-1 is differentially expressed in the cytoplasm and nucleus of wild-type CD-1 dorsal prostates (Figure 37). DJ-1 was predominantly cytoplasmic in 3 week-old developing prostate, but was mainly nuclear in the 15 week old growth quiescent gland. DJ-1 was predominantly

cytoplasmic regardless of age in the 12T-7f dorsal prostate. This suggests that DJ-1 may function similarly during prostate differentiation and tumorigenesis and that sub-cellular localization may determine or affect DJ-1 activity. Currently it is unknown what factors regulate DJ-1 sub-cellular localization. We have observed differential localization in the LNCaP and LAPC4 cell lines following hormonal treatment (Figure 23). It is possible that DJ-1 is transported between sub-cellular compartments as part of a multi-protein complex. We showed that DJ-1 binds AR, which translocates to the nucleus after hormonal treatment. Since DJ-1 binds AR and DJ-1:AR co-localization increases after hormonal treatment, it is possible that DJ-1 is complexed with AR during nuclear translocation. Another important aspect of DJ-1 differential sub-cellular localization is that location may determine which proteins DJ-1 interacts with, and subsequently, what pathways/cellular processes DJ-1 regulates.

The DJ-1 yeast two-hybrid identified multiple putative DJ-1 binding partners. Since DJ-1 is differentially expressed in the nucleus and cytoplasm, it could interact with proteins in both cellular compartments. Several cell adhesion proteins were identified in the yeast two-hybrid screen, including ADAM 15 and P-cadherin. Both proteins are membrane bound, but it is possible that DJ-1 binds the intracellular portion. PLOD1 is also membrane bound, but is localized to the ER. DJ-1 is expressed throughout the cytoplasm, so PLOD1 is a potential cytoplasmic DJ-1 binding partner. The majority of the proteins identified in this screen have not been studied in PCa, and some have not been studied at all. Determining the number of real binding partners from this list was

beyond the scope of this research project, but hopefully will be a useful starting point for future DJ-1 research.

The initial experiments performed to investigate DJ-1 in PCa were varied because of the initial lack of published data on DJ-1. Multiple small projects were started in an attempt to elucidate the function of this protein. The role of DJ-1 in modulating AR signaling became my project of interest. However, the preliminary data presented in this section can be utilized to begin elucidating the regulation of DJ-1 expression in prostate cancer. Furthermore, the interaction of DJ-1 with novel binding proteins and the effects of DJ-1 sub-cellular localization could provide new insight and avenues of research into the functions of this diverse protein.

CHAPTER VI

FUTURE DIRECTIONS AND CONCLUDING REMARKS

This research project determined that some primary HPE cells from moderately differentiated prostate tumors have molecular changes that allowed the anti-androgen flutamide to act as an AR agonist. We found increased levels of DJ-1 and AR after flutamide treatment in primary HPE and LNCaP cells and further determined that this increase was due to protein stabilization. These results supported known hypotheses for mechanisms that would promote androgen-independent disease. Upon further investigation, we determined that DJ-1 directly bound the AR and modulated its transcriptional activity in prostate cancer cells providing a new mechanism for DJ-1 to regulate AR. The DJ-1:AR interaction was hormonally regulated in two PCa cell lines and hormonal treatment increased DJ-1 nuclear localization. The most compelling evidence that DJ-1 is involved in PCa progression is that DJ-1 expression increases after prolonged ADT in primary tumor samples. These results provide evidence that DJ-1 may play an important role in the progression of PCa to an androgen-independent status and fit with previously published accounts of AR co-regulators allowing epithelial cells to gain a growth advantage in the presence of low-levels of androgens (48).

Many aspects of the precise role of DJ-1 in PCa remain unclear. Although DJ-1 expression was increased after ADT in primary tumors, this study did not address whether the increase in DJ-1 correlated with PCa recurrence or time-to-recurrence. This will be an interesting future direction, but unfortunately, may be very difficult to address

since the types of samples needed are very hard to obtain, especially in large enough numbers to be statistically significant. Another future direction that will be easier to address is whether or not DJ-1 correlates with PCa risk. This type of study could be performed by comparing DJ-1 expression to PSA level, tumor volume, tumor stage, etc. This study could be completed more easily because it does not involve samples from patients who received therapy or metastatic samples.

Although we determined that DJ-1 and AR directly interact, we did not determine what other proteins are in the complex. There are many known AR-binding proteins, so this will likely be a long term project, but one that may elucidate the precise function of DJ-1 regulation of AR. Further, there were other proteins identified in the DJ-1 yeast two-hybrid that may be important in PCa and AR signaling, but the interaction between these putative binding proteins must first be confirmed. This could lead to identification of multiple other pathways in PCa that are affected by DJ-1. Beyond protein-protein interactions, DJ-1 acts as a transcription factor in neuronal cells, it is possible that there are DJ-1 regulated genes in prostate epithelial cells (113). This will be an interesting project, but to date there are no known DJ-1 target genes in prostate. Tyrosine hydroxylase, which was identified as the DJ-1 target gene in neuronal cells, is involved in dopamine synthesis and is neuron specific so it is unlikely to be expressed in prostate cancer.

Finally, multiple preliminary experiments were performed in mouse prostates which may provide interesting future research projects. DJ-1 expression was increased in

12T-7f prostate tumors as compared to wild-type prostates, and also was differentially expressed. DJ-1 was cytoplasmic in the 3 week old wild-type prostate and in the 12T-7f tumors, but was predominantly nuclear in the 15 week old growth quiescent wild-type prostate. We demonstrated that hormonal treatment changed DJ-1 subcellular localization in human PCa cell lines, but it is unknown whether changing hormone levels affect the localization of mouse DJ-1. Since DJ-1 was cytoplasmic regardless of age in the 12T-7f mice, it seems more likely that transformation with SV40 Large-TAg affects DJ-1 sub-cellular localization. SV40 TAg inhibits p53 (163) and Rb (164), and it is possible that alterations in one or both of these signaling pathways affects/regulates DJ-1 sub-cellular localization.

This research began to elucidate the role of DJ-1 in PCa. When this project was started there were no reports of DJ-1 in prostate, nor was there any indication that DJ-1 directly interacted with AR. This project shed some light on the potential important role of DJ-1 in AIPC or as a marker of PCa risk. Obviously future research will be required in order to conclusively answer the questions raised by this research. However, this project answered several fundamental questions regarding the function of DJ-1 and provided ample preliminary data for future DJ-1 research in PCa. Therefore, this project represents a first-step in the ongoing process of unraveling the multiple functions of human DJ-1 in prostate.

REFERENCES

1. Krongrad A, Droller M. Prostatic Diseases: W.B. Saunders Publishing; 1993.

2. Abate-Shen C, Shen MM. Molecular Genetics of Prostate Cancer. Genes and Development 2000;14:2410-34.

3. DeMarzo A, Nelson C, Isaacs WB, Epstein J. Pathological and molecular aspects of prostate cancer. Lancet 2003;361:955-64.

4. Thomson A, Cunha G. Prostatic growth and development are regulated by FGF10. Development 1999;126:3693-701.

5. Marker P, Donjacour A, Dahiya R, Cunha G. Hormonal, cellular, and molecular control of prostatic development. Developmental Biology 2003;253(2):165-74.

6. MacLennan GT, Eisenberg R, Fleshman RL, et al. The Influence of Chronic Inflammation in Prostatic Carcinogenesis: A 5-Year Followup Study. The Journal of Urology 2006;176(3):1012-6.

7. Zheng SL, Liu W, Wiklund F, et al. A comprehensive association study for genes in inflammation pathway provides support for their roles in prostate cancer risk in the CAPS study. The Prostate 2006;66(14):1556-64.

8. Sutcliffe S, Giovannucci E, De Marzo AM, Leitzmann M, Willett W, Platz E. Gonorrhea, syphilis, clinical prostatitis, and the risk of prostate cancer. Cancer Epidemiology Biomarkers and Prevention 2006;15(11):2160-6.

9. Wasserman NF. Benign Prostatic Hyperplasia: A Review and Ultrasound Classification. Radiologic Clinics of North America 2006;44:689-710.

10. Berry S, Coffey D, Walsh P. The development of human benign prostatic hyperplasia with age. Journal of Urology 1984;132:474-9.

11. Gann PH. Risk Factors for Prostate Cancer. Reviews in Urology 2002;4(Supplement 5):S3-S10.

12. Smith J, Freije D, Carpten JD, et al. Major susceptibility locus for prostate cancer on chromosome 1 suggested by a genome-wide search. Science 1996;274(5291):1371-4.

13. Xu J, Meyers D, Freije D, et al. Evidence for a prostate cancer susceptibility locus on the X chromosome. Nature Genetics 1998;20(2):175-9.

14. McNeal J, Bostwick D. Intraductal dysplasia: A premalignant lesion of the prostate. Human Pathology 1986;17:64-71.

15. Macintosh CA, Stower M, Reid N, Maitland NJ. Precise Microdissection of Human Prostate Cancers Reveals Genotypic Heterogeneity. Cancer Research 1998;58(1):23-8.

16. Bostwick DG, Shan A, Qian J, et al. Independent origin of multiple foci of prostatic intraepithelial neoplasia. Cancer 1998;83(9):1995-2002.

17. Gleason D. Classification of prostate carcinomas. Cancer Chemotherapeutic Reports 1966;50:125-8.

18. Gleason D. The Veteran's Administration Cooperative Urologic Research Group: Histologic grading and clinical staging of prostatic carcinoma, in Urologic Pathology. The Prostate 1977:171-97.

19. Gleason D, Mellinger G. The Veterans Administration Cooperative Urological Research Group: Prediction of prognosis for prostatic adenocarcinoma by combined histologic grading and clinical staging. Journal of Urology 1974;111:58-64.

20. Baillar J, Mellinger G, Gleason D. Survival rates of patients with prostatic cancer, tumor stage and differentiation - a preliminary report. Cancer Chemotherapeutic Reports 1966;50:129-36.

21. Gleason D. Histologic grading of prostate cancer: A perspective. Human Pathology 1992;23:273-9.

22. Chang M, Tsuchiya K, Batchelor R, et al. Deletion mapping of chromosome 8p in colorectal carcinoma and dysplasia arising in ulcerative colitis, prostatic carcinoma, and malignant fibrous histiocytomas. American Journal of Pathology 1994;144(1):1-6.

23. Fujiwara Y, Ohata H, Emi M, et al. A 3-Mb physical map of the chromosome region 8p21.3-p22, including a 600-kb region commonly deleted in human hepatocellular carcinoma, colorectal cancer, and non-small cell lung cancer. Genes, Chromosomes, and Cancer 1994;10(1):7-14.

24. Matsuyama H, Pan Y, Skoog L, et al. Deletion mapping of chromosome 8p in prostate cancer by fluorescence in situ hybridization. Oncogene 1994;9(10):3071-6.

25. Voeller HJ, Augustus M, Madike V, Bova GS, Carter KC, Gelmann EP. Coding Region of NKX3.1, a Prostate-Specific Homeobox Gene on 8p21, Is Not Mutated in Human Prostate Cancers. Cancer Research 1997;57(20):4455-9.

26. Bhatia-Gaur R, Donjacour AA, Sciavolino PJ, et al. Roles for Nkx3.1 in prostate development and cancer. Genes and Development 1999;13(8):966-77.

27. Whang YE, Wu X, Suzuki H, et al. Inactivation of the tumor suppressor PTEN/MMAC1 in advanced human prostate cancer through loss of expression. Proceedings of the National Academy of Sciences 1998;95(9):5246-50.

28. Steck PA, Pershouse MA, Jasser SA, et al. Identification of a candidate tumour suppressor gene, MMAC1, at chromosome 10q23.3 that is mutated in multiple advanced cancers. Nat Genet 1997;15(4):356.

29. Li J, Yen C, Liaw D, et al. PTEN, a Putative Protein Tyrosine Phosphatase Gene Mutated in Human Brain, Breast, and Prostate Cancer. Science 1997;275(5308):1943-7.

30. Vliestra RJ vAD, Hermans KG, van Steenbrugge GJ, Trapman J. Frequent inactivation of PTEN in prostate cancer cell lines and xenografts. Cancer Research 1998;58:2720-3.

31. Wu X, Senechal K, Neshat MS, Whang YE, Sawyers CL. The PTEN/MMAC1 tumor suppressor phosphatase functions as a negative regulator of the phosphoinositide 3-kinase/Akt pathway. Proceedings of the National Academy of Sciences 1998;95(26):15587-91.

32. Li C, Larsson C, Futreal A, et al. Identification of two distinct deleted regions on chromosome 13 in prostate cancer. Oncogene 1998;16:481-7.

33. Melamed J, Einhorn JM, Ittmann MM. Allelic loss on chromosome 13q in human prostate carcinoma. Clinical Cancer Research 1997;3(10):1867-72.

34. Cooney KA, Wetzel JC, Merajver SD, Macoska JA, Singleton TP, Wojno KJ. Distinct Regions of Allelic Loss on 13q in Prostate Cancer. Cancer Research 1996;56(5):1142-5.

35. Bookstein R, Shew J, Chen P, Scully P, Lee W. Suppression of tumorigenicity of human prostate carcinoma cells by replacing a mutated RB gene. Science 1990;247(4943):712-5.

36. Bookstein R, Rio P, Madreperla SA, et al. Promoter Deletion and Loss of Retinoblastoma Gene Expression in Human Prostate Carcinoma. Proceedings of the National Academy of Sciences 1990;87(19):7762-6.

37. Phillips S, Barton C, Lee S, et al. Loss of the retinoblastoma susceptibility gene (RB1) is a frequent and early event in prostatic tumorigenesis. British Journal Cancer 1994;70:1252-7.

38. Ittmann M, Wieczorek R. Alterations of the retinoblastoma gene in clinically localized, stage B prostate adenocarcinoma. Human Pathology 1996;27(1):28-34.

39. Zhao X, Gschwend JE, Powell CT, Foster RG, Day KC, Day ML. Retinoblastoma Protein-dependent Growth Signal Conflict and Caspase Activity Are Required for Protein Kinase C-signaled Apoptosis of Prostate Epithelial Cells. Journal of Biological Chemistry 1997;272(36):22751-7.

40. Bowen C, Spiegel S, Gelmann EP. Radiation-induced Apoptosis Mediated by Retinoblastoma Protein. Cancer Research 1998;58(15):3275-81.

41. Yeh S, Miyamoto H, Nishimura K, et al. Retinoblastoma, a Tumor Suppressor, Is a Coactivator for the Androgen Receptor in Human Prostate Cancer DU145 Cells. Biochemical and Biophysical Research Communications 1998;248(2):361.

42. Saric T, Brkanac Z, Troyer DA, et al. Genetic pattern of prostate cancer progression. International Journal of Cancer 1999;81(2):219-24.

43. Henke R, Kruger E, Ayhan N, Hubner D, Hammerer P, Hulan H. Immunohistochemical detection os p53 protein in human prostatic cancer. Journal of Urology 1994;152:1297-301.

44. Voeller HJ, Sugar L, Pretlow TG, Gelmann EP. p53 oncogene mutations in human prostate cancer specimens. Journal of Urology 1994;151:492-5.

45. Bookstein R, MacGrogan D, Hilsenbeck SG, Sharkey F, Allred DC. p53 Is Mutated in a Subset of Advanced-Stage Prostate Cancers. Cancer Research 1993;53(14):3369-73.

46. Effert P, McCoy R, Walther P, Liu E. p53 gene alterationsa in human prostate carcinoma. Journal of Urology 1993;150:257-61.

47. Navone N, Troncoso P, Pisters L, et al. p53 protein accumulation and gene mutation in the progression of human prostate carcinoma. Journal of the National Cancer Institute 1993;85:1657-69.

48. Feldman BJ, Feldman D. The Development of Androgen-Independent Prostate Cancer. Nature Reviews Cancer 2001;1(1):34.

49. Heinlein CA, Chang C. Androgen Receptor in Prostate Cancer. Endocrine Reviews 2004;25(2):276-308.

50. Cunha G, Donjacour A, Cooke P, et al. The endocrinology and developmental biology of the prostate. Endocrine Reviews 1987;3:338-62.

51. Roy A, Lavrovsky Y, Song C, et al. Regulation of androgen action. Vitamins and Hormones 1999;55:309-52.

52. Yeh S, Tsai M, Xu Q, et al. Generation and characterization of androgen receptor knockout mice: an in vivo model for the study of androgen function in selective tissues. Proceedings of the National Academy of Sciences 2002;99:13498-503.

53. Quigley C, De Bellis A, Marschke K, El-Awady M, Wilson EM, French FS. Androgen receptor defects: historical, clinical, and molecular perspectives. Endocrine Reviews 1995;16:271-321.

54. Lyon M, Hawkes S. X-linked gene for testicular feminization in the mouse. Nature 1970;227:1217-9.

55. Stenman U. Prostate-specific antigen, clinical use and staging: an overview. British Journal of Urology 1997;79(Supplement 1):53-60.

56. Stenman U, Leinonen J, Zhang W, Finne P. Prostatic Specific Antigen. Seminars in Cancer Biology 1999;9:83-93.

57. Huggins C, Hodges C. The Effect of Castration and of Androgen Injection on Serum Phosphatases in Metastatic Carcinoma of the Prostate. Cancer Research 1941;1:293-7.

58. Taplin M-E, Bubley GJ, Shuster TD, et al. Mutation of the Androgen-Receptor Gene in Metastatic Androgen-Independent Prostate Cancer. New England Journal of Medicine 1995;332(21):1393-8.

59. Brewster SF, Simons J. Gene Therapy in Urological Oncology: principles, strategies and potential. European Urology 1994;25:177-82.

60. Labrie F, Belanger A, Simard J, Labrie C. Dupont A: Combination therapy for prostate cancer. Endocrine and biologic basis of its choice as new standard first-line therapy. Cancer 1993;71:1059-67.

61. Moreau J-P, Delavault P, Bulumberg J. Lutenizing hormone-releasing hormone agonists in the treatment of prostate cancer: A review of their discovery, development, and place in therapy. Clinical Therapeutics 2006;28(10):1485-508.

62. Koivisto P, Kononen J, Palmberg C, et al. Androgen receptor gene amplification: a possible molecular mechanism for androgen deprivation therapy failure in prostate cancer. Cancer Research 1997;57:314-9.

63. Visakorpi T, Hyytinen E, Koivisto P, et al. In vivo amplification of the androgen receptor gene and progression of human prostate cancer. Nat Genet 1995;9(4):401.

64. Linja MJ, Savinainen KJ, Saramaki OR, Tammela TLJ, Vessella RL, Visakorpi T. Amplification and Overexpression of Androgen Receptor Gene in Hormone-Refractory Prostate Cancer. Cancer Res 2001;61(9):3550-5.

65. Gregory CW, Johnson RT, Jr., Mohler JL, French FS, Wilson EM. Androgen Receptor Stabilization in Recurrent Prostate Cancer Is Associated with Hypersensitivity to Low Androgen. Cancer Res 2001;61(7):2892-8.

66. Balk SP. Androgen receptor as a target in androgen-independent prostate cancer. Urology 2002;60(3):132.

67. Buchanan G, Greenberg NM, Scher HI, Harris JM, Marshall VR, Tilley WD. Collocation of Androgen Receptor Gene Mutations in Prostate Cancer. Clin Cancer Res 2001;7(5):1273-81.

68. Marcelli M, Ittmann M, Mariani S, et al. Androgen Receptor Mutations in Prostate Cancer. Cancer Research 2000;60(4):944-9.

69. Taplin M-E, Bubley GJ, Ko Y-J, et al. Selection for Androgen Receptor Mutations in Prostate Cancers Treated with Androgen Antagonist. Cancer Research 1999;59(11):2511-5.

70. Tilley WD, Buchanan G, Hickey TE, Bentel JM. Mutations in the androgen receptor gene are associated with progression of human prostate cancer to androgen independence. Clinical Cancer Research 1996;2(2):277-85.

71. Craft N, Chhor C, Tran C, et al. Evidence for Clonal Outgrowth of Androgen-independent Prostate Cancer Cells from Androgen-dependent Tumors through a Two-Step Process. Cancer Research 1999;59(19):5030-6.

72. Veldscholte J, Ris-Stalpers C, Kuiper G, et al. A mutation in the ligand binding domain of the androgen receptor of human LNCaP cells affects steroid binding characteristics and response to anti-androgens. Biochemical and Biophysical Research Communications 1990;173(2):534-40.

73. Veldscholte J, Berrevoets CA, Brinkman AO, Grootegoed J, Mulder E. Anti-androgens and the mutated androgen receptor of LNCaP cells: differential effects on binding affinity, heat-shock protein interaction, adn transcription activation. Biochemistry 1992;31(8):2393-9.

74. Zhao X-Y, Malloy PJ, Krishnan AV, et al. Glucocorticoids can promote androgen-independent growth of prostate cancer cells through a mutated androgen receptor. Nature Medicine 2000;6(6):703.

75. Gaddipati JP, McLeod DG, Heidenberg HB, et al. Frequent Detection of Codon 877 Mutation in the Androgen Receptor Gene in Advanced Prostate Cancers. Cancer Research 1994;54(11):2861-4.

76. Small EJ, Srinivas S. The antiandrogen withdrawl syndrome. Experience in a large cohort of unselected patients with advanced prostate cancer. Cancer 1995;76(8):1428-34.

77. Kelly W, Scher H. Prostate Specifc Antigen decline after anti-androgen withdrawl: the flutamide withdrawl syndrome. Journal of Urology 1993;149:607-9.

78. Kelly W, Slovin S, Scher H. Steroid hormone withdrawl syndromes. Urologic Clinics of North America 1997;24:421-31.

79. Heinlein CA, Chang C. Androgen Receptor (AR) Coregulators: An Overview. Endocrine Reviews 2002;23(2):175-200.

80. Gregory CW, He B, Johnson RT, et al. A Mechanism for Androgen Receptor-mediated Prostate Cancer Recurrence after Androgen Deprivation Therapy. Cancer Research 2001;61(11):4315-9.

81. Agoulnik IU, Vaid A, Bingman WE, III, et al. Role of SRC-1 in the Promotion of Prostate Cancer Cell Growth and Tumor Progression. Cancer Research 2005;65(17):7959-67.

82. Culig Z, Comuzzi B, Steiner H, Bartsch G, Hobisch A. Expression and function of androgen receptor coactivators in prostate cancer. Journal of Steroid Biochemistry and Molecular Biology 2004;92:265-71.

83. Halkidou K, Gnanapragasam V, Mehta P, et al. Expression of Tip60, and androgen receptor coactivator, and its role in prostate cancer development. Oncogene 2003;22(16):2466-77.

84. Berrevoets CA, Umar A, Trapman J, Brinkman AO. Differential modulation of androgen receptor transcriptional activity by the nuclear receptor co-repressor (N-CoR). Biochemical Journal 2004;379:731-8.

85. Lavinsky RM, Jepsen K, Heinzel T, et al. Diverse signaling pathways modulate nuclear receptor recruitment of N-CoR and SMRT complexes. Proceedings of the National Academy of Sciences 1998;95(6):2920-5.

86. Craft N, Shostak Y, Carey M, Sawyers CL. A mechanism for hormone-independent prostate cancer through modulation of androgen receptor signaling by the HER-2/neu tyrosine kinase. Nature Medicine 1999;5(3):280.

87. Wen Y, Hu MCT, Makino K, et al. HER-2/neu Promotes Androgen-independent Survival and Growth of Prostate Cancer Cells through the Akt Pathway. Cancer Research 2000;60(24):6841-5.

88. Suzuki H, Ueda T, Ichikawa T, Ito H. Androgen receptor involvement in the progression of prostate cancer. Endocrine Related Cancer 2003;10(2):209-16.

89. Torchia J, Glass C, Rosenfeld MG. Co-activators and co-repressors in the integration of transcriptional responses. Current Opinion in Cell Biology 1998;10(3):373-83.

90. Bonifati V, Rizzu P, van Baren MJ, et al. Mutations in the DJ-1 Gene Associated with Autosomal Recessive Early-Onset Parkinsonism. Science 2003;299(5604):256-9.

91. Bonifati V, Rizzu P, Squitieri F, et al. DJ-1(PARK7), a novel gene for autosomal recessive, early onset parkinsonism. Neurological Sciences 2003;24(3):159.

92. Macedo MG, Anar B, Bronner IF, et al. The DJ-1L166P mutant protein associated with early onset Parkinson's disease is unstable and forms higher-order protein complexes. Human Molecular Genetics 2003;12(21):2807-16.

93. Nagakubo D, Taira T, Kitaura H, Ikeda M, Iguchi-Ariga S, Ariga H. DJ-1, a novel oncogene which transforms mouse NIH3T3 cells in cooperation with ras. Biochemical and Biophysical Research Communications 1997;231(2):509-13.

94. Junn E, Taniguchi H, Jeong BS, Zhao X, Ichijo H, Mouradian MM. Interaction of DJ-1 with Daxx inhibits apoptosis signal-regulating kinase 1 activity and cell death. Proceedings of the National Academy of Sciences 2005;102(27):9691-6.

95. Kim RH, Peters M, Jang Y, et al. DJ-1 a novel regulator of the tumor suppressor PTEN. Cancer Cell 2005;7:263-73.

96. Sekito A, Taira T, Niki T, Iguchi-Ariga S, Ariga H. Stimulation of transforming activity of DJ-1 by Abstract, a DJ-1 binding protein. International Journal of Cancer 2005;26(3):685-9.

97. Shinbo Y, Taira T, Niki T, Iguchi-Ariga S, Ariga H. DJ-1 restores p53 transcriptional activity inhibited by Topors/p53BP3. International Journal of Cancer 2005;26(3):641-8.

98. Takahashi K, Taira T, Niki T, Seino C, Iguchi-Ariga SMM, Ariga H. DJ-1 Positively Regulates the Androgen Receptor by Impairing the Binding of PIASxalpha to the Receptor. Journal of Biological Chemistry 2001;276(40):37556.

99. Yaacov H. Differential control of apoptosis by DJ-1 in prostate benign and cancer cells. Journal of Cellular Biochemistry 2004;92(6):1221-33.

100. Wilson MA, Collins JL, Hod Y, Ringe D, Petsko GA. The 1.1-A resolution crystal structure of DJ-1, the protein mutated in autosomal recessive early onset Parkinson's disease. Proceedings of the National Academy of Sciences 2003;100(16):9256-61.

101. Tao X, Tong L. Crystal Structure of Human DJ-1, a Protein Associated with Early Onset Parkinson's Disease. Journal of Biological Chemistry 2003;278(33):31372-9.

102. Honbou K, Suzuki NN, Horiuchi M, et al. The Crystal Structure of DJ-1, a Protein Related to Male Fertility and Parkinson's Disease. Journal of Biological Chemistry 2003;278(33):31380-4.

103. Moore D, Zhang L, Dawson T, Dawson V. A missense mutation (L166P) in DJ-1, linked to familial Parkinson's disease, confers reduced protein stability and impairs homo-oligomerization. Journal of Neurochemistry 2003;87:1557-67.

104. Miller DW, Ahmad R, Hague S, et al. L166P Mutant DJ-1, Causative for Recessive Parkinson's Disease, Is Degraded through the Ubiquitin-Proteasome System. Journal of Biological Chemistry 2003;278(38):36588-95.

105. Yokota T, Sugawara K, Ito K, Takahashi R, Ariga H, Mizusawa H. Down regulation of DJ-1 enhances cell death by oxidative stess, ER stress, and proteasome inhibition. Biochemical and Biophysical Research Communications 2003;312:1342-8.

106. Taira T, Saito Y, Niki T, Iguchi-Ariga S, Takahashi K, Ariga H. DJ-1 has a role in antioxidant stress to prevent cell death. EMBO Reports 2004;5(2):213-8.

107. Yang Y, Gehrke S, Haque ME, et al. Inactivation of Drosophila DJ-1 leads to impairments of oxidative stress response and phosphatidylinositol 3-kinase/Akt signaling. Proceedings of the National Academy of Sciences 2005;102(38):13670-5.

108. Menzies F, Yenisetti S, Min K-T. Roles of Drosophila DJ-1 in Survival of Dopaminergic Neurons and Oxidative Stress. Current Biology 2005;15:1578-82.

109. Kim RH, Smith PD, Aleyasin H, et al. Hypersensitivity of DJ-1-deficient mice to 1-methyl-4-phenyl-1,2,3,6-tetrahydropyrindine (MPTP) and oxidative stress. Proceedings of the National Academy of Sciences 2005;102(14):5215-20.

110. Goldberg M, Pisani A, Haburcak M, et al. Nigrostriatal Dopaminergic Deficits and Hypokinesia Caused by Inactivation of the Familial Parkinsonism-Linked Gene DJ-1. Neuron 2005;45:489-96.

111. Choi J, Sullards MC, Olzmann JA, et al. Oxidative Damage of DJ-1 Is Linked to Sporadic Parkinson and Alzheimer Diseases. Journal of Biological Chemistry 2006;281(16):10816-24.

112. Xu J, Zhong N, Wang H, et al. The Parkinson's Disease Associated DJ-1 Protein is a Transcriptional Co-Activator that Protects Against Neuronal Apoptosis. Human Molecular Genetics 2005;14(9):1231-41.

113. Zhong N, Kim CY, Rizzu P, et al. DJ-1 Transcriptionally Up-regulates the Human Tyrosine Hydroxylase by Inhibiting the Sumoylation of Pyrimidine Tract-binding Protein-associated Splicing Factor. Journal of Biological Chemistry 2006;281(30):20940-8.

114. Deocampo N, Huang H, Tindall D. The Role of PTEN in the Progression and Survival of Prostate Cancer. Minerva Endocrinology 2003;28(2):145-53.

115. Kasper S. Survey of genetically engineered mouse models for prostate cancer: Analyzing the molecular basis of prostate cancer development, progression, and metastasis. Journal of Cellular Biochemistry 2005;94(2):279-97.

116. Mulholland DJ, Dedhar S, Wu H, Nelson CC. PTEN and GSK3[beta]: key regulators of progression to androgen-independent prostate cancer. Oncogene 2006;25(3):329.

117. Nan B, Snabboon T, Unni E, X-J Y, Whang YE, Marcelli M. The PTEN tumor suppressor is a negative modulator of androgen receptor transcriptional activity. Journal of Molecular Endocrinology 2003;31(1):169-83.

118. Niki T, Takahashi-Niki K, Taira T, Iguchi-Ariga SMM, Ariga H. DJBP: A Novel DJ-1-Binding Protein, Negatively Regulates the Androgen Receptor by Recruiting Histone Deacetylase Complex, and DJ-1 Antagonizes This Inhibition by Abrogation of This Complex. Molecular Cancer Research 2003;1(4):247-61.

119. Jeong H, Kim M-S, Kwon J, Kim K-S, Seol W. Regulation of the transcriptional activity of the tyrosine hydroxylase gene by androgen receptor. Neuroscience Letters 2006;396(1):57.

120. Zhang J, Thomas TZ, Kasper S, Matusik RJ. A Small Composite Probasin Promoter Confers High Levels of Prostate-Specific Gene Expression through Regulation by Androgens and Glucocorticoids in Vitro and in Vivo. Endocrinology 2000;141(12):4698-710.

121. Hayward S, Cox S, Mitchell I, Hallowes R, N D, J T. The effects of interferons on the activity of alpha-glycerolphosphate dehydrogenase in benign prostatic hyperplasia cells in primary culture. Journal of Urology 1987(138):648-53.

122. Kasper S, Rennie PS, Bruchovsky N, et al. Cooperative binding of androgen receptors to two DNA sequences is required for androgen induction of the probasin gene. Journal of Biological Chemistry 1994;269:31763-9.

123. Ghosh R, Gu G, Tillman JE, et al. Increased Expression and Differential Phosphorylation of Stathmin May Promote Prostate Cancer Progression. The Prostate 2007;In Press.

124. Tilley WD, Marcelli M, Wilson J, McPhaul M. Characterization and expression of a cDNA encoding the human androgen receptor. Proceedings of the National Academy of Sciences 1989;86:327-31.

125. Yates J, III, Speicher S, Griffin P, Hunkapiller T. Peptide mass maps: a highly informative approach to protein identification. Analytical Biochemistry 1993;214:397-408.

126. Mann M, Hojrup P, Roepstorff P. Use of mass spectrometric molecular weight information to identify proteins in sequence databases. Biological Mass Spectrometry 1993;22:338-45.

127. Henzel W, Billeci T, Stults J, Wong S, Grimley C, Watanabe C. Identifying proteins from two-dimentional gels by molecular mass searching of peptide f ragments in protein sequence databases. Proceedings of the National Academy of Sciences 1993;90:5011-5.

128. Pitkanen-Arsiola T, Tillman JE, Gu G, et al. Androgen and anti-androgen treatment modulates androgen receptor activity and DJ-1 stability. The Prostate 2006;66(11):1177-93.

129. Zhang J, Gao N, Kasper S, Reid K, Nelson C, Matusik RJ. An Androgen-Dependent Upstream Enhancer Is Essential for High Levels of Probasin Gene Expression. Endocrinology 2004;145(1):134-48.

130. Kemppainen J, Wilson E. Agonist and antagonist activites of hydroxyflutamide and Casodex relate to androgen receptor stabilization. Urology 1996;48(1):157-63.

131. Dalrymple S, Antony L, Xu Y, et al. Role of Notch-1 and E-Cadherin in the Differential Response to Calcium in Culturing Normal versus Malignant Prostate Cells. Cancer Research 2005;65(20):9269-79.

132. Yasunaga Y, Nakamura K, Ewing CM, Isaacs WB, Hukku B, Rhim JS. A Novel Human Cell Culture Model for the Study of Familial Prostate Cancer. Cancer Research 2001;61(16):5969-73.

133. Xu Y, Iyengar S, Roberts R, Shappell S, Peehl DM. Primary culture model of peroxisome proliferator-activated receptor? activity in prostate cancer cells. Journal of Cellular Physiology 2003;196(1):131-43.

134. McManaman JL, Zabaronick W, Schaack J, Orlicky DJ. Lipid droplet targeting domains of adipophilin. Journal of Lipid Research 2003;44(4):668-73.

135. van Bokhoven A, Varella-Garcia M, Korch C, et al. Molecular characterization of human prostate carcinoma cell lines. The Prostate 2003;57(3):205-25.

136. Rowley D, Tindall D. Responses of NBT-II bladder carcinoma cells to conditioned medium from normal urogenital sinus. Cancer Research 1987;47:2955-60.

137. Tan J-a, Sharief Y, Hamil KG, et al. Dehydroepiandrosterone Activates Mutant Androgen Receptors Expressed in the Androgen-Dependent Human Prostate Cancer Xenograft CWR22 and LNCaP Cells. Molecular Endocrinology 1997;11(4):450-9.

138. Kasper S, Rennie PS, Bruchovsky N, et al. Selective activation of the probasin androgen responsive region by steroid hormones. Journal of Molecular Endocrinology 1999;22:313-25.

139. Kotaja N, Aittomaki S, Silvennoinen O, Palvimo JJ, Janne OA. ARIP3 (Androgen Receptor-Interacting Protein 3) and Other PIAS (Protein Inhibitor of Activated STAT) Proteins Differ in Their Ability to Modulate Steroid Receptor-Dependent Transcriptional Activation. Molecular Endocrinology 2000;14(12):1986-2000.

140. Chodak D, Kranc D, Puy L, Takeda H, Johnson K, Chang C. Nuclear Localization of Androgen Receptor in heterogeneous samples of normal, hyperplastic, and neoplastic human prostate. Journal of Urology 1992;147(3 part 2):798-803.

141. Hobisch A, Culig Z, Radmayr C, Bartsch G, Klocker H, Hittmair A. Androgen Receptor Status on Lymph Node Metastases from Prostate Cancer. Prostate 1996;28(2):129-35.

142. Mohler JL, Chen Y, Hamil K, et al. Androgen and glucocorticoid receptors in the stroma and epithelium of prostatic hyperplasia and carcinoma. Clinical Cancer Research 1996;2(5):889-95.

143. Sadi M, Walsh P, Barrack E. Immunohistochemical Study of Androgen Receptors in metastic prostate cancer comparison of receptor content and response to hormonal therapy. Cancer 1991;67(12):3057-64.

144. van der Kwast T, Schalken J, Ruizeveld de Winter, JA, van Vroonhoven CC, Mulder E, Boersma, W, Trapman J. Androgen Receptors in endocrine-therapy-resistant human prostate cancer. International Journal of Cancer 1991;48(2):189-93.

145. Sharifi N, Farrar WL. Androgen Receptor as a Therapeutic Target or Androgen Independent Prostate Cancer. American Journal of Therapeutics 2006;13:166-70.

146. Sharifi N, Gulley JL, Dahut WL. Androgen Deprivation Therapy for Prostate Cancer. Journal of American Medicine 2005;294(2):238-44.

147. Klein K, Reiter R, Redula J, et al. Progression of metastatic human prostate cancer to androgen independence in immunodeficient SCID mice. Nature Medicine 1997;3(4):402-8.

148. Bhowmick NA, Ghiassi M, Aakre M, Brown K, Singh V, Moses HL. From the Cover: TGF-{beta}-induced RhoA and p160ROCK activation is involved in the inhibition of Cdc25A with resultant cell-cycle arrest. Proceedings of the National Academy of Sciences 2003;100(26):15548-53.

149. Masahisa K, Hiroaki A, Fumiaki T, Gen S. Spinal and bulbar muscular atrophy: ligand-dependent pathogenesis and therapeutic perspectives. Journal of Molecular Medicine 2004;V82(5):298.

150. Waller AS, Sharrard RM, Berthon P, Maitland NJ. Androgen receptor localisation and turnover in human prostate epithelium treated with the antiandrogen, casodex. Journal of Molecular Endocrinology 2000;24(3):339-51.

151. Spector DL, Fu X-D, Maniatis T. Associations between distinct pre-mRNA splcing components and the cell nucleus. The EMBO Journal 1991;10(11):3467-81.

152. Taira T, Takahashi K, Kitagawa R, Iguchi-Ariga SMM, Ariga H. Molecular cloning of human and mouse DJ-1 genes and identification of Sp1-dependent activation of the human DJ-1 promoter. Gene 2001;263(1-2):285.

153. Stone K, Mickey D, Wunderli H, Mickey G, Vollmer R, Paulson D. Isolation o a human prostate carcinoma cell line (DU 145). International Journal of Cancer 1978;21:274-81.

154. Mickey D, Stone K, Wunderli H, Mickey G, Vollmer R, Paulson D. Heterotransplantation of a human prostatic adenocarcinoma cell line in nude mice. Cancer Research 1977;37:4049-58.

155. Kaighn M, Narayan K, Ohnuki Y, Lechner J, Jones L. Establishment ad characterization of a human prostatic carcinoma cell line (PC-3). Investigative Urology 1979;17:16-23.

156. Berrevoets CA, Veldscholte J, Mulder E. Effects of antiandrogens on transformation and transcription activation of wild-type and mutated (LNCaP) androgen receptors. J Steroid Biochemical Molecular Biology 1993;46(6):731-6.

157. Horoszewicz J, Leong S, Chu T, et al. The LNCaP cell line - A new model for studies on human prostatic carcinoma. Progress in Clinical and Biological Research 1980;37:115-32.

158. Horoszewicz J, Leong S, Kawinski E, et al. LNCaP Model of Human Prostatic Carcinoma. Cancer Research1983;43:1809-18.

159. Hayward SW, Dahiya R, Cunha G, Bartek J, Deshpande N, Narayan P. Establishment and characterization of an immortalized but non-tumorigenic prostate epithelial cell line: BPH-1. In Vitro Cellular and Developmental Biology - Animal 1995;31(1):14-24.

160. Gu G, Yuan J, Wills ML, Kasper S. Prostate Cancer Cells With Stem Cell Characteristics Reconstitute the Original Human Tumor In Vivo. Cancer Research 2007;In Press.

161. Huang W, Shostak Y, Tarr P, Sawyers CL, Carey M. Cooperative Assembly of Androgen Receptor into a Nucleoprotein Complex That Regulates the Prostate-specific Antigen Enhancer. Journal of Biological Chemistry 1999;274(36):25756-68.

162. Jainchill J, Aaronson S, Todaro G. Murine sarcoma and leukemia viruses: assay using clonal lines of contact-inhibited mouse cells. Journal of Virology 1969;4(5):549-53.

163. Pipas JM, Levine AJ. Role of T antigen interactions with p53 in tumorigenesis. Seminars in Cancer Biology 2001;11(1):23-30.

164. DeCaprio J, Ludlow J, Figge J, et al. SV40 large tumor antigen forms a specific complex with the product of the retinoblastom susceptibility gene. Cell 1988;54(2):275-83.

165. Asamoto M, Hokaiwado N, Cho Y-M, Shirai T. Effects of genetic background on prostate and taste bud carcinogenesis due to SV40 T antigen expression under probasin gene promoter control. Carcinogenesis 2002;23(3):463-7.

166. Kasper S, Sheppard P, Yan Y, et al. Development, progression and androgen dependence of prostate tumors in probasin-large T antigen transgenic mice: a model for prostate cancer. Laboratory Investigation 1998;78(3):319-33.

167. Masumori N, Thomas TZ, Chaurand P, et al. A Probasin-Large T Antigen Transgenic Mouse Line Develops Prostate Adenocarcinoma and Neuroendocrine Carcinoma with Metastatic Potential. Cancer Research 2001;61(5):2239-49.

168. Karin M, Liu Z-g, Zandi E. AP-1 functiona nd regulation. Current Opinion in Cell Biology 1997;9:240-6.

169. Angel P, Karin M. The role o Jun, Fos, and the AP-1 complex in cell-proliferation and transformation. Biochimica et Biophysica Acta 1991;1972:129-57.

170. Furlong EEM, Keon NK, Thornton FD, Rein T, Martin F. Expression of a 74-kDa Nuclear Factor 1(NF1) Protein Is Induced in Mouse Mammary Gland Involution. Journal of Biological Chemistry 1996;271(47):29688-97.

171. Roy R, Guerin S. The 30-kDa rat liver transcription factor nulcear facotr 1 binds the rat growth-hormone proximal silencer. European Journal of Biochemistry 1994;219(3):799-806.

172. Jackson D, Rowader K, Stevens K, Jiang C, Milos P, Zaret K. Modulation of liver-specific transcription by interactions between hepatocyte nuclear factor 3 and nuclear factor 1 binding DNA in close apposition. Molecular and Cellular Biology 1993;13(4):2401-10.

173. Archer T, Lefebvre P, Wolford R, Hager G. Transcription factor loading on the MMTV promoter: a bimodal mechanism for promoter activation. Science 1992;255(5051):1573-6.

174. Chong T, Apt D, Gloss B, Isa M, Bernard H. The enhacer of human papillomavirus type 16: binding sites for the ubiquitous transcription factors oct-1, NFA, TEF-2, NF1, and AP-1 participate in epithelial cell-specific transcription. Journal of Virology 1991;65(11):5933-43.

175. Kannius-Janson M, Johansson EM, Bjursell G, Nilsson J. Nuclear Factor 1-C2 Contributes to the Tissue-specific Activation of a Milk Protein Gene in the Differentiating Mammary Gland. Journal of Biological Chemistry 2002;277(20):17589-96.

176. Belikov S, Holmqvist P-H, Astrand C, Wrange O. Nuclear Factor 1 and Octamer Transcription Factor 1 Binding Preset the Chromatin Structure of the Mouse Mammary Tumor Virus Promoter for Hormone Induction. Journal of Biological Chemistry 2004;279(48):49857-67.

177. Lange CA. Making Sense of Cross-Talk between Steroid Hormone Receptors and Intracellular Signaling Pathways: Who Will Have the Last Word? Molecular Endocrinology 2004;18(2):269-78.

178. Lange CA, Gioeli D, Hammes SR, Marker PC. Integration of Rapid Signaling Events with Steroid Hormone Receptor Action in Breast and Prostate Cancer. Annual Review of Physiology 2007;69(1).

179. Zaret K. Developmental competence of the gut endoderm: genetic potentiation by GATA and HNF3/forkhead proteins. Developmental Biology 1999;209(1):1-10.

180. Gao N, Zhang J, Rao MA, et al. The Role of Hepatocyte Nuclear Factor-3{alpha} (Forkhead Box A1) and Androgen Receptor in Transcriptional Regulation of Prostatic Genes. Molecular Endocrinology 2003;17(8):1484-507.

181. Mirosevich J, Gao N, Gupta A, Shappell SB, Jove R, Matusik RJ. Expression and role of Foxa proteins in prostate cancer. The Prostate 2006;66(10):1013-28.

182. Wang Y, Kasper S, Yuan J, et al. Androgen-dependent prostate epithelial cell selection by targeting ARR2PBneo to the LPB-Tag model of prostate cancer. Laboratory Investigations 2006;86(10):1074.

183. Ghosh AK, Steele R, Ray RB. Knockdown of MBP-1 in Human Prostate Cancer Cells Delays Cell Cycle Progression. Journal of Biological Chemistry 2006;281(33):23652-7.

184. Wirth T, Soeth E, Czubayko F, Juhl H. Inhibtion of endogenous carcinoembryonic antigen (CEA) increases the apoptotic rate of colon cancer cells and inhibits metastatic tumor growth. Clinical and Experimental Metastasis 2002;19(2):155-60.

185. Paredes J, Albergaria A, Oliveira JT, Jeronimo C, Milanezi F, Schmitt FC. P-Cadherin Overexpression Is an Indicator of Clinical Outcome in Invasive Breast Carcinomas and Is Associated with CDH3 Promoter Hypomethylation. Clinical Cancer Research 2005;11(16):5869-77.

186. Ashraf N, Zino S, MacIntyre A, et al. Altered Sirtuin Expression is Associated with Node-positive Breast Cancer. British Journal Cancer 2006;95:1056-61.

187. Kuefer R, Day KC, Kleer CG, et al. ADAM15 Disintegrin Is Associated with Aggressive Prostate Cancer and Breast Cancer Disease. Neoplasia 2006;8(4):319-29.

188. Bachelder RE, Lipscomb EA, Lin X, et al. Competing Autocrine Pathways Involving Alternative Neuropilin-1 Ligands Regulate Chemotaxis of Carcinoma Cells. Cancer Research 2003;63(17):5230-3.

189. Goldstein M, Mitchell E. Carcinoembryonic antigen in the staging and follow-up of patients with colorectal cancer. Cancer Investigations 2005;23(4):338-51.

190. Tai P, Chang H, Alders M, Schreiber S, Toft D, Faber L. P59 (FK506 binding protein 59) interaction with heat shock proteins is higly conserved and may involve proteins other than seroid receptors. Biochemistry 1993;31(34):8842-7.

191. Cheung-Flynn J, Prapapanich V, Cox MB, Riggs DL, Suarez-Quian C, Smith DF. Physiological Role for the Cochaperone FKBP52 in Androgen Receptor Signaling. Molecular Endocrinology 2005;19(6):1654-66.